Analysis of Energy-Delay Performance in Multi-hop Wireless Sensor Networks

Ruifeng Zhang

Numéro d'ordre: 2009-ISAL-0109 Year 2009

Thsis

ANALYSIS OF ENERGY-DELAY PERFORMANCE IN MULTI-HOP WIRELESS SENSOR NETWORKS

defend at
L'Institut National des Sciences Appliquées de Lyon

for the degree of
Doctor of Philosophy

Ecole doctorale : Informatique et Mathématiques

submitted at 19 October 2009

by
Ruifeng ZHANG

Defend at 16 December 2009 before the commission of exam
Jury

Dohler Mischa	*Doctor* Centre Tecnològic de Telecomunicacions de Catalunya, Espagne	Rapporteur
CLAVIER Laurent	*Maître de conférence (HDR)* Institut TELECOM/GET TELECOM Lille 1	Rapporteur
Fijalkow Inbar	*Professeur* Universités ENSEA	Examinanteur
Al Agha Khaldoun	*Professeur* Universités Paris Sud	Examinanteur
gorce Jean-Marie	Professeur Université de Lyon, INSA de Lyon	Directeur de thèse

This thesis is prepared at Centre d'Innovation en Télécommunications et Intégration de Services (CITI),
INSA de Lyon - INRIA Rhône-Alpes

To my lovely wife.

To my parents.

Acknowledgements

I would like to express my deep and sincere gratitude to my advisor, Professor Jean-Marie GORCE, who is most responsible for helping me complete this thesis as well as the challenging research that lies behind it. His wide knowledge and her logical way of thinking have been of great value for me. He was always there to meet and talk about my ideas, to proofread and mark up my papers, and to ask me good questions to help me think through my problems. Without his encouragement and constant guidance, I could not have finished this thesis. He has set an example as a smart, hardworking, persistent and passionate researcher that I can only hope to emulate.

Besides my advisor, I am thankful to the rest of my thesis committee members: PhD. Mischa Dohler, Maître de conférence (HDR): Laurent Clavier, Professor: Inbar Fijalkow Professor: Khaldoun Al Agha. Their broad perspective and suggestions have helped me in refining this thesis.

I am very thankful for my officemates at the CITI Laboratory: Amira Ben Hamida, PhD. Fatiha Benali, PhD. Karel Heurtefeux Fei Yang and team members: PhD. Claire Goursaud , PhD. Katia Jaffres-Runser PhD. Nikolai Lebedev, PhD. Jialiang Lu.

Most importantly, I am specially indebted to my wife, Rongping Dong, for staying with me abroad and supporting me all the time. Rongping left her family and friends, and rejected a job offer in China three years ago to come to France living with me in Lyon. I am grateful to Rongping for her love and all the sacrifices she has made for me.

I am greatly indebted to my father, Qiyuan ZHANG, and my mother, Donglan SUN. Thank you, mom and dad, for giving me life in the first place, for educating me to be a honest and responsible person, and for unconditional support and encouragement to pursue my interests.

I am grateful for the financial support of the CSC through UT-INSA project. I want to also thank INRIA for its financial assistance. I also wish to thank BANET project team for its financial support.

Abstract

Wireless sensor networks (WSNs) have introduced a new paradigm of communication between devices, which are applied to different scenarios: from environment monitoring to military. These applications demand three important performance parameters: the end-to-end reliability, the end-to-end delay and the overall energy consumption. Due to the fundamentality of reliability in many applications, we consider it in this thesis as a hard constraint, and the other two performance criteria, i.e., energy and delay are exploited as a couple of competing criteria in order to optimize the parameters of a network including physical and protocol layers.

In wireless channels, unreliability is an inherent property. However, most of works which research the energy-delay performance of WSNs are based on the reliable link of each hop and abandon unreliable links. In this work, unreliable links are efficiently utilized to improve the energy-delay performance of a network.

This thesis begins with the energy-delay performance analyses in traditional multi-hop communications. We propose firstly a metric for energy efficiency: mean energy distance ratio per bit ($\overline{EDRb}$) and a metric for mean delay: mean delay distance ratio ($\overline{DDR}$), which are both derived for unreliable links. Using these two metrics and a realistic unreliable link model, the lower bound and the Pareto front of energy-delay trade-off for one-hop transmissions are derived. Then, these results are extended to multi-hop transmissions and the close-form expression of energy-delay tradeoff is obtained. The lower bound is subsequently validated using simulations in 2-dimension Poisson distributed networks. Theoretical analyses and simulations show that unreliable links in multi-hop transmissions contribute to improve the energy efficiency of the system under a delay constraint, especially for Rayleigh flat fading and Rayleigh block fading channels. On the basis of the close-form expression of lower bound of energy-delay tradeoff, a cross-layer framework is provided to optimize the parameters of the physical, MAC and routing layers under a delay constraint.

Besides the unreliability, broadcasting is another important feature of wireless channels. Opportunistic communications take advantage of these two properties of wireless links to improve the performance of a network. The energy-delay performance of opportunistic communications and related parameter optimization are analyzed in the second

part of this thesis. We firstly propose an analytical framework to evaluate the energy efficiency of opportunistic communications, which provides a method for optimizing the different opportunistic schemes. Further, the lower bound of energy-delay tradeoff in opportunistic communications are deduced considering the mechanism of selecting the optimal forwarding candidates. A close-form expression of the lower bound is obtained on the condition of a fixed number of forwarding candidates, and an algorithm for searching the optimal number of forwarding candidates is proposed. According to the theoretical analyses, a new opportunistic scheme integrating MAC and routing layers is proposed to minimize energy consumption satisfying a mean delay limit. Simulations in a 2-dimension Poisson network using the proposed opportunistic scheme verify the theoretical lower bound of energy-delay tradeoff. Moreover, the optimization of physical parameters is introduced.

In opportunistic communications, only the cooperation at the receiver side is utilized, while in cooperative communications, the cooperation at both the receiver and the transmitter sides is considered. In the third part, cooperative communications are presented by cooperative MIMO (CMIMO) scheme. Firstly, the lower bound of energy-delay tradeoff of CMIMO is analyzed by exploiting an unreliable link model when the number of cooperative transmitters and receivers is fixed. Then, an algorithm for searching the optimal number of cooperative nodes in both two sides is introduced.

Finally, the lower bounds of the above three communication schemes are compared in different channels respectively. The results show that in order to achieve better energy-delay performance, the corresponding communication scheme should be adopted for different channel type: traditional multi-hop communications for AWGN channel, opportunistic communications for Rayleigh block fading channel and CMIMO for Rayleigh flat fading channel.

Résumé

Les réseaux de capteurs sans fil représentent un nouveau paradigme dans les réseaux de communication qui permet de développer de nombreuses applications allant de la surveillance de l'environnement aux applications militaires. Les performances de ces réseaux peuvent être caractérisées par trois fonctions objectives caractérisant les transmissions de bout en bout: la fiabilité, le délai et la consommation d'énergie. Cette thése a pour but de trouver les param¨¨tres optimaux afin d'améliorer les performances de la couche physique, la couche MAC ainsi que la couche protocolaire des réseaux de capteurs. Dans ce travail, nous considérons la fiabilité comme un critère prépondérant et la traitons comme une contrainte dure. La consommation d'énergie et le délai de transmission sont considérés comme des contraintes secondaires concurrentes.

Comme dans tous les réseaux radio, dans les réseaux de capteurs sans fil, les canaux radios ne sont pas fiables. Pour assurer la fiabilité bout-en-bout, la plupart des travaux existants, excluent les liens radios non fiables de la communication et se focalisent sur la sélection des liens fiables. Nous nous différencions par rapport à ces travaux par la prise en compte aussi bien des liens fiables que des liens non fiables. Nous démontrons aussi que les performances telles que la consommation d'énergie et le délai de transmission sont considérablement améliorées en exploitant efficacement les liens non fiables dans les réseaux, et tout en garantissant une fiabilité de bout en bout importante.

Dans une première partie de la thèse, nous analysons le compromis entre la consommation d'énergie et le délai dans les réseaux multi-saut classiques. Nous proposons deux métriques. La première exprime l'efficacité énergétique sous la forme du rapport moyen énergie-distance par bit. La seconde exprime le délai sous la forme du rapport moyen délai-distance par bit. En utilisant ces deux métriques et un mod¨¨le réaliste de liaison radio à erreur, nous déduisons l'ensemble des solutions de compromis Energie-Délai sous la forme du front de Pareto à partir des performances d'une transmission à un saut, et obtenons une formule exprimant le compromis Energie-Délai. Ces résultats sont étendus aux transmissions multi-sauts. Ensuite, nous validons la limite inférieure à l'aide de simulations, sur des réseaux 2-D, issues d'une distribution Poissonnienne. Les analyses théoriques et les simulations montrent que les liens non-fiables dans les transmissions multi-sauts contribuent à améliorer l'efficacité énergétique du syst¨¨me

évanouissements rapides de Rayleigh et le canal à évanouissements de Rayleigh par blocs. Sur la base de l'expression de la borne inférieure du compromis Energie-Délai, un cadre multi-couche est fourni pour optimiser les param¨¨tres des couches physique, MAC et routage sous contrainte de délai.

Dans la seconde partie de la thèse, nous abordons après la non-fiabilité, une autre caractéristique importante des canaux sans fil, qui a trait à la nature diffusante des communications radio. Les communications opportunistes exploitent ces deux propriétés pour améliorer la performance du réseau. Nous analysons les performances d'énergie et de délai des communications opportunistes ainsi que l'optimisation des param¨¨tres connexes. D'abord, nous proposons un cadre de conception pour évaluer l'efficacitè énergétique des communications opportunistes. Ce dernier fournit une méthode pour optimiser les différents mécanismes opportunistes. Ensuite, nous déduisons la borne inférieure du compromis Energie-Délais dans les communications opportunistes, tout en tenant compte du mécanisme de sélection des candidats pour une transmission optimale. La fromule exprimant la borne inférieure est obtenue sous l'hypothèse d'un nombre fixe de candidats à retransmettre. Un algorithme de recherche du nombre optimal de candidats est également proposé. Selon les analyses théoriques obtenues, nous proposons un nouvel algorithme opportuniste pour minimiser la consommation d'énergie face à une limite de délai moyen et intégrant les couches MAC et routage. Les résultats des simulations sur les mécanismes opportunistes proposés dans un réseau issu d'une distribution Poissonnienne correspondent à la limite inférieure théorique du compromis Energie-Délai. Enfin, nous discutons l'optimisation des paramètres de la couche physique.

Dans la troisième partie de la thèse, nous considérons l'aspect coopératif des transmissions. Dans les communications opportunistes, seule la coopération de réception est réalisée, tandis que dans les communications coopératives prennent en compte une coopération des deux côtés : récepteur et émetteur. Dans cette partie, nous considérons l'approche CMIMO (cooperative multiple input multiple output). D'abord, nous analysons la baisse liée au compromis Energie-Délai de CMIMO par l'exploitation d'un modèle de liaison non fiable lorsque le nombre d'émetteurs et de récepteurs coopératifs est fixe. Ensuite, nous fournissons un algorithme de recherche du nombre optimal de nœuds coopératifs de chaque côté. Enfin, nous comparons les limites inférieures de ces trois schémas de communication dans les différents canaux respectivement. Les résultats obtenus montrent que pour parvenir à une meilleure performance Energie-Délai, les mécanismes de communication suivants devraient être adoptés selon le type de canal : les communications multi-saut traditionnelles sont les plus performantes pour le canal à bruit additif blanc Gaussien, alors que les communications opportunistes le sont pour les canaux à évanouissements de Rayleigh par blocs et enfin le CMIMO pour les canaux

à évanouissements rapides de Rayleigh.

Contents

List of Tables

List of Figures

Acronyms

Acronyms

ACK	Acknowledgement
AWGN	Additive White Gaussian Noise
BER	Bit Error Rate
BLAST	Bell Laboratories Layered Space Time
BPSK	Binary Phase Shift Keying
$\overline{DDR}$	mean Delay Distance Ratio
CTS	Clear To Send
dB	Decibel
ETD	Effective Transmission Distance
QPSK	Quaternary Phase Shift Keying
$\overline{EDRb}$	mean Energy Distance Ratio per bit
MIMO	Multiple-Input-Multiple-Output
MAC	Medium Access Control
MHz	Mega Hertz
MIMO	Multi-Input-Multi-Output
MISO	Multi-Input-Single-Output
MPSK	M-ary Phase Shift Keying
MQAM	M-ary Quadrature Shift Keying
PER	Packet Error Rate
PRR	Packet Reception Ratio
RST	Request to Send
SISO	Single-Input-Single-Output
SIMO	Single-Input-Multi-Output
STBC	Space-Time Block Code
SNR	Signal-to-Noise Ratio
SER	Symbol Error Rate
SINR	Signal to Interference Noise Ratio
WSN	Wireless Sensor Network

Notations

Notations

α	Path-loss exponent (≥ 2)
β_{amp}	Amplifier proportional offset (> 1)
γ	Signal Noise ration
τ_{ack}	ACK Ratio
τ_{head}	Overhead Ratio
b	modulation order
B	Bandwidth of channel
d_0	Minimum transmission distance
d_{hop}	one-hop transmission distance
$\mathcal{D}$	a destination node
E_{ACK}	Energy consumption for an ACK packet
E_p	Energy consumption for transmitting one packet
E_{Tx}	Energy consumption at the transmitter side
E_{Rx}	Energy consumption at the receiver side
${}_2F_1$	Gauss's hypergeometric function
F_1	Appell's hypergeometric function
f_c	Carrier frequency
G_{Rant}	Receiver antenna gain
G_{Tant}	Transmitter antenna gain
L	Circuitry loss (≥ 1)
N_0	Noise level
N_b	Number of bits per packet
N_{ack}	Number of bits in an ACK packet
N_{head}	Number of bits in the overhead of a data packet
N_R	Number of cooperative receivers
N_{Ropt}	Optimal number of cooperative receivers
N_{R0}	Minimum number of cooperative receivers
N_T	Number of cooperative transmitters
N_{Topt}	Optimal number of cooperative transmitters
N_{T0}	Minimum number of cooperative transmitters

pl	Link probability
P_0	Minimum transmission power
P_{broagg}	Transmission power for broadcast and aggregation
P_{opt}	Optimal transmission power
P_{rxElec}	Receiver circuitry power
P_{start}	Startup power
P_{txElec}	Transmitter circuitry power
R_b	Bit rate
R_s	Symbol rate
R_{code}	Code rate
R_c	STBC code rate
T_{start}	Startup time
T_{queue}	Time from queueing
R_b	Bit rate
R_s	Symbol rate
R_{code}	Code rate
R_c	STBC code rate
$\mathcal{S}$	a source node
T_{start}	Startup time

1 Introduction

Wireless technologies have changed the way of people communication. Traditional wireless cellular networks allow people on the move to communicate with anyone or anything using a range of multimedia services. Now, wireless sensor networks (WSNs) have the potential to expand the communication capability to devices in order to co-operate on the monitoring of stress and strain in buildings and bridges, detection of hazardous events, tracking of enemy targets, and the support of unmanned robotic vehicles and so on. Wireless broadband access networks allow people and devices to have high-speed connections to the backbone network from any place at any time.

Of all potential wireless applications, WSNs are special due to their emphasis on communication among devices. In addition, these networks have hard energy constraints since each node is powered by a small battery that may not be rechargeable or renewable. Moreover, wireless links are unreliable and unstable. Therefore, how to make best use of unreliable links to reduce energy consumption is an important design consideration for such networks. Since all the layers in the network protocol stack affect the overall system performance, synergies between the design of different layers must be exploited to optimize the system performance under resource constraints [33].

In this chapter, we first give an introduction to sensor networks as well as their applications in Section 1.1. Then, the technical challenges for implementing efficient sensor networks are presented in Section 1.2. In Section 1.3, the organization of this thesis is introduced. Finally, in Section 1.4, we give an overview of the main contributions of this thesis.

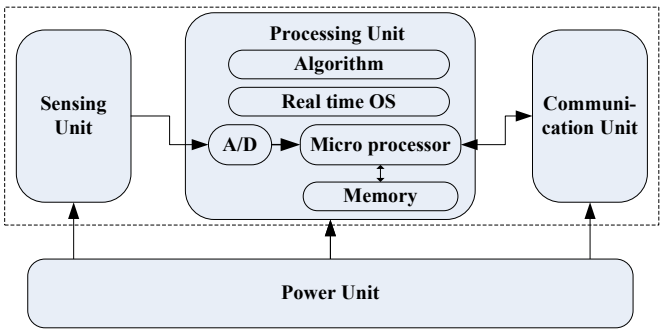

Figure 1.1: Architecture of wireless sensor node

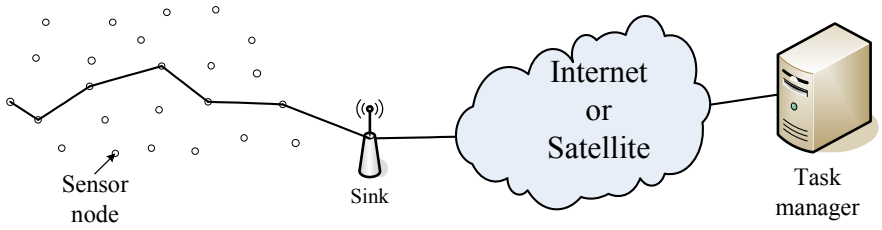

Figure 1.2: Architecture of wireless sensor network

1.1 Overview of wireless sensor networks

Wireless technology has been traditionally used to connect people to each other. Cellular systems, wireless local area networks and broadband wireless access aim to provide voice and data communication. While advances in Micro Electro-Mechanical Systems (MEMS) technology, wireless communications, and digital electronics have enabled the manufacturing of small, low priced, low power, multi-functional sensor nodes that can be connected via a wireless network [47]. Wireless sensor networks (WSNs) have introduced a new paradigm of communication among devices.

These tiny sensor nodes consist of sensing module, data processing module, communication module and power supply module [76] as shown in Fig. 1.1. The sensing module collects information from the surrounding environment; the data processing module performs some local information processing such as quantization and compression; and the communication module is responsible for transmitting the locally processed data to a fusion center (also called a sink node) where the information from different sensor nodes are aggregated and fused to generate the final intelligence.

A sensor network is composed of dozens, or even thousands of nodes, connected in a systematic way, as shown in Fig. 1.2. This figure indicates that the information from the sensors flows into a sink node. As shown, if the source node is far away from the sink node, intermediate nodes can help with relaying via multi-hop transmissions. These networked sensors are distributed to collect information on entities of interest,

e.g., they can be deployed on the ground, in the air, inside buildings, on bodies [79], and in vehicles to detect events of interests and monitor environmental parameters.

Wireless Sensor Networks have wide applications [6, 55] such as environment control [41, 59, 65], traffic control [73, 74, 23], vital sign monitoring, [7, 9, 75], biodiversity mapping , intelligent buildings, human imaging and tracking, and military applications [63]. Consequently, WSNs are slowly becoming an integral part of our lives. Recently, extensive research efforts have enabled the actual implementation of sensor networks designed for the unique objective of sensing and monitoring applications [65].

1.2 Motivation

The applications of WSNs can be classified as event detection, periodic measurements and tracking [47, 55], and most of applications belong to the former two kinds. Therefore, this thesis mainly concentrates on these two types of applications. Regarding event detection and periodic measurement applications, data traffic is low, that is to say, the throughput is not a constraint for these two kinds of applications. Because of this characteristic, interference can be neglected.

For these kinds of applications, three important performance parameters are usually considered: the end-to-end reliability, the end-to-end delay and the end-to-end energy consumption [13].

Energy is a scarce resource for nodes in multi-hop WSNs [33] because the power of node is supplied by a battery which is difficult to charge or impossible to change in a large-scale network. Therefore, the energy efficiency is of paramount importance in most of these applications to prolong the lifetime of network.

Secondly, since transmitted data are often of a timely nature, the end-to-end transmission delay becomes an important performance metric.

As shown in Fig. 1.3, the loss of a packet during data transmission period maybe result in a mischance, for instance, a grievous forest fire. Due to the fundamentality of reliability, we consider it in this thesis as a hard constraint. The use of acknowledged transmissions is to fulfill this constraint, at least from a theoretical point of view. The other two constraints, i.e., energy and latency, are considered as two competing objective functions that should be simultaneously minimized.

Therefore, WSNs are desired to be reliable, expandable, and easily implementable. They should also be able to collect information with low delay and have a long lifetime. Before we can achieve these goals, we must be able to address the research problems arising from the following three areas: firstly, we need to design sensitive and low cost sensors to collect information [1, 3]; secondly, from the data transmission viewpoint, we need to explore optimal algorithms to process and abstract the core intelligence from the raw data collected from all the nodes, i.e, data fusion, and we need to develop efficient

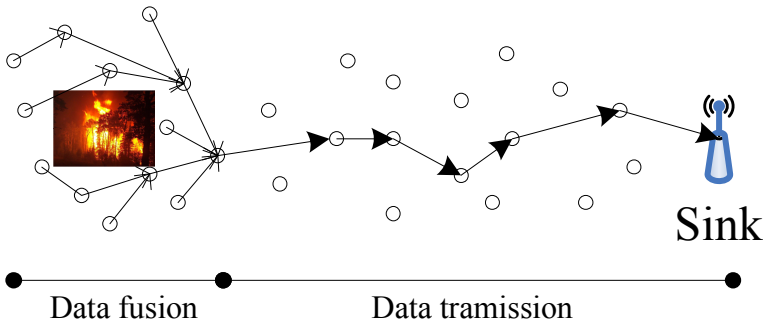

Figure 1.3: Data processes of wireless sensor networks

networking protocols and optimize all parameters in each layer to transmit information from the source nodes to a sink node efficiently as illustrated in Fig. 1.3. These three technology areas are not isolated from each other due to the interdisciplinary nature of sensor network design. For example, the types of sensors deployed will define the data rate generated at each node, which in turn defines the throughput required for the underlying wireless networks. The corresponding network protocols need to be designed to support this throughput under the system resource constraints. Given limited system resources, there is always data loss or delay introduced in the network. Therefore, the information processing algorithms at the fusion center need to be robust and adaptive to deal with the imperfections of the data network. Consequently, to achieve an optimal sensor network design, interdisciplinary work across the research sectors is needed. Numerous works, e.g., [42, 49, 81, 31] focus on data fusion phase, data will be aggregated to reduce the total energy consumption of a network and arrive at a node. In this thesis, the work is mainly focusing on efficient network designs during the data transmission phase. Extensions of this work to incorporate data processing and sensing will be described as future work in Chapter 8.

Protocol design based on layered structures provides reasonable performance in wired networks for the main following reasons: individual layer dynamics are limited given the closed communication media, and each layer can be over-designed to compensate for the dynamics of neighboring layers since system resources such as power and bandwidth are relative unconstrained. However, this is not the case for systems built on top of wireless channels, since wireless links exhibit large random dynamics due to multipath fading, Doppler shift, and interference that are inevitable in a wireless communication medium. In addition, wireless systems have more stringent resource constraints: bandwidth is expensive as companies must spend billions of dollars to acquire licensed spectrum; and power is limited, due to interference to other users and finite battery life. Therefore, we cannot afford to over-design each layer to deal with the dynamics in other layers. Moreover, as for WSNs, there are some special characteristics

such as: high node density, non-rechargeable battery. And a lot of MAC protocols, e.g., [24, 40, 80, 17] and routing protocols, e.g., [48, 84, 10, 52] were designed especially for WSNs.

Cross-layer design is a joint design optimization across all or several layers in the protocol stack under given resource constraints, and it overcomes the drawbacks of layered design to improve the network performance. Cross-layer design can include information exchange between different layers (not necessarily neighboring layers), adaptivity at each layer to this information, and diversity built into each layer to insure robustness [34]. Generally speaking, the link layer can employ adaptive parameters such as modulation and coding to exploit or compensate for the time-varying wireless channel. Then, this adaptivity at the link layer can be used by higher layers to achieve better performance: the MAC layer can assign a longer channel usage time to links with low-rate modulation schemes to meet the throughput constraint; the routing layer can reroute traffic to links supporting high-rate modulation schemes to minimize congestion; and the application layer can use multi-description codes to leverage the diversity of different routes. Significant performance gain can be achieved by these interactions between different layers [34]. Numerous attentions, e.g., [22, 58, 31, 21, 89, 77] are payed to cross layer design to maximize the performance of a network. More detailed technical surveys for cross-layer design will be given in the corresponding chapters.

However, All of the aforementioned works are based on the assumption of a disc link model or a switched link model under which the transmission between two nodes x and x' succeeds if and only if the signal to noise ratio (SNR) $\bar{\gamma}(x, x')$ at the receiver is above a minimal value $\bar{\gamma}_{min}$, i.e, BER is under a threshold value, for example, 10^{-5} in most of works. That means perfect reliable links are used for communication and all unreliable links are abandoned. In fact, experiments in different environments and theoretical analyzes in [29, 78, 88, 83, 91, 69, 57] have proved that unreliable links have a strong impact on the performance of upper layers such as MAC and routing layer. In our previous work [35], we have shown how unreliable link improve the connectivity of WSNs.

In this thesis, packet error rate (PER) is used to model the unreliability of wireless links. In Fig.1.4, the link probability is presented as an example in AWGN channel and Rayleigh block fading channel where all parameters are same for the transmitter and the receiver but the type of channel. By the link probability, we can divide the communication area into three zones: reliable link zone, unreliable link zone and no link zone. In reliable link zone, the link probability is almost equal to 1 and in no link zone, the link probability approximates 0. In unreliable link zone, the link probability drops form 1 to 0. It is obvious that the unreliable link zone is very small in AWGN channel but it expends greatly in Rayleigh block fading channel because of the introduction

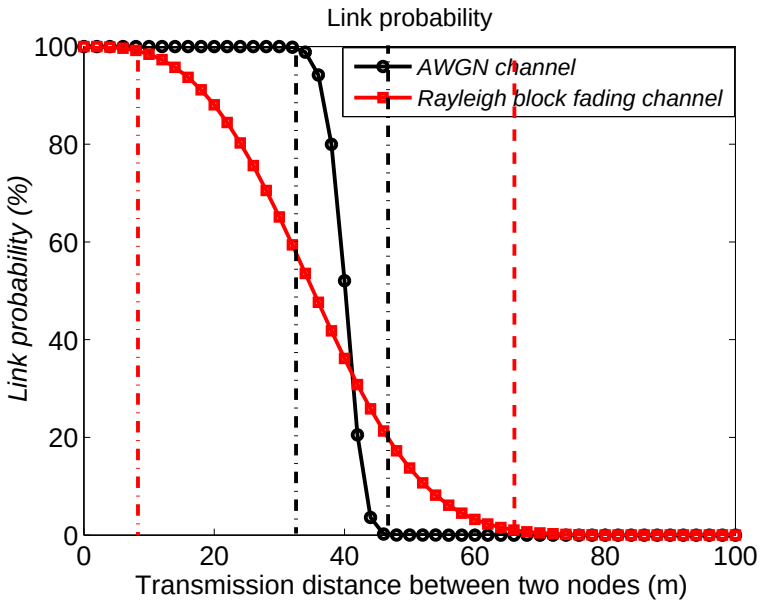

Figure 1.4: Link probability in different channels

of fading and the reliable link zone becomes very small. Then, if we abandon the unreliable zone in Rayleigh block fading channel, the communication area will shrink greatly and the resource including transmission energy, channel capacity and so on will be wasted. How to configure physical parameters of a network to make best use of unreliable links is the aim of this thesis.

Finally, in this thesis, the energy-delay performance and the optimization of cross-layer parameters of WSNs will be exploited by making best use of unreliable links in different scenarios.

1.3 Organization of thesis

This thesis is structured as follows. We start with a traditional multi-hop transmission scheme in chapter 2. We propose a metric for energy efficiency: mean energy distance ratio per bit ($\overline{EDRb}$), and a metric for mean delay: mean delay distance $\overline{DDR}$, which are combined with the unreliable link model and reveal the relationship between the energy consumption and delay of one hop and the transmission distance which contributes to determine optimal route at the routing layer. Using these two metrics and a realistic unreliable link model, the lower bounds of energy-delay trade-off and energy efficiency are obtained in AWGN, Rayleigh flat fading, Rayleigh block fading channels respectively for one-hop transmissions. Then, these results are extended to multi-hop transmissions and the close-form expression of energy-delay tradeoff is obtained.

These two lower bounds are then validated using the simulations in 2-dimension Poisson distributed networks. Theoretical analyses and simulations show that accounting for unreliable links contributes to improve the energy efficiency of the system under delay constraints, especially for Rayleigh flat fading and Rayleigh block fading channels. The close-form expression of energy-delay tradeoff provides a framework to evaluate the energy-delay performance of a network according to its parameters of the physical, MAC and Routing layers. Moreover, a cross-layer parameter optimization process is provided to configure physical parameters such as optimal transmission power, coding scheme, type and order of modulation, protocol parameters such as number of bits in a packet and network parameters: node density.

An important feature of wireless networks is the time varying channel caused by wireless channel propagation effects, mainly multi-path fading, which can result in large fluctuations in signal strength and therefore intermittent link behavior. In addition, the wireless medium is broadcast in nature. Opportunistic communications take advantage of these two properties of wireless links to improve the performance of a network. In Chapter 5 and 6, the energy-delay performance of opportunistic communications and related parameter optimization are analyzed. We firstly propose an analytical framework of energy efficiency of classical opportunistic communications in Chapter 5, which provides a method for optimizing the different opportunistic schemes. Meanwhile, the energy efficiency of opportunistic communications with respect to different forwarding areas is studied with regard to the optimal transmission power and the optimal node density in AWGN and Rayleigh block fading channels. The analyses show that opportunistic communications are more efficient in Rayleigh block fading channel than that in AWGN channel from an energy point of view. Further, the lower bound of energy-delay tradeoff in opportunistic communications are deduced in Chapter 6 considering the mechanism of selecting the optimal forwarding candidates. A close-form expression of the lower bound is obtained on the condition of a fixed number of forwarding candidates and an algorithm for searching the optimal number of forwarding candidates is proposed. According to the theoretical analyses, a new opportunistic scheme integrating MAC and Routing layers is proposed to minimize energy consumption satisfying a mean delay constraint. Simulations in a 2-dimension Poisson network using the proposed opportunistic scheme verify the theoretical lower bound of energy-delay tradeoff. Moreover, the optimization of physical parameters is analyzed.

In opportunistic communications, only the cooperation at the receiver side is utilized, while in cooperative communications, the cooperation at both receiver and transmitter sides is considered. In Chapter 7, cooperative communications are introduced by cooperative MIMO (CMIMO) scheme. Firstly, the lower bound of energy-delay tradeoff of CMIMO is analyzed by exploiting an unreliable link model when the number of

cooperative transmitters and receivers is fixed. Then, an algorithm for searching the optimal number of cooperative nodes at both two sides is introduced. Next, the effect of physical parameters on the lower bound is explained. Finally, the lower bounds of the above three communication schemes are compared in different channels respectively. The results show that in order to achieve better energy-delay performance, the corresponding communication scheme should be adopted for different channel type: traditional multi-hop communications for AWGN channel, opportunistic communications for Rayleigh block fading channel and CMIMO for Rayleigh flat fading channel.

In Chapter 8, the conclusions are drawn, and some possible extensions of the work covered in this thesis are discussed.

1.4 Contributions of thesis

The main contributions of this thesis are listed as follows:

In traditional multi-hop communication part:

- The close-form expressions of the optimal transmission range and the corresponding optimal transmission power are derived in AWGN channel, Rayleigh flat fading channel and Rayleigh block fading channel employing both a comprehensive energy model and an unreliable link model.
- The closed form expression of the lower bound of energy-delay trade-off for a linear and a Poisson network in the three types of channels aforementioned is obtained and validated by simulations in 2-dimension Poisson networks.
- The closed form expression of the lower bound of energy efficiency of a multi-hop communication and its corresponding maximum mean delay are obtained and validated by simulation in 2-dimension Poisson networks.
- A cross-layer parameter optimization process is proposed.

In opportunistic communication part:

- A more precise energy model for classical opportunistic communication is proposed, which integrates a realistic unreliable link model and the effect of acknowledgements and retransmissions. This proposed model enhances the precision by an exact integral computation instead of a simplified summation approximation.
- A general framework for evaluating the maximal efficiency of the opportunistic routing principle is provided. Energy and delay are compromised under an end-to-end reliability constraint.

- The lower bound of energy efficiency is derived and its corresponding maximal delay is obtained.
- The Pareto front of energy-delay trade-off is derived for different scenarios. A close-form expression of energy-latency tradeoff when the number of relay candidates is fixed, and an algorithm to find the optimal number of relay candidates is proposed. The simulation results verify this lower bound in a 2-dimension Poisson distributed network. The numerical analyses show that opportunistic routing is inefficient in Additive White Gaussian Noise (AWGN) channel, while efficient in Rayleigh block fading channel in the condition of a small cluster size.
- An opportunistic protocol is proposed to minimize energy consumption under a delay constraint.

In cooperative communication part:

- The lower bound of energy-delay tradeoff of CMIMO is obtained when the number of cooperative transmitters and receivers is fixed and an algorithm for searching the optimal number of cooperative nodes in both two sides is introduced.
- The lower bound of energy efficiency of CMIMO is obtained and the corresponding optimal parameters are deduced.
- A cross-layer framework to optimize the parameters at the physical and MAC layers in CMIMO scheme is introduced.
- The lower bounds of the above three communication schemes are compared in different channels respectively. The results show that in order to achieve better energy-delay performance, the corresponding communication scheme should be adopted for different channel type: traditional multi-hop communications for AWGN channel, opportunistic communications for Rayleigh block fading channel and CMIMO for Rayleigh flat fading channel.

Part I

Traditional multi-hop communications

2

Energy-Delay Tradeoff Analysis

2.1 Abstract

Wireless sensor networks (WSNs) have various application scenarios from health-care to military [47]. In these applications, lots of them have low data traffic compared with the capacity of networks such as forest fires surveillance, that is to say, the throughput is not a constraint for this kind of applications. There performance of WSNs is measured with respect to three criteria: the end-to-end reliability, the end-to-end delay (refereed to latency in the following) and the energy consumption are crucial requirements for this type of applications [13]. Due to the fundamentality of reliability, we consider it in this thesis as a hard constraint, and acknowledged transmissions is to used to fulfill this constraint, at least from a theoretical point of view. The other two constraints, i.e., energy and delay, are considered as two competing objective functions that should be simultaneously minimized.

In this chapter, we will explore the Pareto front of energy-delay trade-off while adopting a very generic network layer/routing model for low-traffic applications. This Pareto front can serve as a benchmark for preliminary performance evaluation and is suitable in the early phases of network planning and design to optimize physical parameters. To find this bound, a comprehensive energy model is used which includes energy consumption for both data packet and control packet. Meanwhile, a realistic unreliable link model is introduced into the energy model by the metric, mean energy distance ratio, $\overline{EDRb}$. We focus on two factors which are tightly related energy efficient

and latency performance: mean hop length and transmission power.

2.2 State of the art

Routing protocols have a significant impact on energy efficiency and latency performances and choosing an efficient routing scheme is a multi-objective optimization problem [43]. Long-hop routes demand substantial transmission power but minimize the energy cost for reception, computation and etc, meanwhile, decrease the number of hops, i.e, reduce the end to end delay. On the opposite, routes made of shorter hops use fewer transmission power but maximize the energy cost for reception since there is an increase in the number of hops which means more delay. M. Haenggi points out several advantages of using long-hop routing in [38, 39], among which high energy efficiency is one of the most important factors. These works reveal the importance of the transmission range and its impact on the energy conservation but don't provide a theoretical analysis on the optimal hop length regarding various networking scenarios.

Some works analyze the optimal transmission range from the viewpoint of physical layer. [14] defines the optimal one-hop length for multi-hop communications that minimizes the total energy consumption and analyzes the influence of channel parameters on this optimal transmission range in a linear network. The same issue is studied in [30] with a *Bit-Meter-per-Joule* metric where the authors study the effects of the network topology, the node density and the transceiver characteristics on the overall energy expenditure. This work is improved by [25] which showed the effects of network parameters such as node density, network radius on the optimal transmission range and the impacts of the path loss exponent in a 2-dimension Poisson network. [22] solve a cross-layer optimization problem to minimize the energy consumption and delay for a TDMA based small-scale sensor networks. However, all of the aforementioned works are based on the assumption of a disc link model as described in Chapter 1.

Recently, unreliable links are taken into account in the routing scheme design by introducing a link probability and the effect of link error rate, e.g., in [8, 46]. In [8], the authors derive the minimum energy paths for a given pair of source and destination nodes and propose the corresponding routing algorithm. However, the energy model used in this thesis includes the transmission power only and does not consider circuitry energy consumption at the transmitter and receiver side. In fact, such a model leads to an unrealistic conclusion which states that the smaller hop distance, the higher energy efficiency. As we show in this thesis, considering a constant circuitry power according to [47] results in completely different conclusions. In [46], a routing scheme is proposed whose metric for the relay selection is $PRR \times distance$, where PRR is short for Packet Reception Ratio. This routing scheme makes best use of unreliable links to improve the energy efficiency.

These efforts are devoted to the various low-energy routing scheme design while keeping non-protocol system parameters fixed such as the transmission power, transceiver power characteristics, node density and etc. However, very few works address the relationship between the network performance and the network parameters, in other words, the best networks performance that could be obtained by setting all parameters of physical layer, MAC layer and routing layer in a network as a whole.

In this chapter, we will explore the Pareto front of energy-latency trade-off while adopting a very generic network layer/routing model for low-traffic applications. This Pareto front can serve as a benchmark for preliminary performance evaluation and is suitable in the early phases of network planning and design to optimize physical parameters. To find this bound, a comprehensive energy model is used which includes energy consumption for both data packet and control packet. Meanwhile a realistic unreliable link model is introduced into the energy model by the metric, mean energy distance ratio, $\overline{EDRb}$. We focus on two factors which are tightly related energy efficient and latency performance: mean hop length and transmission power.

The contributions of this chapter are:

- The closed form expression of the lower bound of energy-delay trade-off for a linear and a Poisson network is achieved in AWGN, Rayleigh flat fading and Rayleigh block fading channels employing both a comprehensive energy model and an unreliable link model.

- The close-form expressions of the optimal transmission range and for the corresponding optimal transmission power are derived in three types of channel aforementioned .

- The closed form expression of the lower bound of energy efficiency of a multi-hop communication and its corresponding maximum mean delay are obtained.

The rest of this chapter is organized as follows: Section 2.3 concentrates on presenting the models and metrics used in the chapter. Next, two scenarios are considered: minimizing the energy consumption with and without delay constraint. Section 2.4 focuses on the optimal trade-off between the energy consumption and the delay in linear networks. we derive the lower bound of energy-delay tradeoff and a closed form expression of optimal transmission range and optimal transmission power with mean delay request. In Section 2.5 the close-form expression of the lower bound in three kinds of channel is provided. Finally, section 2.6 concludes our work and explains the applications of the all theoretical analyses.

2.3 Models and metrics

In this section, the energy model, the realistic unreliable link model, the delay model and the metric $\overline{EDRb}$ and $\overline{DDR}$ in traditional multi-hop communications are introduced.

2.3.1 Energy consumption model

In this chapter, we do not consider any specific protocol and assume the corresponding overhead to be negligible. We consider energy efficient nodes, i.e., nodes that only listen to the packets intended to themselves and that send an acknowledgment packet (ACK) to the source node after a correct packet reception. As such, the energy consumption for transmission of one packet E_p is composed of three parts: the energy consumed by the transmitter E_{Tx}, by the receiver E_{Rx} and by the acknowledgement packet exchange E_{ACK}:

$$E_p = E_{Tx} + E_{Rx} + E_{ACK}. \tag{2.1}$$

The energy model for transmitters and receivers [47] are given respectively by:

$$E_{Tx} = T_{start} \cdot P_{start} + \frac{N_{head} + N_b}{R_b R_{code}} \cdot (P_{txElec} + \beta_{amp} \cdot P_t), \tag{2.2}$$

and

$$E_{Rx} = T_{start} \cdot P_{start} + \frac{N_{head} + N_b}{R_b R_{code}} \cdot P_{rxElec}, \tag{2.3}$$

where P_t is transmission power, N_{head} is the number of bit in the overhead of a packet for the synchronization of physical layer, R_{code} is the code rate. The other parameters are described in Table 2.1.

The energy expenditure model of acknowledgment is given by:

$$E_{ACK} = \tau_{ack} \cdot (E_{Tx} + E_{Rx}), \tag{2.4}$$

where

$$\tau_{ack} = \frac{N_{ack} + N_{head}}{N_b + N_{head}} \tag{2.5}$$

is the ratio between the length of a ACK packet and that of a DATA packet.

The analysis of E_p shows that the energy consumption can be classified into two parts: the first part is constant, including $T_{start} \cdot P_{start}$, P_{txElec} and P_{rxElec}, which are constant and independent of the transmission range; the second part is variable and depends on the transmission energy P_t which is tightly related to the transmission

Table 2.1: Some parameters of the transceiver energy consumption referring to [4]

Symbol	Description	Value
α	Path-loss exponent (≥ 2)	3
β_{amp}	Amplifier proportional offset (> 1)	14.0
τ_{ack}	ACK Ratio	0.08125
B	Bandwidth of channel	250 $Kbps$
f_c	Carrier frequency	$2.4GHz$
G_{Tant}	Transmitter antenna gain	1
G_{Rant}	Receiver antenna gain	1
L	Circuitry loss (≥ 1)	1
N_b	Number of bits per packet	2560
N_{head}	Number of bits of overhead in a packet	0
N_0	Noise level	-150 dBm/Hz
P_{start}	Startup power	38.7 mW
P_{txElec}	Transmitter circuitry power	59.1 mW
P_{rxElec}	Receiver circuitry power	59.1 mW
R_b	Transmission bit rate	250 $Kbps$
T_{start}	Startup time	0 μs
T_{ACK}	ACK duration	1 mS

range. Accordingly, the energy model for each bit follows:

$$E_b = \frac{E_p}{N_b} = E_c + K_1 \cdot P_t, \tag{2.6}$$

where E_b, E_c and $K_1 \cdot P_t$ are respectively the total, the constant and the variable energy consumption per bit. Substituting (2.1), (2.2), (2.3) and (2.4) into (2.6) yields:

$$E_c = (1+\tau_{ack})\left(\frac{2T_{start} \cdot P_{start}}{N_b} + (1+\tau_{head})\frac{P_{txElec}+P_{rxElec}}{R_b R_{code}}\right) \tag{2.7}$$

$$K_1 = (1+\tau_{ack})(1+\tau_{head})\frac{\beta_{amp}}{R_b R_{code}}, \tag{2.8}$$

where

$$\tau_{head} = \frac{N_{head}}{N_b} \tag{2.9}$$

.

2.3.2 Realistic unreliable link model

The unreliable radio link model is defined using the packet error rate (PER) [35]:

$$pl(\gamma_{x,x'}) = 1 - \mathrm{PER}(\gamma_{x,x'}) \tag{2.10}$$

where PER(γ) is the PER obtained from a signal to noise ratio (SNR) γ. The PER depends on the transmission chain technology (modulation, coding, diversity ...). And $\gamma_{x,x'}$ is defined as usually [47]:

$$\gamma_{x,x'} = K_2 \cdot P_t \cdot d_{hop}^{-\alpha}, \tag{2.11}$$

with

$$K_2 = \frac{G_{Tant} \cdot G_{Rant} \cdot \lambda^2}{(4\pi)^2 N_0 \cdot R_s \cdot L}, \tag{2.12}$$

where d_{hop} is the distance between node x and x', λ is the wavelength, R_s is the symbol rate, and other parameters are presented in Table 2.1. Note that $R_b = R_s \cdot b$ where b is the order of modulation.

The function of PER varies with the type of channel. Here, we give the close-from expression of link probability in AWGN, Rayleigh flat fading and Rayleigh block fading channel.

AWGN

In AWGN channel, the PER is:

$$PER_g(\gamma) = 1 - (1 - \text{BER}(\gamma))^{N_b}, \tag{2.13}$$

where BER(γ) is the Bit Error Rate (BER). In [34], the expression of BER is approximated in high SNR by:

$$\text{BER}_g(\gamma) = \alpha_m Q(\sqrt{\beta_m \gamma}), \tag{2.14}$$

where $Q(\cdot)$ represents the Q function, α_m and β_m rely on the modulation type and order, e.g., for Multiple Quadrature Amplitude Modulation (MQAM) $\alpha_m = 4(1 - 1/\sqrt{M})/\log_2(M)$ and $\beta_m = 3\log_2(M)/(M-1)$. For BPSK, $\alpha_m = 1$ and $\beta_m = 2$.

Substituting (2.13) into (2.10), we have the link probability in AWGN channel:

$$pl_g(\gamma) = (1 - \alpha_m Q(\sqrt{\beta_m \gamma}))^{N_b}, \tag{2.15}$$

Rayleigh flat fading channel

In Rayleigh flat fading channel, the PER is:

$$PER_f(\bar{\gamma}) = 1 - (1 - \text{BER}(\bar{\gamma}))^{N_b} \text{ with } BER(\bar{\gamma}) = \int_{\gamma=0}^{\infty} BER(\gamma) p(\gamma|\bar{\gamma}) d\gamma, \tag{2.16}$$

where $p(\gamma|\bar{\gamma}) = \exp(-\gamma/\bar{\gamma})/\bar{\gamma}$. A general expression of BER in Rayleigh flat fading channel is provided in [34] in case of $\bar{\gamma} \geq 5$, it is:

$$\mathrm{BER}_f(\bar{\gamma}) \approx \frac{\alpha_m}{2\beta_m\bar{\gamma}}, \tag{2.17}$$

where α_m and β_m are the same as those in (2.14).

Substituting (2.16) into (2.10), we have the link probability in this kind of channel:

$$pl_f(\bar{\gamma}) = \left(1 - \frac{\alpha_m}{2\beta_m\bar{\gamma}}\right)^{N_b}, \tag{2.18}$$

Block fading channel

In block fading channel, the fading state is assumed constant for all bits in a block. In [35], the exact link model in Nakagami-m block fading channel is introduced as:

$$pl(\bar{\gamma}) = \int_{\gamma=0}^{\infty} (1 - \mathrm{BER}(\gamma))^{N_b} p(\gamma|\bar{\gamma}) d\gamma \tag{2.19}$$
$$\text{with } p(\gamma|\bar{\gamma}) = \frac{m^m \gamma^{m-1}}{\bar{\gamma}\Gamma(m)} \exp\left(-\frac{m\gamma}{\bar{\gamma}}\right),$$

where $\mathrm{BER}(\gamma)$ refers to (2.14), m presents the strength of fading in Nakagami-m fading model [62]. When $m = 1$, a Nakagami-m block fading channel become a Rayleigh block fading channel. It should be noted that the average PER ensures that errors in several packets are not correlated, i.e., fading state is independent between successive packets.

2.3.3 Reliable transmission

Because of the unreliability of each transmission, retransmissions and acknowledgement mechanism are adopted in this thesis to ensure a reliable transmission. Here, $\overline{N}_{tx}$ is the average number of transmissions needed to ensure a successful reception computed by:

$$\begin{aligned} \overline{N}_{tx} &= \sum_{n=1}^{\infty} n \cdot pl_{data} \cdot pl_{ack} \cdot (1 - pl_{data} \cdot pl_{ack})^{(n-1)} \\ &= \frac{1}{pl_{data} \cdot pl_{ack}}, \end{aligned} \tag{2.20}$$

where n is the number of transmissions, pl_{data} and pl_{ack} are the link probability of DATA packet and ACK packet respectively.

In the acknowledgment process, it is assumed that an ACK packet can be successfully transmitted in a single attempt which is based on the following facts: firstly, since ACK packets are much smaller data packets, their link probability is greater than that

of data packet. For instance, for respectively ACK and Data packets of 26 and 320 bytes each, if the successful transmission probability of the data packet is 80%, the link probability of the ACK packet is 98%; secondly, because of channel correlation as shown in experiments in [12], if the data packet experienced a good channel, the return path experiences the same beneficial channel conditions. Hence, we can assume that $pl_{ack} \approx 1$, in other words, only one ACK packet is sent with high probability of success to the source of the message. Therefore, $\overline{N}_{tx}$ can be approximated by:

$$\overline{N}_{tx} \approx \frac{1}{pl(d_{hop}, P_t)}, \tag{2.21}$$

where $pl(d_{hop}, P_t)$ replaces for $pl_{data}(d_{hop}, P_t)$ because of simplification.

2.3.4 Mean energy distance ratio per bit ($\overline{EDRb}$)

Depending on the application, the energy efficiency has a different significance [47]. A periodic monitoring application is assumed here, so that the energy spent per correctly received bit is a crucial energy metric. Moreover, in wireless communications, the energy cost augments with the increase of the transmission distance. Hence, we also adopt the mean Energy Distance Ratio per bit ($\overline{EDRb}$) metric in $J/m/bit$ proposed in [30] which is defined as the energy consumption for transmitting one bit over one meter. This criterion allows to compare different transmission strategies, with different hop lengths.

The mean energy consumption per bit for the successful transmission over one hop E_{1hop} including the energy needed for retransmissions is given by $E_{1hop} = E_b(P_t) \cdot \overline{N}_{tx}$,

According to the definition, $\overline{EDRb}$ is formulated as:

$$\overline{EDRb} = \frac{\overline{E}_{1hop}}{d_{hop}} = \frac{E_b}{d \cdot pl} = \frac{E_c + K_1 \cdot P_t}{d_{hop} \cdot pl}. \tag{2.22}$$

2.3.5 mean Delay Distance Ratio ($\overline{DDR}$)

The delay of a packet to be transmitted over one hop, D_{hop}, is defined as the sum of three delay components:

$$D_{hop} = T_{queue} + T_{tx} + T_{ACK}. \tag{2.23}$$

The first component is the queuing delay during which a packet waits for being transmitted, T_{queue}. The second component, T_{tx}, is the transmission delay that is equal to $T_{tx} = \frac{N_b + N_{head}}{R_b R_{code}}$. The third component is $T_{ACK} = \tau_{ack} \cdot T_{tx}$. Note that we neglect the propagation delay because the transmission distance between two nodes is usually short in multi-hop networks.

Furthermore, a reliable one-hop transmission will suffer from the delay caused by retransmissions. According to (2.21), the mean delay of a reliable one-hop transmission is:

$$\overline{D}_{hop} = D_{hop}\overline{N}_{tx}. \tag{2.24}$$

Since delay raises with the increase of the distance between the source node and the destination node, we propose a new delay metric Delay Distance Ratio ($\overline{DDR}$) which is defined as:

$$\overline{DDR} = \frac{D_{hop}\overline{N}_{tx}}{d_{hop}} = \frac{D_{hop}}{d_{hop} \cdot pl}, \tag{2.25}$$

2.4 Energy-delay trade-off

A trade-off between energy and delay exists. For instance, when considering a long range transmission, a direct single-hop transmission needs a lot of energy but yields a shorter delay while a multi-hop transmission uses less energy but suffers from an extended delay as we will show in Fig. 2.3. This section concentrates on the analysis of the energy-delay trade-off of multi-hop transmissions.

2.4.1 On the optimality of a uniform repartition

The lower bound of energy-delay trade-off can be abstracted as an optimization problem:

$$\text{minimize}: \ \overline{E}_{tot} \quad \text{subject to}: \ \overline{D}_{tot} = \text{delay constraint}, \tag{2.26}$$

where $\overline{E}_{tot}$ and $\overline{D}_{tot}$ are the end to end energy consumption and delay between the source and destination nodes. To solve this optimization problem, two related theorems about energy and delay are introduced firstly:

Theorem 1. *In a homogeneous linear network, a source node x sends a packet of N_b bits to a destination node x' using n hops. The distance between x and x' is d, and the path-loss exponent is greater than 2, $\alpha > 2$. The length of each hop is d_1, d_2, $\ldots$, d_n respectively and the average EDRb of each hop is denoted as $\overline{EDRb}(d_i)$ where $i = 1, \cdots, n$. The minimum mean total energy consumption $\overline{Etot}_{min}$ is obtained if and only if $d_1 = d_2 = \ldots = d_n$:*

$$\overline{E}tot_{min} = N_b \cdot \overline{EDRb}(d/n) \cdot d. \tag{2.27}$$

Proof. The average energy consumption for each hop of index m is set to $\overline{E}_m = N_b \cdot \overline{EDRb}(d_m) \cdot d_m$, $m = 1, 2, \ldots, n$. Since each hop is independent from the other hops, the mean total energy consumption is $\overline{Etot} = \overline{E}_1 + \overline{E}_2 + \ldots + \overline{E}_n$. Hence, the problem

of finding the minimum mean total energy consumption can be rewritten as:

$$\begin{array}{ll} \text{minimize} & \overline{Etot} \\ \text{subject to} & d_1 + d_2 + \ldots + d_n = d. \end{array}$$

Set

$$F = \overline{E}_1 + \overline{E}_2 + \ldots + \overline{E}_n + \lambda(d_1 + d_2 + \ldots + d_n - d),$$

where $\lambda \neq 0$ is the Lagrange multiplier.

According to the method of the Lagrange multipliers, we obtain:

$$\begin{cases} \dfrac{\partial \overline{E_1}}{\partial d_1} + \lambda = 0 \\ \dfrac{\partial \overline{E_2}}{\partial d_2} + \lambda = 0 \\ \ldots \\ \dfrac{\partial \overline{E_n}}{\partial d_n} + \lambda = 0 \\ d_1 + d_2 + \ldots + d_n = d \end{cases} \tag{2.28}$$

(2.28) shows that the minimum value of F is obtained in the case: $\frac{\partial \overline{E_1}}{\partial d_1} = \frac{\partial \overline{E_2}}{\partial d_2} = \ldots = \frac{\partial \overline{E_n}}{\partial d_n} = -\lambda$. Moreover, in a homogeneous linear network, the properties of each node are identical. Therefore,

$$\frac{\partial \overline{E_m}}{\partial d_m} = \left.\frac{\partial \overline{E}}{\partial d}\right|_{d=d_m}$$

where $m = 1, 2, \ldots, n$. Because $\frac{\partial \overline{E}}{\partial d}$ is a monotonic increasing function of d when the path-loss exponent follows $\alpha \geq 2$, the unique solution of (2.28) is $d_1 = d_2 = \ldots = d_n = \frac{d}{n}$. Finally, we obtain: $\overline{Etot}_{min} = N_b \cdot \overline{EDRb}(d/n) \cdot d$. This theorem is valid if and only if $\frac{\partial \overline{E}}{\partial d}$ is a monotonic increasing function of d which holds with the attenuation model in (2.11) having $\alpha \geq 2$ in many practical scenarios. ■

Theorem 2. *In a homogeneous linear network, a source node x sends a packet of N_b bits to a destination node x' using n hops. The distance between x and x' is d. The length of each hop is d_1, d_2, ..., d_n respectively and the mean hop delay per meter is referred to as $\overline{DDR}(d_i)$ where $i = 1, \cdots, n$. The minimum mean end to end delay $\overline{Dtot}_{min}$ is given, if and only if $d_1 = d_2 = \ldots = d_n$, by:*

$$\overline{Dtot}_{min} = \overline{DDR}(d/n) \cdot d. \tag{2.29}$$

Proof. The mean delay of each hop is defined by $\overline{D}_m$, $m = 1, 2, \ldots, n$. Since each hop is independent of the other hops, the mean end to end delay is obtained by:

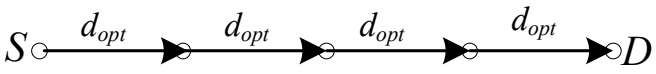

Figure 2.1: Equivalent hop distance transmission

$\overline{Dtot} = \overline{D}_1 + \overline{D}_2 + \ldots + \overline{D}_n$. Hence, the problem can be rewritten as:

$$\text{minimize } \overline{Dtot}, \text{ subject to: } d_1 + d_2 + \ldots + d_n = d.$$

We set

$$F = \overline{D}_1 + \overline{D}_2 + \ldots + \overline{D}_n + \lambda(d_1 + d_2 + \ldots + d_n - d),$$

where $\lambda \neq 0$ is the Lagrange multiplier. According to the method of the Lagrange multipliers, we obtain:

$$\begin{cases} \dfrac{\partial \overline{D_1}}{\partial d_1} + \lambda = 0 \\ \dfrac{\partial \overline{D_2}}{\partial d_2} + \lambda = 0 \\ \ldots \\ \dfrac{\partial \overline{D_n}}{\partial d_n} + \lambda = 0 \\ d_1 + d_2 + \ldots + d_n = d. \end{cases} \tag{2.30}$$

(2.30) shows that the minimum value of F is obtained in the case: $\frac{\partial \overline{D_1}}{\partial d_1} = \frac{\partial \overline{D_2}}{\partial d_2} = \ldots = \frac{\partial \overline{D_n}}{\partial d_n} = -\lambda$. Moreover, in a homogeneous network the properties of each node are identical. Therefore,

$$\frac{\partial \overline{D_m}}{\partial d_m} = \frac{\partial \overline{D}}{\partial d}\Big|_{d=d_m}$$

where $m = 1, 2, \ldots, n$. Because $\frac{\partial \overline{D}}{\partial d}$ is a monotonic increasing function of d when the path-loss exponent follows $\alpha \geq 2$, the unique solution of (2.30) is $d_1 = d_2 = \ldots = d_n = \frac{d}{n}$. Finally, we obtain: $\overline{Dtot}_{min} = \overline{D}(d/n) \cdot n$. ■

Based on Theorem 1 and 2, we conclude that, regarding a pair of source and destination nodes with a given number of hops, the single scenario which minimizes both mean energy consumption and mean transmission delay, corresponds to each hop with uniform distance along a linear path as shown in Fig. 2.1. As a result, the optimization about energy and delay for a single hop will bring the optimization of the same performance for the multi-hop transmission. Hence, the optimization problem (2.26) can be converted to:

$$\text{minimize}: \ \overline{EDRb}(d, P_t) \quad \text{subject to}: \ \overline{DDR}(d, P_t) = ddr, \tag{2.31}$$

where ddr is a delay constraint. Consequently, minimizing energy and delay in a multi-hop transmission can be achieved by finding the best couple of parameters $(d_{opt},\ P_{opt})$ for one-hop transmission, where d_{opt} is the optimal hop distance and P_{opt} is the optimal transmission power.

2.4.2 Delay constrained optimization

To solve (2.31), we use the definition of γ (2.11) and the the link probability (2.10) inside the definition of $\overline{EDRb}$ (2.22) and $\overline{DDR}$ (2.25) leading to:

$$\overline{EDRb}(\gamma, P_t) = \frac{E_c + K_1 P_t}{(K_2 P_t)^{\frac{1}{\alpha}}} \cdot g(\gamma) \tag{2.32}$$

$$\overline{DDR}(\gamma, P_t) = \frac{D_{hop}}{(K_2 P_t)^{\frac{1}{\alpha}}} \cdot g(\gamma) \tag{2.33}$$

where $g(\gamma) = \frac{\gamma^{\frac{1}{\alpha}}}{pl(\gamma)}$.

Note that the initial variables of our optimization problem $(d,\ P_t)$ have been replaced by γ, P_t since γ_{opt} is directly related to d and P_t according to (2.11).

Theorem 3. *The optimal $\overline{EDRb}$ under a given delay constraint $\overline{DDR}(\gamma, P_t) = ddr$ is obtained when*

$$\gamma_{opt} = \arg\min_{\gamma} g(\gamma).$$

Proof. Without loss of generality, let us introduce a new function $v = \frac{1}{(K_2 P_t)^{\frac{1}{\alpha}}}$ and let $\hat{g}$ the minimum value of $g(\gamma)$ and $D_{hop} = 1$, then (2.32) and (2.33) are rewritten as:

$$\overline{EDRb}_{opt} = \hat{g} \cdot f(v) \tag{2.34}$$

$$\overline{DDR}_{opt} = \hat{g} \cdot v, \tag{2.35}$$

where $f(v) = E_c v + \frac{K_1}{K_2} v^{1-\alpha}$.

If (2.34) and (2.35) are not the equations providing the lower bound of energy-delay trade-off, then we assume that there exists another value of $g(\gamma)$, $g' = \varepsilon \cdot \hat{g}$ $(\varepsilon > 1)$ by which the lower bound of energy-delay trade-off can be obtained:

$$\overline{EDRb}'_{opt} = \varepsilon \cdot \hat{g} \cdot f(v') \tag{2.36}$$

$$\overline{DDR}'_{opt} = \varepsilon \cdot \hat{g} \cdot v' \quad \text{with} \quad \varepsilon > 1 \tag{2.37}$$

Notice that, according to this assumption, we can deduce that $\overline{EDRb}'_{opt} < EDRb_{opt}$ when $\overline{DDR}'_{opt} = \overline{DDR}_{opt}$.

Considering $\overline{DDR}'_{opt} = \overline{DDR}_{opt}$, we have:

$$v' = \frac{v}{\varepsilon}. \tag{2.38}$$

Substituting (2.38) into (2.36) yields:

$$\overline{EDRb}'_{opt} = E_c \cdot v + \frac{K_1}{K_2} \cdot v^{1-\alpha} \cdot \varepsilon^{\alpha} > E_c \cdot v + \frac{K_1}{K_2} \cdot v^{1-\alpha} = \overline{EDRb}_{opt} \text{ when } \varepsilon > 1. \tag{2.39}$$

Therefore, this assumption leads to a contradiction. Finally, we can conclude that (2.33) and (2.32) present a parametric equation of the lower bound of energy-delay trade-off when the minimum value of $g(\gamma)$ is available. ■

Theorem 3 provides an interesting result that achieving Pareto front is constrained by a constant SNR γ_{opt} which is subject to a joint selection (P_{opt}, d_{opt}).

When a delay constraint ddr is set, according to (2.33), the optimal transmission power satisfying this delay constraint, P_{opt}, is calculated by:

$$P_{opt} = \frac{1}{K_2} \left(\frac{g(\gamma_{opt}) \cdot D_{hop}}{ddr} \right)^{\alpha}. \tag{2.40}$$

It is obvious that the optimal transmission power is a monotonic decreasing function with respect to ddr.

Furthermore, when P_{opt} and γ_{opt} are known, the corresponding optimal transmission distance, d_{opt}, is obtained according to (2.11), as follows:

$$d_{opt} = \left(\frac{K_2 P_{opt}}{\gamma_{opt}} \right)^{\frac{1}{\alpha}} = \frac{g(\gamma_{opt}) \cdot D_{hop}}{\gamma_{opt}^{1/\alpha} \cdot ddr}. \tag{2.41}$$

On the basis of Theorem 3, we can obtain the lower bound of energy-delay trade-off when we minimize $g(\gamma)$. Therefore, substituting (2.40) into (2.32), the lower bound of energy-delay trade-off is:

$$\overline{EDRb}_{opt} = E_c \cdot \frac{ddr}{D_{hop}} + g(\gamma_{opt})^{\alpha} \cdot \frac{K_1}{K_2} \cdot \left(\frac{ddr}{D_{hop}} \right)^{1-\alpha}. \tag{2.42}$$

2.4.3 Pareto front of energy-delay tradeoff

In the previous subsection, the lower bound of energy-delay tradeoff (2.42) is derived. Obviously, (2.42) is composed of two components with respect to ddr. Therefore, it can be deduced easily that $\overline{EDRb}_{opt}$ is a convex function with respect to ddr when $g(\gamma_{opt})$ is given, and a lowest point is existed as shown in Fig. 2.2. The curve at left side of the lowest point is exactly the Pareto front of energy-delay tradeoff, this is to say, the

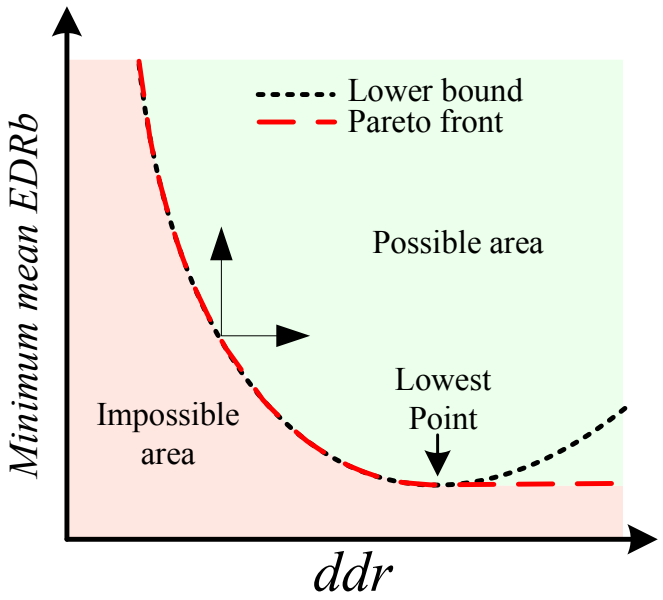

Figure 2.2: Lower bound and Pareto front of energy-delay tradeoff

Pareto front is a subset of the lower bound of energy-delay tradeoff.

Pareto front separates the ddr-$\overline{EDRb}$ area into two parts: Feasible area (green area in Fig. 2.2) and impossible area (red area in Fig. 2.2).

Hence, in order to obtain the Pareto front of energy-delay tradeoff, we need not only the lower bound of energy-delay tradeoff but also the lowest point in the lower bound , i.e., the minimum $\overline{EDRb}$: $\overline{EDRb}_{min}$, and its corresponding ddr, ddr_{max}. Following, we analyze the lowest point.

2.4.4 Minimal energy point

It should be note that the $\overline{EDRb}$ and ddr that correspond to the lowest point exits in the lower bound of energy-delay trade-off are the lower bound of energy efficiency, $\overline{EDRb}_{min}$ and the max delay, ddr_{max}, respectively. In this subsection, as to the lowest point, we derive $\overline{EDRb}_{min}$, ddr_{max} and the corresponding energy-optimal transmission power and distance without the delay constraints to optimize these parameters.

Through Lagrange method, letting $\frac{\partial \overline{EDRb}_{opt}}{\partial ddr} = 0$, we obtain:

$$ddr_{max} = g(\gamma_{opt}) \cdot D_{hop} \cdot \left(\frac{K_1(\alpha-1)}{E_c \cdot K_2}\right)^{\frac{1}{\alpha}} \tag{2.43}$$

and

$$\overline{EDRb}_{min} = g(\gamma_{opt}) \cdot \frac{E_c \cdot \alpha}{\alpha - 1} \cdot \left(\frac{K_1(\alpha-1)}{E_c \cdot K_2}\right)^{\frac{1}{\alpha}}. \tag{2.44}$$

Note that $\overline{EDRb}_{min}$ provide the lower bound of energy efficiency of a system.

Energy-optimal transmission power P_0

In order to get the minimum value of $\overline{EDRb}$, it is obvious that we should minimize $g(\gamma)$ and $f(P_t) = \frac{E_c + K_1 P_t}{(K_2 P_t)^{\frac{1}{\alpha}}}$ at the same time according to (2.32).

Letting $\gamma = \gamma_{opt}$, we have the minimum value of $g(\gamma)$. Then, employing Lagrange algorithm, we have:

$$\frac{d}{dP_t}\left(\frac{E_c + K_1 P_t}{(K_2 P_t)^{\frac{1}{\alpha}}}\right) = 0. \tag{2.45}$$

Solving the above equation yields:

$$P_0 = \frac{E_c}{K_1(\alpha - 1)}, \tag{2.46}$$

which is the transmission power minimizing $f(P_t)$.

Substituting (2.7) and (2.8) into (2.46) yields:

$$P_0 = \frac{P_{start}}{\beta_{amp}(\alpha - 1)} \cdot \frac{2T_{start}}{\frac{N_b + N_{head}}{R_b R_{code}}} + \frac{P_{txElec} + P_{rxElec}}{\beta_{amp}(\alpha - 1)} \tag{2.47}$$

where $\frac{N_b + N_{head}}{R_b R_{code}}$ is the transmission duration of a packet. Since $\frac{N_b + N_{head}}{R_b R_{code}} \gg T_{start}$ generally, the first part of (2.47) can be neglected. Thus, we get:

$$P_0 \approx \frac{P_{txElec} + P_{rxElec}}{\beta_{amp}(\alpha - 1)}. \tag{2.48}$$

In (2.47), it should be noted that P_0 is independent of $p_l(\gamma)$ and consequently independent of modulation and the type of channel. Based on this result, we can set the transmission power of a node according to (2.48) to minimize the total energy consumption for the applications without delay request. Moreover, P_0 provides a threshold of transmission power under which a node will be running in an inefficient stat such as the right side curve of the lowest point as shown in Fig. 2.3, Fig. 2.4 and Fig. 2.3.

(2.48) shows that the characteristics of the amplifier have a strong impact on P_0. When the efficiency of the amplifier is high, i.e., $\beta_{amp} \to 1$, P_0 reaches its maximum value. It coincides with the result of [36]. Moreover, it is clear that when the environment of transmission deteriorates, namely, α increases, P_0 decreases correspondingly.

Energy-optimal transmission range d_0

When P_0 and γ_{opt} are given, the corresponding transmission distance, d_0, may be calculated according to (2.11), as follows:

$$d_0 = \left(\frac{K_2 P_0}{\gamma_{opt}}\right)^{\frac{1}{\alpha}} = \left(\frac{K_2 E_c}{K_1 \cdot \gamma_{opt} \cdot (\alpha - 1)}\right)^{\frac{1}{\alpha}} \tag{2.49}$$

Consequently, when $g(\gamma_{opt})$ is obtained, the Pareto front energy-delay tradeoff, the lower bound of energy-delay tradeoff and the lower bound of energy efficiency are achieved at the same time.

γ_{opt} and $g(\gamma_{opt})$ are available by solving $\frac{\partial g(\gamma)}{\partial \gamma} = 0$. Thus, we get:

$$\gamma_{opt} = \frac{pl(\gamma_{opt})}{\alpha \cdot pl'(\gamma_{opt})} \tag{2.50}$$

where $pl'(\cdot)$ is the first derivation of $pl(\cdot)$. (2.50) shows that γ_{opt} and $g(\gamma_{opt})$ depend on the kind of channel. In Section 2.5, the lower bound of energy-delay tradeoff in different channels is presented.

2.5 Application to specific channels

In this section, the lower bound of energy-delay trade-off is analyzed in AWGN, Rayleigh flat fading and Rayleigh block fading channel and a general solution is given for all other scenarios.

2.5.1 AWGN

Using (2.15) and (2.50), we derive:

$$\gamma_{optg} = \frac{-1 - \alpha N_b \mathrm{W}_{-1}\left[\frac{-\exp(\frac{-1}{\alpha N_b})}{0.1826\alpha_m N_b \alpha}\right]}{0.5415\beta_m \cdot \alpha \cdot N_b} \tag{2.51}$$

where $\mathrm{W}_{-1}[\cdot]$ is the branch of the Lambert W function satisfying $\mathrm{W}(x) < -1$ [16], α_m and β_m rely on the modulation type and order referring to [34]. The derivation is provided in Appendix A.1

Substituting (2.51) into (2.40) and (2.41) respectively, we have P_{opt} and d_{opt} in AWGN channel under a delay constraint ddr as follows:

$$\begin{aligned} P_{opt_g} &= \left(\frac{D_{hop}}{ddr}\right)^{\alpha} \left(1 - 0.1826\alpha_m \exp\left(\frac{1}{\alpha N_b} + \mathrm{W}_{-1}\left[\frac{-\exp(\frac{-1}{\alpha N_b})}{0.1826\alpha_m N_b \alpha}\right]\right)\right)^{-\alpha N_b} \\ &\quad \cdot \frac{-1 - \alpha N_b \mathrm{W}_{-1}\left[\frac{-\exp(\frac{-1}{\alpha N_b})}{0.1826\alpha_m N_b \alpha}\right]}{0.5415\beta_m \cdot \alpha \cdot N_b \cdot K_2} \\ &\approx -\frac{1 + \alpha N_b \mathrm{W}_{-1}\left[\frac{-\exp(\frac{-1}{\alpha N_b})}{0.1826\alpha_m N_b \alpha}\right]}{0.5415\beta_m \cdot \alpha \cdot N_b \cdot K_2} \left(\frac{D_{hop}}{ddr}\right)^{\alpha} \quad \text{when } N_b > 100 \end{aligned} \tag{2.52}$$

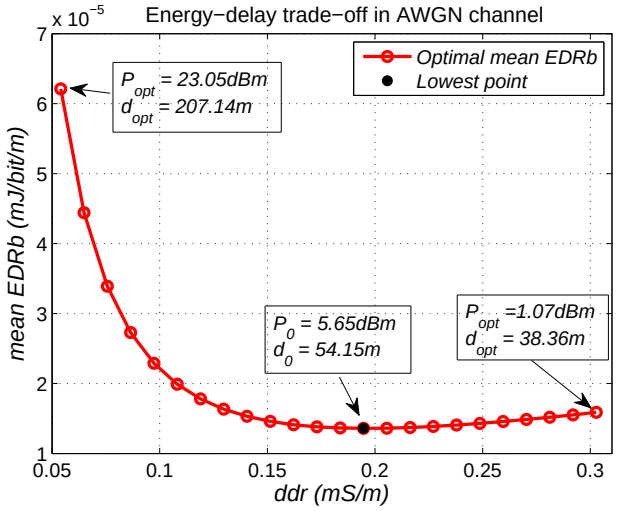

Figure 2.3: Theoretical lower bound in AWGN channel

and

$$d_{opt_g} = \frac{D_{hop}}{ddr}\left(1 - 0.1826\alpha_m \exp\left(\frac{1}{\alpha N_b} + \mathrm{W}_{-1}\left[\frac{-\exp(\frac{-1}{\alpha N_b})}{0.1826\alpha_m N_b \alpha}\right]\right)\right)^{-N_b} \approx \frac{D_{hop}}{ddr}. \tag{2.53}$$

Meanwhile, the energy-optimal transmission range d_{0g} is obtained by substituting (2.51) and (2.46) into (2.49):

$$d_{0g} = \left(\frac{-0.5415\beta_m K_2 N_b E_c \alpha}{K_1(\alpha-1)(1+\alpha N_b \mathrm{W}_{-1}\left[\frac{-e^{-\frac{1}{N_b\cdot\alpha}}}{0.1826\alpha_m N_b \alpha}\right])}\right)^{\frac{1}{\alpha}}. \tag{2.54}$$

Substituting (2.51) into (2.15), we have the optimal link probability in AWGN channel:

$$\begin{aligned} pl_{optg} &= \left(1 - 0.1826\alpha_m \exp\left(\frac{1}{\alpha N_b} + \mathrm{W}_{-1}\left[\frac{-\exp(\frac{-1}{\alpha N_b})}{0.1826\alpha_m N_b \alpha}\right]\right)\right)^{N_b} \\ &\approx 1 \text{ when } N_b > 100. \end{aligned} \tag{2.55}$$

This means that in the optimal configuration, the radio links are reliable.

The lower bounds of energy-delay trade-off according to (2.42) and its corresponding P_{opt} and d_{opt} in AWGN channel are shown in Fig. 2.3 where the related parameters are listed in Table 2.1. Here, $\gamma_{optg} = 9.43dB$ and $pl_{optg} = 96.55\%$

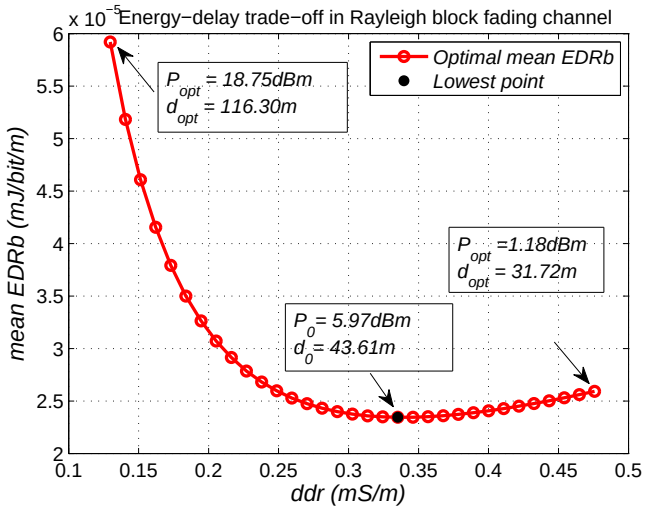

Figure 2.4: Theoretical lower bound in Rayleigh block fading channel

2.5.2 Rayleigh Block fading

When $\alpha_m = 1$ (e.g., for BPSK, BFSK and QPSK), according to the derivation in Appendix A.3, γ_{optb} is obtained by:

$$\gamma_{optb} = \frac{\alpha(4.25 \log 10(N_b) - 2.2)}{\beta_m} \tag{2.56}$$

Substituting (2.56) into (2.40) and (2.41) respectively, we have P_{opt} and d_{opt} in Rayleigh block fading channel under a delay constraint ddr as follows:

$$P_{opt_b} = \frac{e \cdot \alpha \cdot (4.25 \log 10(N_b) - 2.2)}{\beta_m K_2} \left(\frac{D_{hop}}{ddr}\right)^{\alpha} \tag{2.57}$$

and

$$d_{opt_b} = e^{\frac{1}{\alpha}} \cdot \frac{D_{hop}}{ddr} \tag{2.58}$$

Substituting (2.56) and (2.46) into (2.49) yields:

$$d_{0b} = \left(\frac{\beta_m K_2 E_c}{K_1(\alpha^2 - \alpha)(4.25 \log_{10}(N_b) - 2.2)}\right)^{1/\alpha}. \tag{2.59}$$

As for the optimal link probability, substituting (2.56) into (A.4) yields:

$$pl_{optb} = e^{-\frac{1}{\alpha}}. \tag{2.60}$$

The lower bounds of energy-delay trade-off according to (2.42) and its corresponding P_{opt} and d_{opt} in Rayleigh block fading channel are shown respectively, as example, in

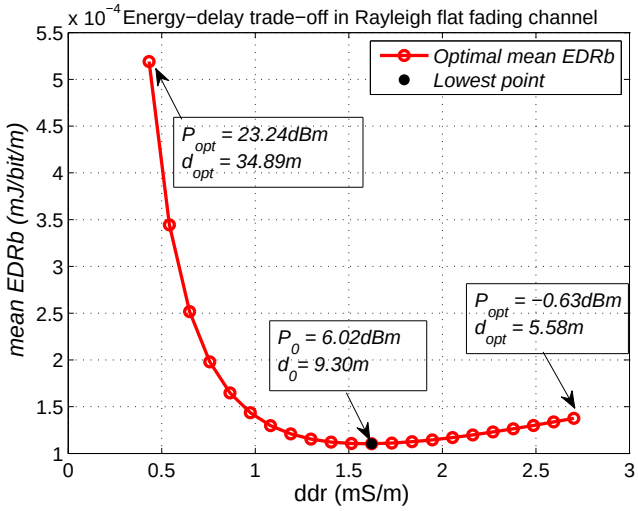

Figure 2.5: Theoretical low bound in Rayleigh flat fading channel

Fig. 2.4 where the related parameters are listed in Table 2.1. Here, $\gamma_{optb} = 12.65dB$ and $pl_{optb} = 71.65\%$

2.5.3 Rayleigh flat fading

According to (2.18) and (2.50), we obtain:

$$\gamma_{optf} = \frac{\alpha_m(1+\alpha N_b)}{2\beta_m}. \tag{2.61}$$

Appendix A.2 gives the detail of the related derivation.

Substituting (2.61) into (2.40) and (2.41) respectively, we have P_{opt} and d_{opt} in AWGN channel under a delay constraint ddr as follows:

$$\begin{aligned} P_{opt_f} &= \frac{\alpha_m(1+\alpha N_b)\cdot\left(1+\frac{1}{\alpha N_b}\right)^{\alpha N_b}}{2K_2\beta_m}\left(\frac{D_{hop}}{ddr}\right)^{\alpha} \\ &\approx \frac{1.359\alpha_m(1+\alpha N_b)}{K_2\beta_m}\left(\frac{D_{hop}}{ddr}\right)^{\alpha} \quad \text{when } N_b > 1 \end{aligned} \tag{2.62}$$

and

$$d_{opt_f} = \left(1+\frac{1}{\alpha N_b}\right)^{N_b}\frac{D_{hop}}{ddr} \approx \sqrt[\alpha]{2.718}\cdot\frac{D_{hop}}{ddr}. \tag{2.63}$$

Substituting (2.61) and (2.46) into (2.49) as follows:

$$d_{0f} = \left(\frac{2\beta_m E_c\cdot K_2}{(\alpha-1)\cdot K_1\alpha_m(\alpha N_b+1)}\right)^{\frac{1}{\alpha}}. \tag{2.64}$$

Meanwhile, the optimal link probability is obtained by substituting (2.61) into (2.18)

as follows:

$$pl_{optf} = \left(1 + \frac{1}{\alpha N_b}\right)^{-N_b} \approx 2.718^{-\frac{1}{\alpha}} \text{ when } N_b > 100. \tag{2.65}$$

The lower bounds of energy-delay trade-off according to (2.42) and its corresponding optimal P_{opt} and d_{opt} in Rayleigh flat fading channel are shown in Fig. 2.5 where the related parameters are listed in Table 2.1. Here, $\gamma_{optf} = 32.83dB$ and $pl_{optf} = 71.65\%$

2.5.4 Other scenarios

Except the above three scenarios, there are a lot of scenarios in which we can not find the close-form expression of γ_{opt} and $g(\gamma_{opt})$.

The first problem arises when the expression of the link probability is derived but the close-form expression of γ_{opt} is not obtained. For example, the type of channel is Nakagami-m block fading channel ($m \neq 1$) or a coding scheme is employed. In this kind of situation, the sequential quadratic programming (SQP) method in [67] can be adopted to solve the optimization problem of minimizing $g(\gamma)$. Then the exact value of γ_{opt} and $g(\gamma_{opt})$ are obtained. Subsequently, (2.42) gives the corresponding lower bound of energy-delay trade-off.

Another problem is drawn when we are not able to get the expression of the link probability. In this situation, we have to estimate the value of $g(\gamma_{opt})$. According to (2.33), when P_t is fixed, $g(\gamma_{opt})$ is obtained by minimizing the value of $\overline{DDR}$. Meanwhile, we deduce that $\frac{\overline{DDR}}{D_{hop}} = \frac{1}{pl \times d_{hop}}$ from (2.25). Hence, the method of finding $g(\gamma_{opt})$ is searching the maximum value of $pl \cdot d_{hop}$. Base on the above analysis, we use two nodes which one is assigned as transmitter and the other is assigned as receiver. Then, these following three steps is introduced to find $g(\gamma_{opt})$:

- Set a transmission power, for example, 0dB.
- Measure the value of $pl \cdot d_{hop}$ in different distance and try to find its maximum value, i.e., $\max(pl \cdot d_{hop})$, and recode the corresponding γ.
- Calculate the value of $g(\gamma_{opt})$ through

$$g(\gamma_{opt}) = \frac{(K_2 P_t)^{\frac{1}{\alpha}}}{max(pl \cdot d_{hop})}. \tag{2.66}$$

So far, the value $g(\gamma_{opt})$ can be obtained in any condition, and the lower bound of energy-delay tradeoff is achieved on the basis of (2.42). The corresponding P_{opt} and d_{opt} are obtained by (2.40) and (2.41) respectively. Meanwhile, the corresponding d_0 is obtained by (2.49).

2.5.5 Discussions

It should be noticed that the lowest point exists in each curve, this is to say, there is the most energy saving point without the delay constraints for each channel. The left side of the lowest point shows the energy consumption increases with the decrease of the delay constraint which coincides with our intuition. However, in the right of the lowest point, the energy consumption increases with the increase of the delay because the transmission power is too small which results to very small hop distance, i.e., the increase of the hop number. Certainly, this is a work state should be avoided in practice. Therefore, it is clear that the transmission power should be adjusted correctly according to a delay constraint in order to avoid too small transmission power. In addition, the transmission power which corresponds to the lowest point is the minimum transmission power because of its monotonic decrease property and the corresponding mean delay is the maximum mean delay of a pair of nodes.

In addition, the trade-off curves reveal the relationship between the transmission power, the transmission delay and the total energy consumption:

1. For smaller delays (fewer hops), more energy is needed due to the high transmission power needed to reach nodes located far away.

2. An increased energy consumption is not only triggered by communications with few hops but also arises for communications with several hops where the use of a reduced transmission power leads to too many retransmissions, and consequently wastes energy, too. Hence, the decrease of the transmission power does not always guarantee a reduction of the total energy consumption.

3. For a given delay constraint, there is an optimal transmission power that minimizes the total energy consumption.

Though the lower bound on the energy-delay trade-off is derived in linear networks, it will be shown by simulations in the following section 3.5 that this bound is proper for 2-dimensional Poisson distributed networks.

Another point that should be noted is the link probability in each channel. According to (2.55), (2.60) and (2.55), we conclude easily that the optimal link probability is independent of ddr in each channel. pl_{optg} and pl_{optf} depend on the type and order of modulation, N_b and α, and pl_{optb} is only related to α. When $Nb > 100$, the link probability in AWGN channel approximates to 1 which means reliable links are the optimal links to minimize both $\overline{EDRb}$ and $\overline{DDR}$. However, in Rayleigh flat fading and block fading channel, the optimal link probability is 71.65% when $\alpha = 3$, which corresponds to an unreliable links clearly. In conclusion, it is helpful to reduce energy consumption by making best use of unreliable links in these two kinds of channels.

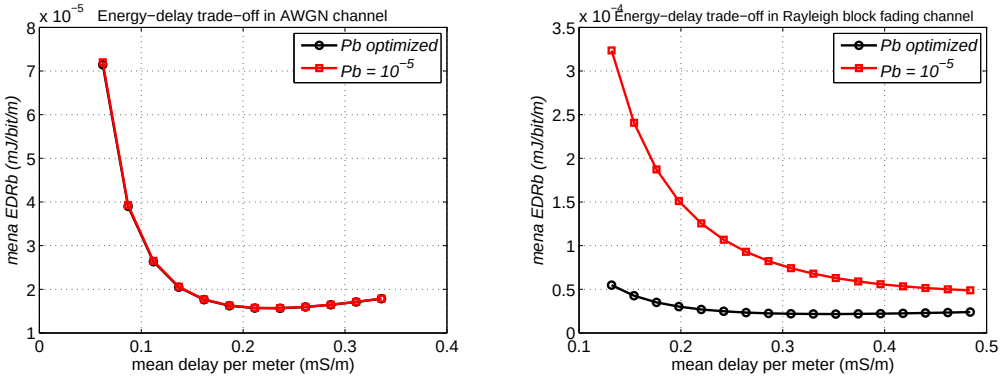

(a) AWGN channel

(b) Rayleigh block fading channel

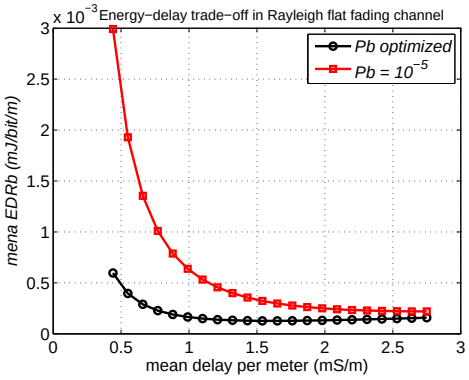

(c) Rayleigh flat fading channel

Figure 2.6: Effect of Pb on energy-delay trade-off in different channels

To explain the effect of unreliable links on energy efficiency, the comparison of energy-delay trade-off is provided in Fig. 2.6 under two conditions: optimized link probability and fixed link probability where the BER is set to 10^{-5}, i.e., $pl = 97.47\%$ according to the most of works such as [19]. These figures show that, in Rayleigh flat fading and block fading channels, the energy consumption is reduced greatly when the link probability is optimized where it is 71.65%, however, the energy consumption is almost the same for two conditions in AWGN channel, which verify our analyses above and indicate the importance of the optimization of link probabilities.

2.6 Summary

This chapter, using realistic unreliable link model, explored the lower bound of energy-delay trade-off and energy efficiency in AWGN channel, Rayleigh flat fading channel and Nakagami block fading channel. Firstly, we proposed a metric for energy efficiency, $\overline{EDRb}$, which is combined with the unreliable link model. It reveals the relation between the energy consumption of a node and the transmission distance which can

contribute to determine an optimal route at the routing layer. By optimizing $\overline{EDRb}$, a closed form expression of the energy-optimal transmission range is obtained for AWGN, Rayleigh flat fading and Nakagami block fading channel. Based on this optimal transmission range, the lower bound on energy-delay trade-off and $\overline{EDRb}$ for a multi-hop transmission using a linear network is derived for the three different kinds of channel. Theoretical analyses and simulations show that accounting for unreliable links in the transmission contributes to improve the energy efficiency of the system under delay constraints, especially for Rayleigh flat fading and Rayleigh block fading channel.

The close-form expression on energy-delay tradeoff provides the framework to evaluate the energy-delay performance of a network according to its parameters of physical layer, MAC layer and Routing layer. This framework can be used in the following applications:

1. *Performance evaluation*

   During the design or planning phase of a network, these results of performance evaluation provide the basis of the choice of sensor node and the choice of routing and MAC layer.

2. *Parameter optimization*

   Likewise in the design phase of a network, we can optimize the parameters such as transmission power according to the request of performance of a network on the basis of the framework.

3. *Benchmark of performance*

   Regarding to the design of protocol, the best performance of network can be obtained using this framework which can act as the benchmark of performance in order to measure the performance of a protocol and to adjust the parameters of protocol.

In Chapter 3, these applications are addressed in detail.

3

Applications of lower bound of energy-delay tradeoff

3.1 Introduction

In the planning phase of a WSN, the first job is to select a node to satisfy the performances of a network and other constraints such as budget. For example, if there are two kinds of node, the performance of these two kinds of nodes can be evaluated directly using this framework as show in previous section, in turn, these results provide a reference of selections.

Another important work in the planning phase of a WSN is to optimize the physical parameters. These parameters includes not only node parameters such as transmit rate, the type and order of modulation, the choice of coding scheme and so on, but also the network parameters such as node density and protocol parameters such as number of bits in a data packet and in a ACK packet.

In Chapter 2, the close-form expression of the lower bound of energy-delay tradeoff, (2.42), is obtained, which include all parameter of the physical, MAC and routing layers. Therefore, (2.42) provides a cross-layer framework to optimize these parameters.

In this chapter, we focus on how to optimize these parameters using this framework. The contributions of this chapter are:

- A parameter optimization process is introduced for the applications with or without a delay constraint.

- The lower bounds of energy-delay trade-off and energy efficiency are validated by simulations in 2-dimension Poisson networks.

The rest of this chapter is organized as follows: The effects of parameters on the lower bound of energy-delay tradeoff are introduced in section 3.2. In section 3.3, the parameter optimization process is addressed for the applications with or without a delay request ddr. Then, the optimization of node density is proposed in Section 3.4. Simulations are given and analyzed in section 3.5 in a 2-dimensional network to verify the theoretical results. Finally, section 3.6 concludes our work.

3.2 Parameters optimization

In this section, the effect of parameters including physical layer and protocol layer on both $\overline{EDRb}_{opt}$ and $\overline{DDR}_{opt}$ are analyzed to optimize these parameters. Firstly, we assume that the transmission power P_t is given. For all the results provided hereafter, the values of physical parameters that are not analyzed are given in Table 2.1.

For the reason of clear explanation, (2.32), (2.33), E_c, K_1, K_2 and D_{hop} are listed as follows:

$$\overline{EDRb}_{opt} = \frac{E_c + K_1 P_t}{(K_2 P_t)^{\frac{1}{\alpha}}} \cdot g(\gamma_{opt})$$
$$\overline{DDR}_{opt} = \frac{D_{hop}}{(K_2 P_t)^{\frac{1}{\alpha}}} \cdot g(\gamma_{opt})$$

$$E_c = \left(1 + \frac{N_{ack} + N_{head}}{N_b + N_{head}}\right)\left(\frac{2T_{start} \cdot P_{start}}{N_b} + \left(1 + \frac{N_{head}}{N_b}\right)\frac{P_{txElec} + P_{rxElec}}{b \cdot R_s \cdot R_{code}}\right)$$
$$K_1 = \left(1 + \frac{N_{ack} + N_{head}}{N_b + N_{head}}\right) \cdot \left(1 + \frac{N_{head}}{N_b}\right)\frac{\beta_{amp}}{b \cdot R_s \cdot R_{code}}$$
$$K_2 = \frac{G_{Tant} \cdot G_{Rant} \cdot \lambda^2}{(4\pi)^2 N_0 \cdot R_s \cdot L}$$
$$D_{hop} = T_{queue} + \frac{N_b + N_{ack} + 2N_{head}}{b \cdot R_s \cdot R_{code}}$$
$$g(\gamma_{opt}) = \frac{\gamma_{opt}^{\frac{1}{\alpha}}}{pl(\gamma_{opt})}$$
$$d_{opt} = \left(\frac{K_2 \cdot P_t}{\gamma_{opt}}\right)^{\frac{1}{\alpha}}$$

3.2.1 Physical layer parameters

First, on the basis of (2.32) and (2.33), the effects of circuitry power, coding scheme, type of modulation and transmit rate on the lower bound of energy-delay trade-off are

studied in this part.

Circuitry power

Circuitry power includes P_{txElec}, P_{rxElec}, $T_{start} \cdot P_{start}$. According to the definition of E_c, it is deduced easily that the increase of circuitry power leads to the increment of E_c. Therefore, we should reduce the circuitry power in the design of sensor node and should select a node which has minimum circuitry power.

Another factor related circuitry power is the amplifier coefficient β_{amp}. Since $\overline{EDRb}_{opt} \propto K_1 \propto \beta_{amp}$, the increase of β_{amp} results in the increase of $\overline{EDRb}_{opt}$, so that an efficient radio amplifier should be used to improve the energy efficiency of a node.

Channel coding

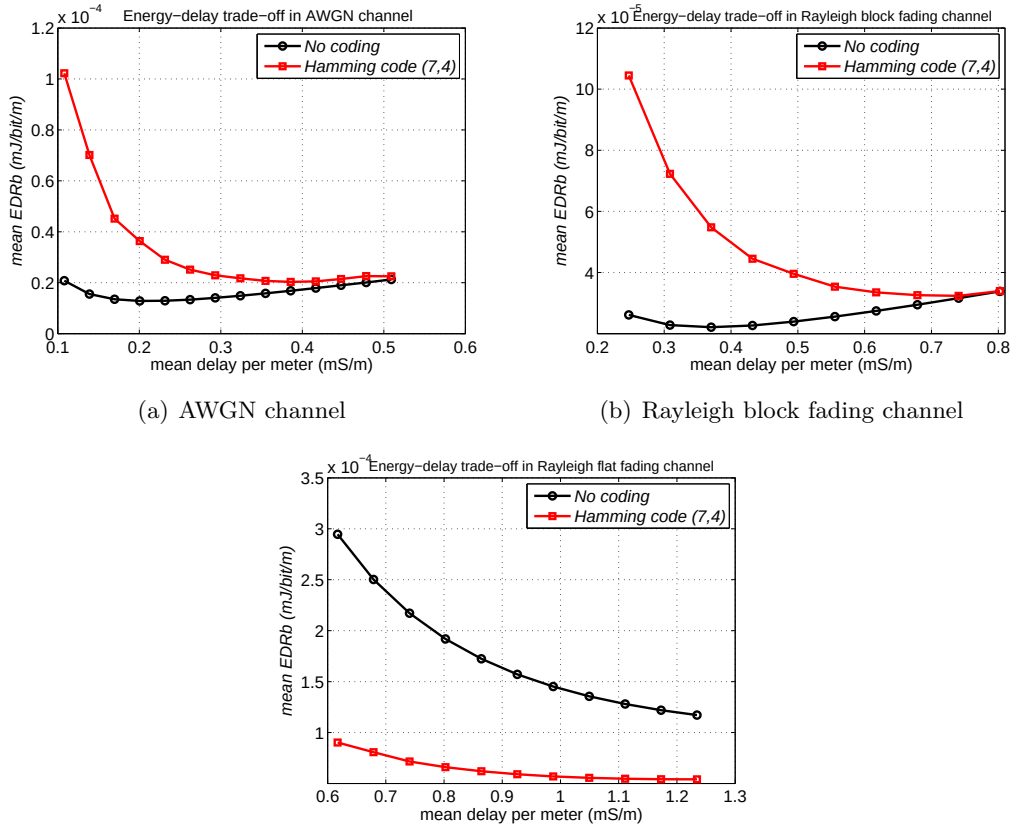

(a) AWGN channel

(b) Rayleigh block fading channel

(c) Rayleigh flat fading channel

Figure 3.1: Effect of a coding scheme on energy-delay trade-off in different channels

Because $R_{code} < 1$ and $\{E_c, K_1, D_{hop}\} \propto 1/R_{code}$, introducing a coding scheme results in the increase of this parameters. However, coding can reduce the probability

of bit or block error, and brings the decrease of $g(\gamma_{opt})$. To show the tradeoff of these two contrary effects on $\overline{EDRb}_{opt}$ and $\overline{DDR}_{opt}$, Hamming code $(7, 4)$ are used as an example in three kinds of channels.

The results in Fig. 3.1 indicate that this kind of coding is efficient only in flat fading channel, i.e., code words are spread over different channel states. However, it introduces more energy expenditure in AWGN channel and Rayleigh block fading channel. Therefore, it is dependent on the type of channel to decide if a coding scheme should be used.

Transmit rate R_s

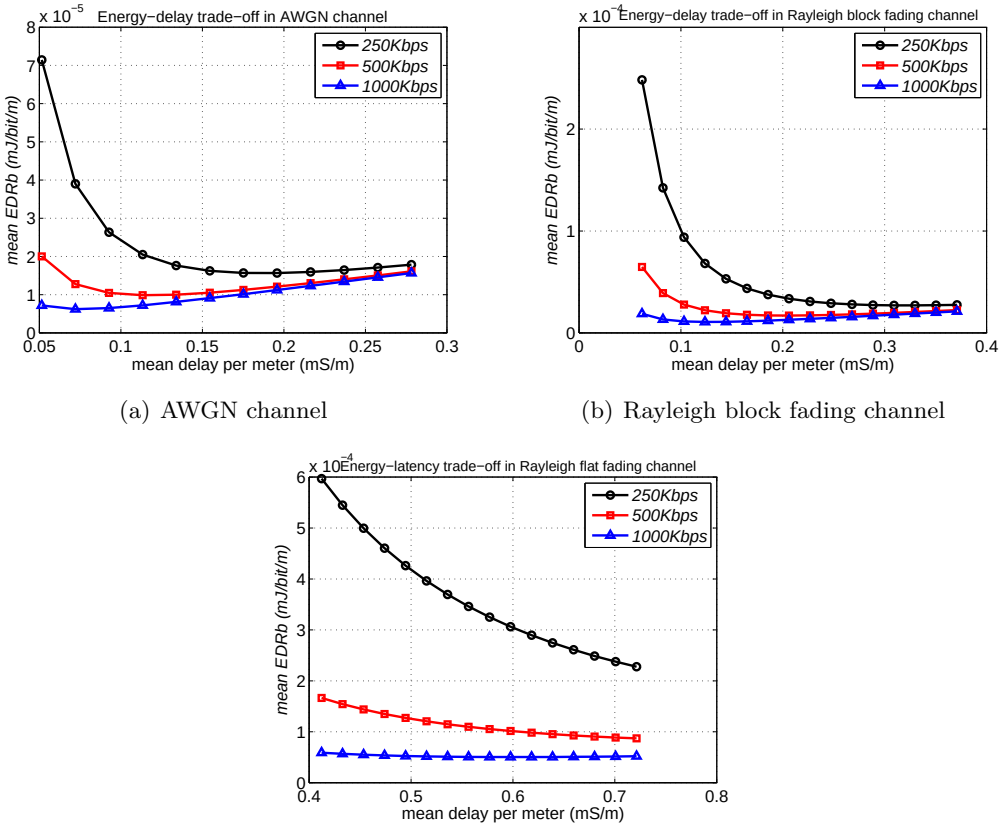

(a) AWGN channel

(b) Rayleigh block fading channel

(c) Rayleigh flat fading channel

Figure 3.2: Effect of transmit rate on energy-delay trade-off in different channels

Because $g(\gamma_{opt})$ is independent of R_s, $K_2 \propto (1/R_s)^{(1/\alpha)}$ and $\{K_1, E_c\} \propto 1/R_s$, it can be deduced easily that the increase of R_s leads to the decrease of $\overline{EDRb}$ and $\overline{DDR}$ simultaneously. The results in Fig. 3.2 in the three kinds of channel verify this analyses. Hence, according to this conclusion, the maximum transmit rate that a node can reach should be used in order to minimize both $\overline{EDRb}$ and $\overline{DDR}$ at the price of the increase

of transmission bandwidth.

Modulation

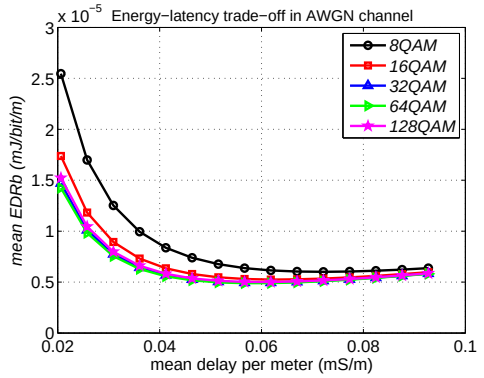

(a) AWGN channel $\alpha = 3$

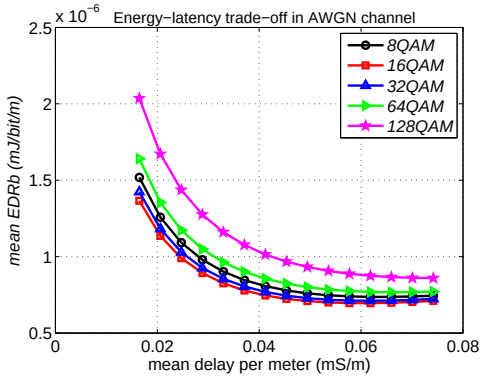

(b) AWGN channel $\alpha = 2$

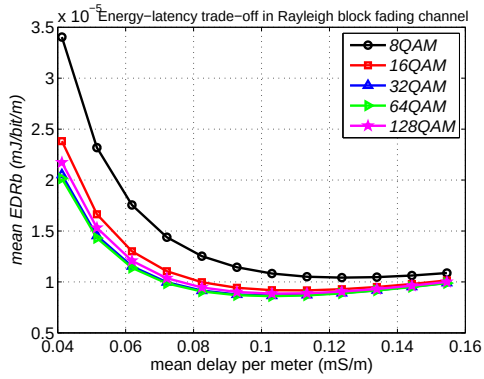

(c) Rayleigh block fading channel $\alpha = 3$

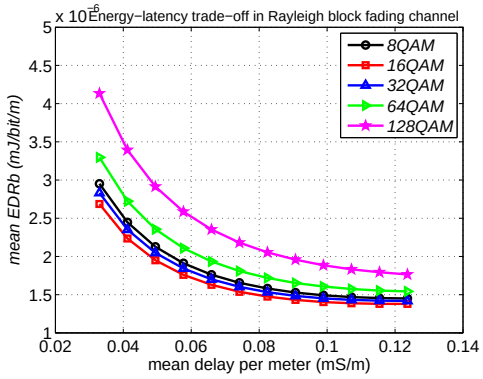

(d) Rayleigh block fading channel $\alpha = 2$

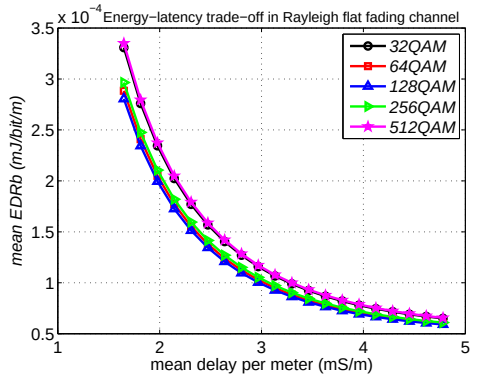

(e) Rayleigh flat fading channel $\alpha = 3$

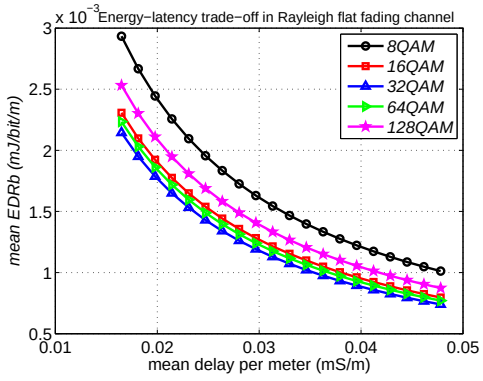

(f) Rayleigh flat fading channel $\alpha = 2$

Figure 3.3: Effect of modulation on energy-delay trade-off in different channels

Here, we assume that the symbol rate R_s is fixed, i.e., the bandwidth is constant. Hence, K_2 has no relationship with modulation. Note that $\{E_c,\ K_1\} \propto 1/b$ and the

increase of the order of a modulation results in the increase of $g(\gamma_{opt})$. Therefore, due to these two opposite effects, an optimal modulation exists for a node. The effect of modulation on the lower bound of energy-delay trade-off in three kinds of channel is shown in Fig. 3.3. Here, 64QAM is the best choice for AWGN channel and Rayleigh block fading channel and 128QAM is suitable for Rayleigh flat fading channel.

The optimal modulation is related with α and the order of optimal modulation decreases with the decrease of α. We found that the optimal modulation is independent of N_b and other parameters of a node. Therefore, we can decide the optimal modulation when the path-loss exponent and type of channel are given.

Additionally, when ddr is given, the increase of order of modulation brings the decrease of the optimal transmission distance d_{opt} according to (2.53), (2.58) and (2.63). This means the node density of a network should be increased to meet d_{opt}, which brings the increase of budget of a network.

3.2.2 The effect of protocol layer parameters

Number of bits in an ACK packet N_{ack}

Because $\{K_1,\ E_c,\ D_{hop}\} \propto N_{ack}$, it is deduced easily that the increase of N_{ack} leads to the increment of total $\overline{EDRb}_{opt}$ and $\overline{DDR}_{opt}$. Therefore, removing the ACK packet is a best solution from the viewpoint of energy saving. However, due to the unreliability of wireless links as described in Chapter 1, a lot of protocols adopt a ACK packet as a feedback mechanism. Consequently, N_{ack} should be reduced as less as possible.

Number of bits in a data packet N_b

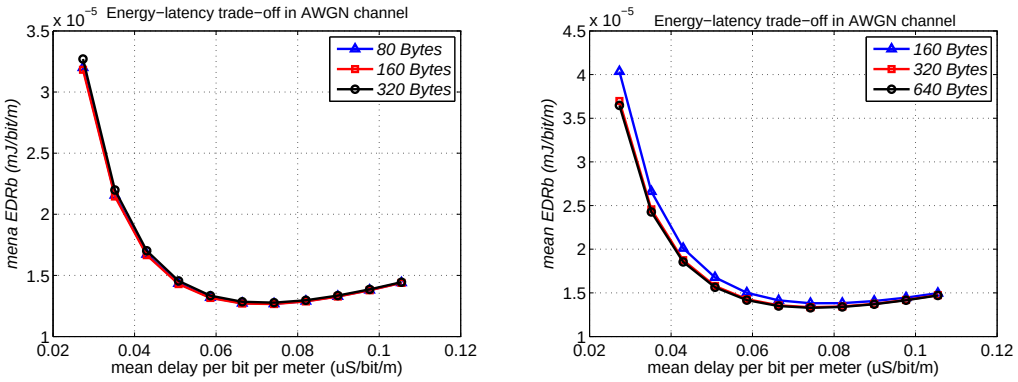

(a) AWGN channel ACK = 5 bytes

(b) AWGN channel ACK = 20 bytes

Figure 3.4: Effect of N_b on energy-delay trade-off in AWGN channel

Since $\{E_c,\ K_1\} \propto 1/N_b$, the increase of N_b diminishes E_c and K_1, but enlarges $g(\gamma_{opt})$. Thus, these two contrary effects on $\overline{EDRb}_{opt}$ bring on an optimal number of

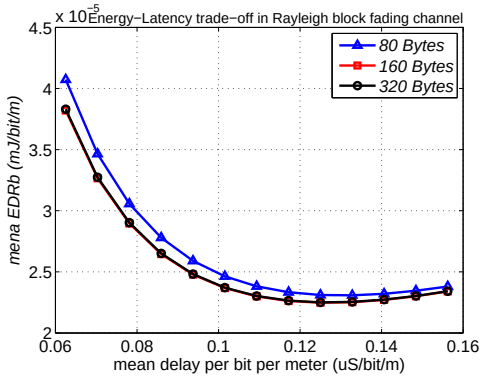

(a) Rayleigh block fading channel ACK = 12 bytes

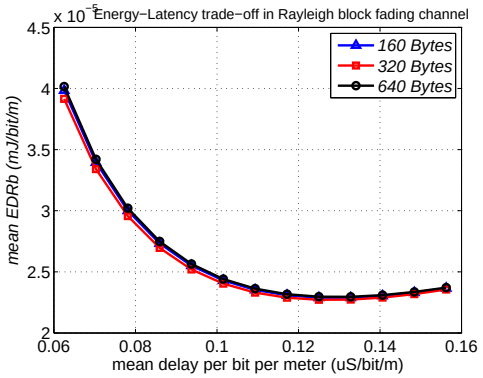

(b) Rayleigh block fading channel ACK = 15 bytes

Figure 3.5: Effect of N_b on energy-delay trade-off in Rayleigh block fading channel

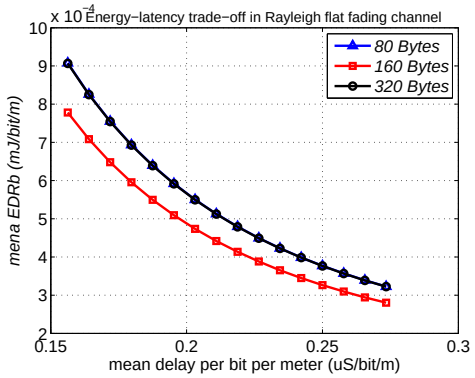

(a) Rayleigh flat fading channel ACK = 78 bytes

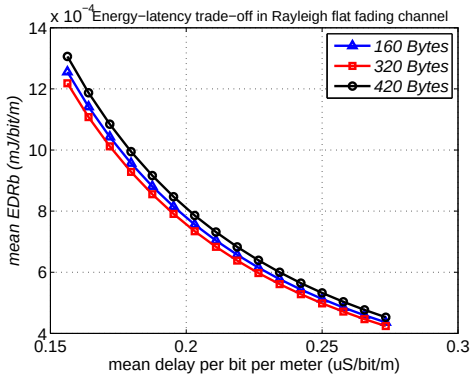

(b) Rayleigh flat fading channel ACK = 120 bytes

Figure 3.6: Effect of N_b on energy-delay trade-off in Rayleigh flat fading channel

bits. The results in Fig. 3.4, Fig. 3.5 and Fig. 2.5 validate our analyses in three kinds of channel. Meanwhile, the result in these figures indicate that the increase N_{ack} leads to the increase of the optimal N_b.

It should be noticed that the difference of $\overline{EDRb}_{opt}$ from the different number of bits is small when N_{ack} is very small especially in AWGN channel and Rayleigh block fading channel. Considering the conclusion about N_{ack}, we should do our best to reduce N_{ack} so that the optimization about N_b can be neglected.

Under a *ddr* constraint, the increase of N_b leads to the increase of d_{opt} and P_{opt} simultaneously in three kinks of channels mentioned, according to (2.53) (2.58), (2.63), (2.52), (2.57) and (2.62). This means a long-hop transmission which decreases the node density of a network.

Delay from MAC protocol T_{queue}

According to (2.25), the increase of T_{queue} will lead to the increment of D_hop and it can be deduced that the transmission power should be increased to satisfy the same delay constraint on the basis of (2.42). In turn, $\overline{EDRb}$ will increase. The results in Fig. 3.7 verify the above analysis. This conclusion shows that the process leading to the increase of T_{queue} should be reduced or removed, such as RTS (Request to Send) and CTS (Clear To Send) process, to improve the energy efficiency of a network.

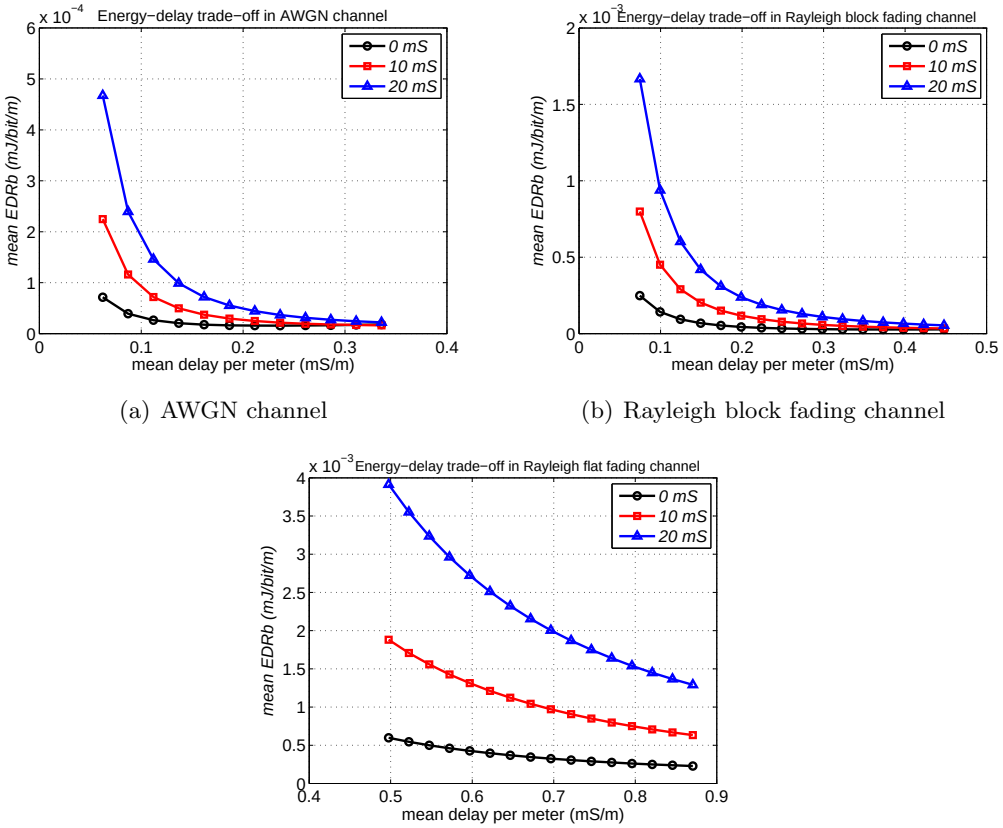

(a) AWGN channel

(b) Rayleigh block fading channel

(c) Rayleigh flat fading channel

Figure 3.7: Effect of T_{queue} on energy-delay trade-off in different channels

Besides the above parameters, the other parameters such as strength of fading of a channel or the integration of several parameters can be analyzed also according to the different applications because this framework includes every physical parameters. On the basis of these analysis result, we can adjust the parameter to obtain the best performance of a network.

3.2.3 Optimal transmission power

According to the analyses in Chapter 2, we know that there exists an optimal transmission power according to (2.40) when a delay constraint ddr is set. When there is no delay request, P_0, obtained by (2.48), is the optimal transmission power for minimizing the total energy consumption. Moreover, P_0 provides a threshold of transmission power under which a node will be running in an inefficient stat as described in Chapter 2. Therefore, the transmission power of each node in a network should not be configured smaller than P_0.

3.3 Process of parameters optimization

Integrating the results of analyzes above, the process of parameter optimization shown in Fig. 3.8 is explained in detail as the flowing steps:

1. The physical parameters of a node should be obtained and E_c, K_1 and K_2 are calculated according to these parameters. Meanwhile, N_{ack} is obtained according to the protocol using in a network.

2. R_s is decided according to the maximum limit value of transmission rate of a node.

3. Coding scheme is selected according to the type of channel.

4. N_b and modulation are optimized using searching method on the framework (2.42) and other optimized parameters.

5. Calculate the optimal transmission power P_{opt} according to (2.40).

6. Calculate the optimal transmission distance d_{opt} and minimal node density ρ on the basis of (2.41) and (3.3) respectively (addressed in the following section).

3.4 Minimum node density

It is clear that the bigger the node density of a network, the closer the performance of network approaches the lower bound of energy-delay because the best node which satisfies d_{opt} can be found more possibly. However, the increase of node density means the increase of the total cost of a network and an increase of idle energy which is nor considered here. Now, we discuss how to config the node density according to d_{opt} from(2.41) under a delay constraint ddr, or d_0 from (2.49) in the condition of no delay request.

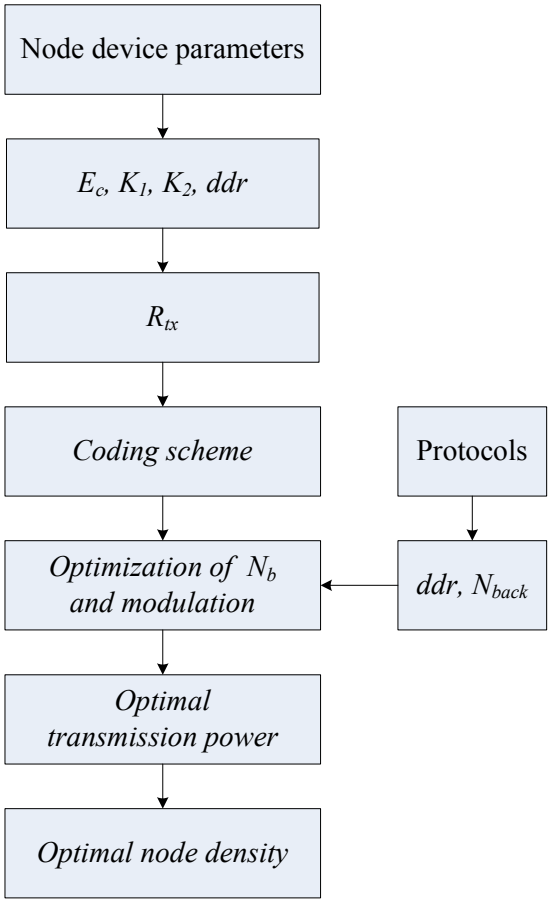

Figure 3.8: The process of parameters optimization

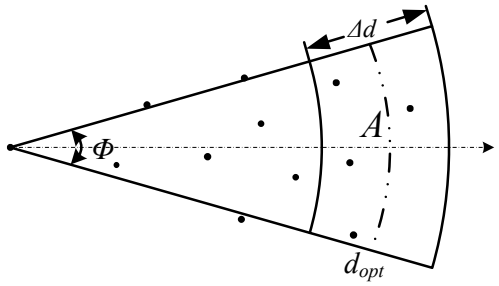

Figure 3.9: Node density

Next, we discuss how to obtain the node density. Here, we assume a Poisson distributed network according to:

$$P(n\ nodes\ in\ S_A) = \frac{(\rho \cdot S_A)^n}{n!} e^{-\rho \cdot S_A}. \tag{3.1}$$

where S_A is the surface of area A and ρ is the node density.

The relationship between node density and the expected distance between two nearest node, $\bar{d}$, is provided in [37] in a 2-dimension Poisson distribution network as follows:

$$\bar{d} = \frac{\sqrt{\pi}}{2\sqrt{\rho \cdot \Phi}}, \tag{3.2}$$

where Φ is shown in Fig. (3.9). According to the previous analysis, we should let $\bar{d} \leq d_{opt}$ or $\bar{d} \leq d_0$ in order to minimize energy consumption, so that we have:

$$\rho \geq \frac{\pi}{4 \cdot \Phi \cdot \{d_{opt} \text{ or } d_0\}^2}. \tag{3.3}$$

Finally, on the basis of (3.3), the minimum node density is obtained to improve the energy efficiency and deduce the transmission latency in a network.

In [61], the mean distance between two nodes are presented and mean distances for Manhattan networks, hypercubes, and shufflenets are presented in [68]. Using similar method, the minimum node density can be deduced in these kinds of networks.

3.5 Simulations

The purpose of this section is to determine the lower bound on the energy-delay tradeoff and on the energy efficiency in a 2-dimensional Poisson distributed network using simulations. The goal is to show that the theoretical results obtained for a linear network still hold for such a more realistic scenario.

3.5.1 Simulation setup

In the simulations, the lower bound on the energy-delay trade-off and on $\overline{EDRb}$ are evaluated in an area $\mathcal{A}$ of surface $S_{\mathcal{A}} = 100 \times 1200m^2$ using the simulator Wsnet [2]. The nodes are uniquely deployed according to a Poisson distribution (3.1).

All the other simulation parameters concerning a node are listed in Table 2.1. The distance between the source node and the destination node is $1000m$. The source node transmits only one DATA packet of 320 bytes to the destination with BPSK modulation. Relay nodes adopt decode and forward transmission mode and will transmit immediately ACK packet of 26 bytes to the transmitter when receiving the DATA packet correctly. For every hop, the transmitter will retransmit the DATA packet until the DATA packet is received by the next relay node, this is to say, there is no retransmission limit in order to ensure the reliability. A simulation will be repeated for 2000 times in each different configuration.

The network model used in the simulations assumes the following statements:

- The network is geographical-aware, i.e., each node knows the position of itself

and all the neighbor nodes in the simulation network.

- Each node in the simulation network has the same fixed transmission power.
- The nodes sleep when they are not the relay nodes based on a perfect duty cycle scheduling algorithm in order to avoid energy consumption by overhearing.

3.5.2 Simulations of the energy-delay trade-off

To verify the lower bound of energy-delay trade-off, two routing schemes are used in the simulations: greedy routing [28] and $PRR \times distance$ routing [46] scheme, and 802.11 DCF protocol are adopted for MAC layer.

The original greedy routing protocol has low performance on energy efficiency and delay [46], so the optimal transmission distance is employed as the maximum transmission distance of every hop, in turn, in this scope the node closest to the destination node is selected as relay node.

The main idea of $PRR \times distance$ routing protocol is that a source node measures the link probability for each neighbor node using Packet Reception Ratio (PRR). Then, the source node calculates the metric $PRR \cdot d$ of each node, where d is the distance between the source and its neighbor. Finally, the source selects the node with the maximum value of $PRR \cdot d$ among its all neighbors in the direction of the destination node. In the simulations, the PRR is computed according to (A.4) for Rayleigh block fading channel and (2.15) for AWGN channel.

In 802.11 DCF protocol, we set the RST (Request to Send) threshold bigger than the length of DATA packet, i.e., RTS and CTS don't be sent before the transmission of DATA packet because there is no collision due to the low traffic. The $\overline{DDR}$ decreases from 0.02 to 0.011 stepped by 0.001 in AWGN channel and from 0.034 to 0.016 stepped by 0.002 in Rayleigh block fading channel and the corresponding optimal transmission power and optimal transmission distance are listed in Table 3.1 obtained by (2.53) (2.58) (2.52) (2.57).

Fig. 3.10 and 3.11 provide the simulation results with different nodes in the simulation area compared with the theoretical lower bound of energy delay trade-off in AWGN channel and Rayleigh block fading channel respectively. These results show that:

1. *The theoretical lower bound on $\overline{EDRb}$ is adequate for a 2-D Poisson network although its derivation is based on a linear network.*

   With the increase of the node density, the simulation result is approaching the the theoretical lower bound because relays node selected by the routing scheme are more and more near the optimal transmission distance of each hop when the

Table 3.1: Simulation parameters

AWGN	Tx Power (dBm)	4.98	5.65	6.36	7.10	7.89
	Hop Distance (m)	52	55	58	61	65
	Tx Power (dBm)	8.73	9.63	10.60	11.64	12.77
	Hop Distance (m)	70	74	80	87	95
Rayleigh block	Tx Power (dBm)	5.18	5.97	6.81	7.71	8.68
	Hop Distance (m)	42	44	47	50	54
	Tx Power (dBm)	9.72	10.85	12.10	13.47	15.00
	Hop Distance (m)	59	64	70	78	88

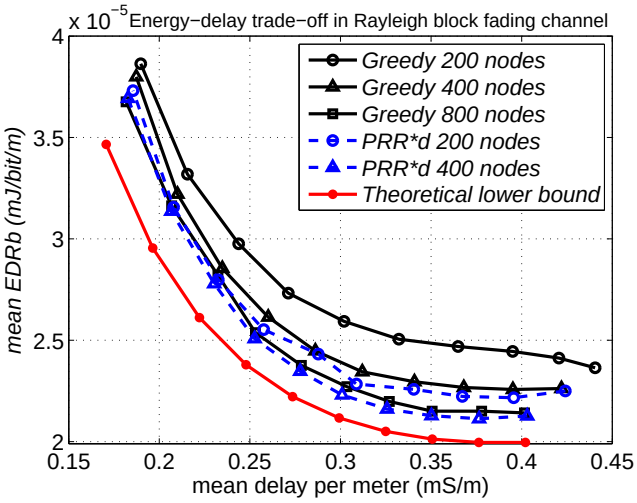

Figure 3.10: Simulation results of energy-delay trade-off in block fading channel

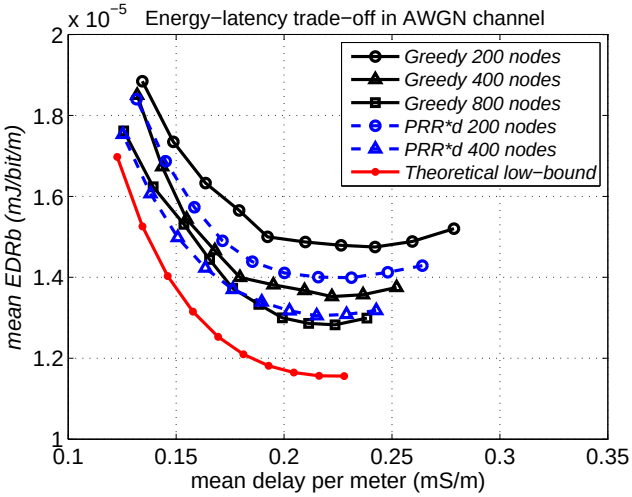

Figure 3.11: Simulation results of energy-delay trade-off in AWGN channel

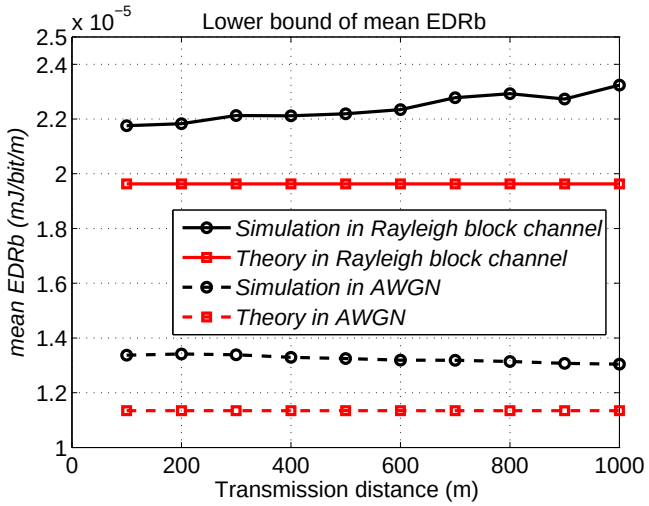

Figure 3.12: Lower bound of $\overline{EDRb}$ in different channels

node density increases. We can deduce the the lower bound can be reached when the node density is big enough. Hence, we can conclude that the theoretical lower bound of energy-delay trade-off is suitable for Poisson networks.

2. *The optimal physical configuration is importance to achieve the best network performance.*

   When the node density is reduced, theoretical and simulation based curves for the lower bound of energy-delay trade-off diverge. In that case, the source node can not find a relay node in the optimal transmission range and has to search for a further or closer relay node which increases both the energy consumption and delay.

3. *Unreliable links play an important role for energy savings in Rayleigh block fading channel.*

   In simulations, the mean link probability is 64% for $PRR \times distance$ routing and 73% for greedy routing protocol respectively. Hence, unreliable links also contribute to reach the lower bound on energy-delay trade-off (as presented Section2.4).

3.5.3 Simulations of the lower bound on $\overline{EDRb}$

The simulations regarding lower bound on $\overline{EDRb}$ are also implemented in AWGN and Rayleigh block fading channel. The lower point of each curve in Fig. 3.10 and 3.11 corresponds to the most energy efficient point which reveals that the increase of node density is helpful to let the network performance on energy efficiency achieving the

theoretical lower bound.

In Fig. 3.12, simulation results are given for different transmission distance. Here 400 nodes are deployed in the simulation area. This result indicates that the theoretical lower bound on the energy efficiency $\overline{EDRb}$ is valid for a Poisson network though its derivation is based on a linear network.

3.6 Summary

In this chapter, applications of the lower bound of energy-delay tradeoff are presented. A parameter optimization process is found to adjust the parameters including physical layer and protocol layers according for the applications with or without delay constraint. Meanwhile, the simulations in a 2-dimension Poisson network is provided to verify the theoretical results about the lower bounds of energy-delay tradeoff and energy efficiency. In simulations, two geography routing schemes are used, while this framework can be used for non-geography routing schemes as well because the transmission distance is an inherent property all routing schemes.

Part II

Cooperative communications

4

State of The Art

Channel fading was traditionally considered as a source of unreliability that has to be mitigated in wireless networks. However, information theory [32] reveals that channel fluctuations can be rather beneficial if strong channel states are opportunistically exploited. To achieve the full capacity of such a system, a virtual Multiple Input Multiple Output (MIMO) system [27] and an opportunistic communication scheme [90] are proposed.

4.1 Opportunistic communications

Compared with traditional point-to-point multi-hop routings, the basic idea of opportunistic routing is that, at each hop, a set of next-hop relay candidates receiving a packet successfully compete for acting as relay as show in Fig. 4.1. For relay selection, a priority is assigned to each relay candidate according to a specified metric, for example, the geographical *closeness* of the relay candidate to the destination [90]. As a consequence, exploiting the spatial diversity is exactly the purpose of opportunistic routing techniques.

The efficiency of opportunistic communications can be evaluated from different points of view. In this part, we keep our analysis approach in Chapter 2: the end to end reliability is a hard constraint while the end to end delay and the ene to end energy consumption are two interaction factors.

In classical opportunistic communications, the neighbors of a source in a certain

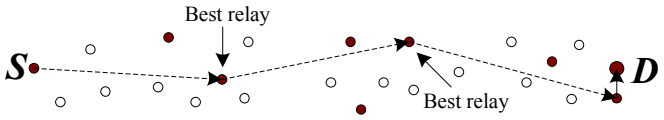

Figure 4.1: Mechanism of opportunistic communications

area serve as the relay candidate. For example, the nodes in the sector with a angle ψ of $\mathcal{S}$ are the relay candidates of $\mathcal{S}$ as shown in Fig. 5.1. Some analytical models have already been proposed for this kind of opportunistic communications in [70, 56]. The modeling framework in [70], which separates the opportunistic routing functionality into three components: routing, medium access and sleep discipline, is proposed to analyze the energy efficiency and latency performances of opportunistic routing in low traffic scenarios. This framework rests on the disc model [35] which relies on the definition of a radio power reception threshold and can not take the realistic channel features into account, such as fading or shadowing. In [56], the proposed model introduces shadowing and fading and defines the expected effective transmission distance (ETD). However, this model still relies on the definition of a reception threshold, now defined as a signal to noise (SNR) threshold, namely, the switched link model. As described in Chapter 1, the disc model and the switched link model are not realistic and have severe weakness that are particularly relevant to opportunistic communications. In addition, the expected ETD model in [56] is a rough approximation of reality by the summation computation. Furthermore, none of the aforementioned models considers the impact of retransmissions caused by link unreliability. In chapter 5, we propose a significant improvement of the expected ETD model proposed in [56].

On the basis of the models previously described, several works provide a thorough analysis of the energy performance of opportunistic routing. In [90, 70], energy and latency performances of an opportunistic routing scheme called *GeRaF* are analyzed, and the effects of node density, traffic load and duty cycle are evaluated. The simulations in [71] show the impact of node density, radio channel quality and traffic rate on the energy consumption at each node, the average packet transmission delay and the goodput of opportunistic protocol. A 10% decrease in power and a 40% of delay reduction is exhibited in this work. Whereas these analyses are based on the previously described unrealistic disc link model. In addition, the energy efficiency of an opportunistic routing called CAGIF [86] is studied in a fading channel, where the whole set of neighbor nodes try to receive the packet from the source node.

However, none of the aforementioned works consider the optimization of the transmission power and the number of relay candidates, which have influence on the energy performance. Consequently, these studies are insufficient to determine whether the

relative low performances of opportunistic routing are intrinsic to this kind of routing or due to the specific protocol implementation (relay selection policy, fixed power choice, etc...). In Chapter 5, we will analyze the minimum energy consumption with opportunistic communications without delay constraint in classical opportunistic communication.

Several previous works on opportunistic routing, such as [90, 70, 71, 86, 85], provide the analyses of energy and latency performances. In [90, 70], energy and latency performances of a routing scheme called *GeRaF* are analyzed, and the effects of node density, traffic load and duty cycle are evaluated. The simulations in [71] show the impacts of node density, radio channel quality and traffic rate on the energy consumption at each node, the average delay of packet and the goodput of opportunistic protocol. It is concluded that the benefit of opportunistic scheme is about 10% decrease in power and 40% reduction in delay. Whereas these analyses are based on an unrealistic disc link model [83, 35] which relies on the definition of a reception threshold level and is not well adapted to the research of opportunistic communications due to the neglect of propagation phenomena, e.g., fading and shadowing. Furthermore, the energy efficiency of the protocol CAGIF [86] is studied in a fading channel, where the whole set of neighbor nodes try to receive the packet from the source node.

However, in aforementioned studies, a fixed transmission power and the node density are considered, without providing any proof of optimality. Therefore, these studies are insufficient to determine whether the relative low performances of opportunistic routing are intrinsic to this kind of routing or due to the specific protocol (relay selection policy, fixed power choice, etc.). In Chapter 5, we propose to answer this question by minimizing the energy consumption of opportunistic relaying schemes with respect to the optimization of the node density and the transmission power.

In the mentioned works, all nodes in the communication area of a source node act as forwarding candidates. While in [85], instead of choosing the whole neighbors as relay candidates, an efficient selection mechanism of relay nodes is proposed in order to optimize energy efficiency. Simulations of [85] in a shadowing channel indicate that the energy efficiency is greatly improved.

Nevertheless, based on the relay selection mechanism, the optimization of parameters is not considered and the delay performance of a system is not analyzed in the papers mentioned. In Chapter 6, these works are performed on the basis of a realistic unreliable link model.

4.2 cooperative MIMO

In opportunistic communications, we introduce the concept of cooperation only in the receiver side. In Chapter 7, the cooperation is extended to both the transmitter side

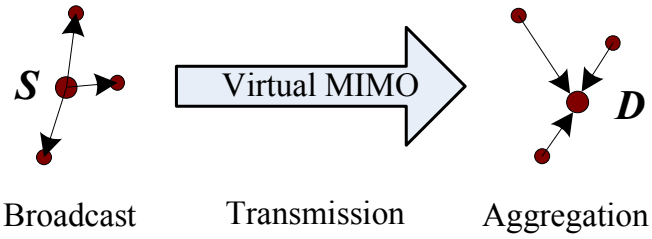

Figure 4.2: Single hop cooperative MIMO communication

and the receiver side by cooperative multi-input multi-output (MIMO) systems.

Multi-antenna systems have been studied intensively in recent years due to their potential to dramatically increase the channel capacity in fading channels. Then, the concept of virtual antenna array is proposed to achieve MIMO capability in a network of single antenna nodes in [27, 26]. In WSNs, a virtual MIMO scheme based on the space-time block code (STBC) is proposed using two [53] or more cooperative sensors [54] to provide transmission diversity with neither antenna array nor transmission synchronization.

A CMIMO transmission is illustrated in Fig. 4.2. In the transmission side, node $\mathcal{S}$ cooperates with its neighbors and broadcasts its data. MIMO techniques, e.g., STBC, STTC and Spatial Multiplexing, are then employed to transmit their data simultaneously to the destination node and cooperative nodes like a multi-antenna diversity system. Each cooperative node acts as one antenna of MIMO system. In the reception side, the cooperative neighbors of $\mathcal{D}$ receive the MIMO modulated symbols and retransmit them separately to $\mathcal{D}$ for joint MIMO signals combination. Multihop transmissions are realized by repeating one-hop transmission as described above.

The importance of energy efficiency and delay for WSNs have been described in Chapter 1. The energy efficiency of a CMIMO scheme with Alamouti code is analyzed for the single-hop transmission in [20], and it is concluded that the energy efficiency of a CMIMO scheme is higher than that of a single input single output (SISO) scheme when the transmission distance is greater than a threshold. Meanwhile, the constellation size of modulation is optimized. In [45], a more complete energy model of CMIMO is considered, which includes the training overheads of a scheme to analyze the energy efficiency of CMIMO communications compared with SISO schemes, and the authors find that the training overheads can be modeled as proportional to the number of cooperative nodes. Whereas, only single-hop SISO transmission is utilized for comparison in [20, 45]. [11] compares the energy efficiency of single hop CMIMO based transmissions with that of multihop SISO transmissions, and determines the thresholds of the physical parameters above which the MIMO-based structure outperforms the multihop transmission. However, the number of cooperative nodes is fixed and non-optimum

in previous works. The joint optimization of the rate and the number of nodes in a cluster is carried out in [15, 66] in order to improve the energy efficiency of cooperative multiple input single output (CMISO) scheme. The optimal number of nodes under CMIMO is also studied in [64], which considers both the transmitter side and the receiver side. The same optimization is implemented from the point of view of uniform energy distribution to prolong the lifetime of a WSN in [5].

The previous optimizations are investigated from the energy efficiency viewpoint, which focus only on the physical layer. [18] proposes a cross-layer design of CMISO scheme by adapting transmission rate to minimize the transmission delay under an energy constraint, and a best energy-delay tradeoff is derived.

However, all of the aforementioned works are based on the assumption of a disc link model or a switched link model under which the transmission between two nodes x and x' succeeds if and only if the bit error rate (BER) $P_b(x, x')$ at the receiver is above a minimal value P_{bmin}. As described in Chapter 1, the unreliability of wireless links can not be avoided.

In [82], the optimization problem of P_{bmin} is analyzed, and an optimized multihop protocol is proposed to meet the end-to-end QoS requirements with a minimum energy expenditure based on CMISO scheme. Nevertheless, in aforementioned studies, a fixed transmission power is considered and the number of cooperative nodes is chosen according to a given routing policy, while without providing any proof of optimality. In Chapter 7, the lower bound of energy-delay tradeoff of CMIMO is exploited under unreliable links with optimized parameters.

5

Energy Efficiency of Classical Opportunistic Communications

5.1 Introduction

As described in Chapter 4, classical opportunistic communications take advantage of spatial diversity to improve the performance of a network by cooperative reception mechanism. In this chapter, the energy efficiency of opportunistic communications is analyzed.

Firstly, we propose a significant improvement of the ETD model proposed in [56] by:

- integrating a realistic unreliable link model into the ETD model,
- considering the effect of acknowledgements and retransmissions,
- enhancing the precision by an exact integral computation instead of a simplified summation approximation.

However, none of the aforementioned works consider the optimization of the transmission power and the number of relay candidates, which have influence on the energy performance. Consequently, these studies are insufficient to determine whether the relative low performances of opportunistic routing are intrinsic to this kind of routing or

due to the specific protocol implementation (relay selection policy, fixed power choice, etc...).

Meanwhile, based on the improved ETD model, we propose to minimize the energy consumption of opportunistic schemes in terms of the optimization of the node density and the transmission power. In order to analyze the effect of fading, AWGN channel and Rayleigh block fading channel are adopted in this chapter, the analyses in other channels can be carried out by following the same method. This chapter also provides the following contributions:

- Classical opportunistic communications are proved to be more efficient in Rayleigh block fading channel than that in AWGN channel from the energy viewpoint.
- The impact of the selection mechanism of relaying candidates on energy efficiency is analyzed. Hence, selecting the relay candidates which locate around the linear path between the source and the destination is more energy efficient than that of selection of all neighbor nodes.

The rest of this chapter is organized as follows: Section 5.2 describes the utilized models and metrics. Using these models, the optimization of one-hop transmission regarding various forwarding areas is implemented in Section 5.3, and the results are extended to multi-hop transmissions. The simulations in Section 5.4 verify the correctness of the analytical models proposed. Finally, Section 5.5 draws some perspectives and conclusions.

5.2 Models and metric

In this section, we adopt the definitions about energy efficiency in Chapter 2 to the case of opportunistic communications: the realistic link models, the metric $\overline{EDRb}$. In addition, the system model, the expected ETD model, the delay model are introduced.

5.2.1 Realistic unreliable link models

As claimed in the introduction, it is very crucial to accurately model transmission errors to ensure a reliable transmission in a realistic channel.

According to the opportunistic relaying principle, the successful transmission means that at least one node in relay candidates receives the packet from the source node correctly. Thus, according to [35], the probability of a successful transmission is:

$$P_s = 1 - P_{iso}, \tag{5.1}$$

where P_{iso} is the probability that no node receives the packet and can be obtained by (5.7).

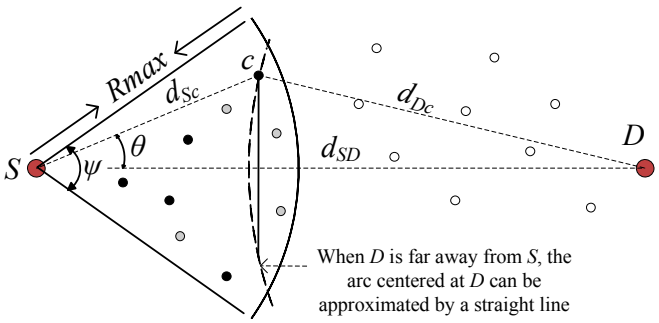

Figure 5.1: Effective transmission distance

For a reliable transmission, retransmission mechanism is adopted also in opportunistic communications as well. Then, the mean number of retransmissions is:

$$\overline{N}_{tx} = \sum_{n=1}^{\infty} n \cdot P_s \cdot (1 - P_s)^{(n-1)} = \frac{1}{P_s} = \frac{1}{1 - P_{iso}}, \tag{5.2}$$

where n stands for the number of transmissions.

5.2.2 System model

The nodes in a network are assumed to be independently and randomly distributed according to a random Poisson process of density ρ defined as (3.1). [1]

We consider the case of a source node $\mathcal{S}$ forwarding a packet to a sink/destination node $\mathcal{D}$. The communication sector of $\mathcal{S}$ is defined as a sector centered at $\mathcal{S}$ and turned towards $\mathcal{D}$ as shown in Fig. 5.1. The radius of this communication sector is the maximum transmission range of $\mathcal{S}$, R_{max}, and the angular aperture is referred to as ψ.

R_{max} depends on the receive sensitivity of node and the transmission power of the source node. In [35], R_{max} is given though the mean node degree. R_{max} is the transmission distance at which the mean node degree of a node reach its plafond as shown in Fig. 5.2 and its corresponding SNR is $\bar{\gamma}_{Rmax}$. In this thesis, without loss of generality, R_{max} is defined as the distance where $\overline{\gamma}_{Rmax} = 1$ since it is low enough such that the probability of longer transmission is negligible. Then, according to (2.11), we obtain:

$$R_{max} = (K_2 \cdot P_t)^{\frac{1}{\alpha}}. \tag{5.3}$$

The communication sector depends on opportunistic routing policies on the assumption that the nodes know their geographical position.

The set of nodes c being in the communication sector of $\mathcal{S}$ is referred to as $\mathcal{C}$. $N_C = |\mathcal{C}|$ is the average number of nodes in $\mathcal{C}$. According to the property of Poisson

[1] Here, the density is calculated by the number of active nodes per area unit. For the systems in which nodes sleep and wake up periodically, the density can be computed according to the duty cycle.

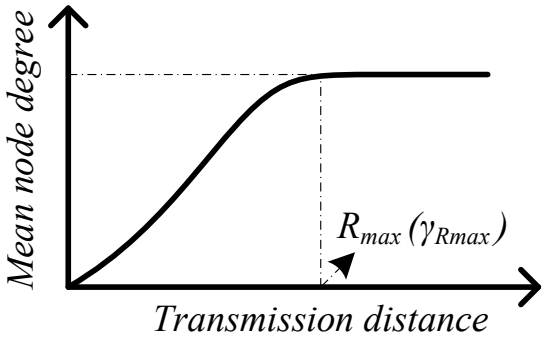

Figure 5.2: Effective transmission distance

distribution, we have:

$$N_C = \rho \cdot \frac{\psi}{2} \cdot R_{max}^2. \tag{5.4}$$

Note that a specific link probability is associated with each link between the source $\mathcal{S}$ and a relay candidate c, according to (2.10).

Let $\mathcal{F}$ denote the forwarding candidate set, which includes all the active nodes in $\mathcal{C}$ that have successfully received the packet from the node $\mathcal{S}$ and compete for forwarding it. N_f presents the average number of nodes in $\mathcal{F}$, which is defined as the *opportunistic mean node degree* in [35] and is computed by:

$$N_f = \int_{s=0}^{R_{max}} s \cdot \rho \cdot \psi \cdot p_l(s) ds. \tag{5.5}$$

Note that $N_f \leq N_C$.

5.2.3 Excepted effective transmission distance

According to the transmission strategy of opportunistic communication, the node c, which is the closest node to $\mathcal{D}$ in $\mathcal{F}$, will act as the relay to forward the packet. We assume that the transmission distance between c and $\mathcal{S}$ is d_{Sc}, the distance between c and $\mathcal{D}$ is d_{Dc} and the distance between $\mathcal{S}$ and $\mathcal{D}$ is d_{SD} as shown in Fig. 5.1. While, from $\mathcal{D}$ viewpoint, the effective transmission distance is $d_{SD} - d_{Dc}$ as shown in Fig 5.1. Following the assumption in [56] that the destination node $\mathcal{D}$ is far away from the $\mathcal{S}$, the arc in Fig 5.1 can be approximated by the straight line. As such, the *effective transmission distance* is obtained by: $d_{tx} = d_{Sc} \cdot \cos(\theta)$ where θ is equal to $\angle cSD$.

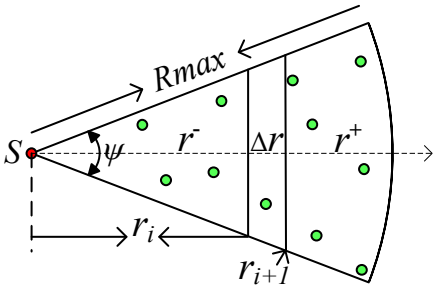

Figure 5.3: The probability of the furthest transmission distance

Definition 5.2.3.1. *The expected effective transmission distance is calculated by:*

$$\overline{d}_{tx} = \int_{r=0}^{R_{max}} \exp\left(\int_{x=r}^{R_{max}} \int_{y=0}^{x\tan(\frac{\psi}{2})} 2\rho \cdot p_l\left(\sqrt{x^2+y^2}\right) dydx\right) \cdot \frac{\int_{y=0}^{r\tan(\frac{\psi}{2})} 2r\rho \cdot p_l\left(\sqrt{r^2+y^2}\right) dy}{1 - e^{-\int_{s=0}^{R_{max}} s\cdot\rho\cdot\psi\cdot p_l(s)ds}} dr.$$

Proof. In order to analyze the expected effective transmission distance for one-hop transmission, we divide the communication sector of $\mathcal{S}$ into three zones: Δr, r^- and r^+, where $\Delta r \to 0$ is located at r_i, as shown in Fig. 5.3.

The expected value of ETD for a reliable transmission including retransmissions is calculated by:

$$\overline{d}_{tx} = \lim_{\Delta r\to 0} \sum_{i=1}^{\infty} r_i P_s(r_i, \Delta r) \cdot P_{iso}(r_i^+) \cdot \frac{1}{1 - P_{iso}(0^+)}, \text{ with } r_{i+1} = r_i + \Delta r, \tag{5.6}$$

where $P_s(r_i, \Delta r)$ is the link probability at the distance r_i, i.e., the probability that at least one node in the zone Δr successfully receives the packet from $\mathcal{S}$; $P_{iso}(r^+)$ is the isolated probability that in , namely, the probability that no node successfully receives the packet from $P_{iso}(r^+)$ in the zone r^+; $P_{iso}(0^+)$ is the probability of failed transmission [35] and is obtained by:

$$P_{iso}(0^+) = \exp\left(-\int_{s=0}^{R_{max}} s\cdot\rho\cdot\psi\cdot p_l(s)ds\right), \tag{5.7}$$

where $p_l(\cdot)$ is link probability defined in (2.10).

$P_{iso}(r^+)$ can be computed by [35]:

$$P_{iso}(r^+) = \exp(-\mu_0(r^+)), \tag{5.8}$$

where $\mu_0(r^+)$ is the opportunistic mean node degree in the zone r^+ [35] as shown in

Fig. 5.3 and is computed by:

$$\mu_0(r^+) = \int_{x=r}^{R_{max}} \int_{y=0}^{x\tan(\frac{\psi}{2})} 2\rho \cdot p_l \left(\sqrt{x^2+y^2}\right) dydx. \tag{5.9}$$

$P_s(r, \Delta r)$ is obtained in the similar way:

$$P_s(r, \Delta r) = 1 - e^{-\mu_0(r,\Delta r)}, \tag{5.10}$$

where $\mu_0(r, \Delta r)$ is the opportunistic mean node degree of node $\mathcal{S}$ in the zone Δr as shown in Fig. 5.3 when $\Delta r \to 0$:

$$\begin{aligned}\mu_0(r, \Delta r) &= \lim_{\Delta r \to 0} \int_{x=r}^{r+\Delta r} \int_{y=0}^{x\tan(\frac{\psi}{2})} 2\rho \cdot p_l \left(\sqrt{x^2+y^2}\right) dxdy \\ &\approx \lim_{\Delta r \to 0} \int_{y=0}^{r\tan(\frac{\psi}{2})} 2\rho \cdot p_l \left(\sqrt{r^2+y^2}\right) dy\Delta r. \end{aligned} \tag{5.11}$$

Substituting (5.11) to (5.10) yields:

$$\begin{aligned}P_s(r, \Delta r) &= 1 - \exp(-\mu_0(r, \Delta r)) \\ &\approx \lim_{\Delta r \to 0} \int_{y=0}^{r\tan(\frac{\psi}{2})} 2\rho \cdot p_l \left(\sqrt{r^2+y^2}\right) dy\Delta r. \end{aligned} \tag{5.12}$$

Integrating all previous analyses, we have the expected effective transmission distance:

$$\begin{aligned}\overline{d}_{tx} = &\int_{r=0}^{R_{max}} \exp\left(\int_{x=r}^{R_{max}} \int_{y=0}^{x\tan(\frac{\psi}{2})} 2\rho \cdot p_l \left(\sqrt{x^2+y^2}\right) dydx\right) \\ &\cdot \frac{\int_{y=0}^{r\tan(\frac{\psi}{2})} 2r\rho \cdot p_l \left(\sqrt{r^2+y^2}\right) dy}{1 - e^{-\int_{s=0}^{R_{max}} s\cdot\rho\cdot\psi\cdot p_l(s)ds}} dr. \end{aligned} \tag{5.13}$$

■

This formula is confirmed by the simulation results depicted in Fig. 5.4. The simulated scenario is described in section 5.4.

5.2.4 Energy consumption models

According to the previous assumptions, the energy consumption for transmitting one packet E_p is composed of three parts: the energy consumed by the transmitter E_{Tx}, by the receiver E_{Rx} and by the acknowledgement packet exchange E_{ACK}:

$$E_p = E_{Tx} + N_C \cdot E_{Rx} + E_{ACK}, \tag{5.14}$$

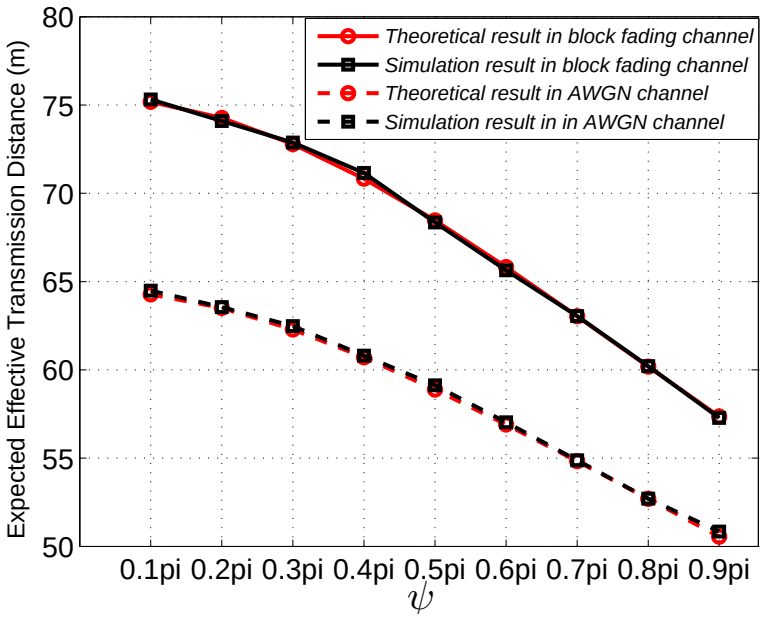

Figure 5.4: The expected effective transmission distance with respect to ψ

The transmission energy model E_{tx} and the receiver energy model E_{rx} [47] are given by (2.2) and (2.3) respectively. During the acknowledgment process, it is assumed that in the period of T_{ACK} an ACK packet can be transmitted to the source node. Furthermore, all the others candidates located in the same communication sector as the ACK sender can detect the ACK packet for the purpose of information exchange about relay selection. The energy expenditure model is given by:

$$E_{ACK} = \tau_{ack} \cdot (E_{tx} + N_C \cdot E_{rx}), \tag{5.15}$$

where τ_{ack} is defined by (2.5).

The mean energy consumption for one-hop successful transmission $\overline{E}_{1hop}$ including retransmissions can be obtained by:

$$\overline{E}_{1hop} = E_p \cdot \overline{N}_{tx} = \frac{E_p}{1 - P_{iso}(0^+)} \tag{5.16}$$

5.2.5 mean Energy Distance Ratio per bit ($\overline{EDRb}$)

In this part, we adopt $\overline{EDRb}$ as a metric of energy efficiency also. Using this metric, the energy efficiency at different transmission distances is measured, so that the optimal energy saving transmission mode can be found. According to its definition, the $\overline{EDRb}$

in opportunistic communications is defined as:

$$\overline{EDRb} := \frac{\overline{E}_{1hop}}{\overline{d}_{tx} \cdot N_b}. \tag{5.17}$$

Note that this metric integrates all factors of physical and link layers.

5.2.6 Delay model

The average delay for a packet to be transmitted over one hop in opportunistic scheme, D_{hop}, is defined as the sum of three delaying components. The first component is the queuing delay during which a packet awaits for being transmitted. The second component is the transmission delay that is equal to N_b/R_b. The third component is T_{ACK}, the time slot during which all nodes wait and receive ACK reply. Note that we neglect the propagation delay because the transmission distance between two nodes is usually short in multi-hop networks.

However, the one-hop delay varies from one link to another due to retransmissions. According to (5.2), the expected delay of a reliable one-hop transmission is:

$$\overline{D} = D_{hop} \cdot \overline{N}_{tx} = \frac{D_{hop}}{1 - P_{iso}}. \tag{5.18}$$

5.3 Minimum energy transmission

One-hop transmissions are the basis of multi-hop communications. In this section, the optimal transmission power, the optimal node density and the corresponding optimal expected ETD of one-hop transmissions are derived in order to optimize the energy efficiency in AWGN and Rayleigh block fading channels. Then, the results are extended to the case of multi-hop transmissions.

5.3.1 Optimization of one-hop transmission

The optimization of the energy efficiency can be abstracted as a nonlinear programming (NP) problem:

$$\begin{aligned} \text{Minimize}: \ & \overline{EDRb} \\ \text{Subject to}: \ & P_t > 0, \rho > 0. \end{aligned} \tag{5.19}$$

The sequential quadratic programming (SQP) method algorithm in [67] is adopted to solve the optimization problem in this works. Fig. 5.5 shows the optimization results in AWGN and Rayleigh block fading channels concerning the different ψ, where the

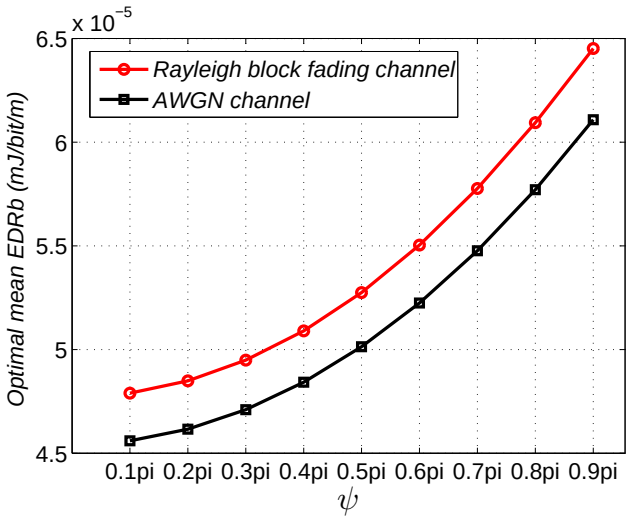

Figure 5.5: Optimal $\overline{EDRb}$ in AWGN and Rayleigh block fading with respect to ψ.

parameters used are given in Table 2.1. The corresponding optimal parameters are provided in Fig. 5.6.

The results in Fig. 5.5 show that the $\overline{EDRb}$ increases energy monotonically, namely, the energy efficiency decreases, in these two kinds of channels with the increase of ψ. Meanwhile, it should be noticed that the $\overline{EDRb}$ in Rayleigh block fading channel is smaller than that in AWGN channel for the same ψ, that is to say, the energy efficiency is improved in Rayleigh block fading channel by opportunistic communications compared with the results in [87]. Moreover, the optimal $\overline{d_{tx}}$ in Rayleigh block fading channel is greater than that in AWGN channel as shown in Fig. 5.6 (c). This result indicates that the opportunistic communication scheme can exploit the benefit of fading.

$\overline{EDRb}$ increases monotonically with the augment of ψ in two kinds of channels. This result suggests that relay candidates should be selected which are close to the linear path between the source and the destination to improve the energy efficiency. In addition, using directional antennas will prove to be more efficient because the antenna gain in (2.11) increases with the reduction of the aperture angle.

Another point should be noted that the links are still unreliable even when there are multiple receivers as shown in Fig. 5.6 (d), which indicates that the trad-off between the multiuser diversity introduced by the opportunistic communications and the temporal diversity introduced inherently by retransmissions exits in the opportunistic communication.

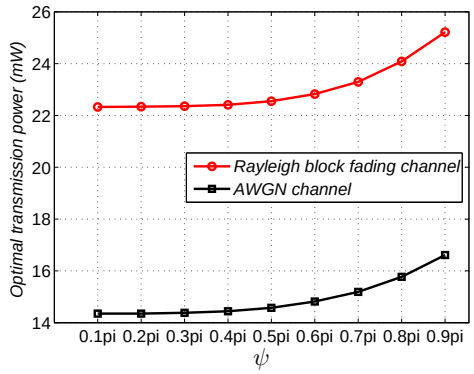

(a) Optimal transmission power Pt_0

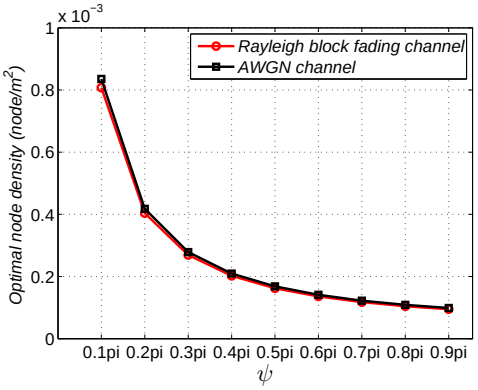

(b) Optimal node density ρ_0

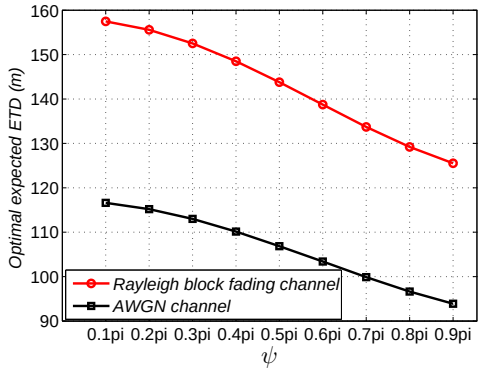

(c) Optimal expected ETD $\overline{d}_{0tx}$

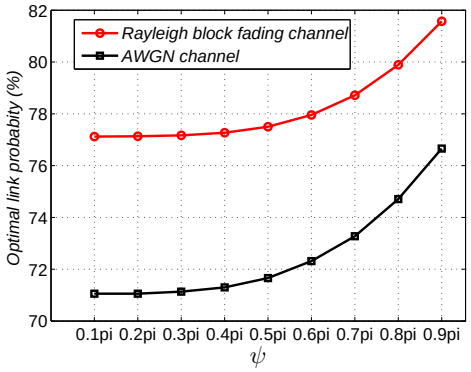

(d) Optimal link probability

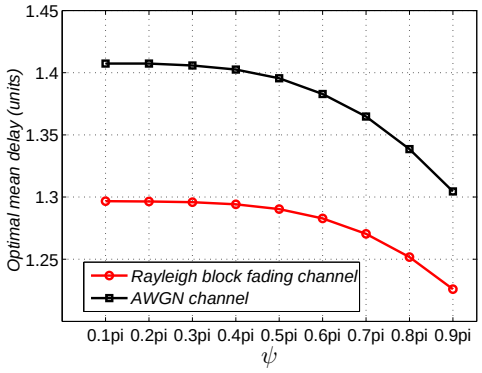

(e) Optimal mean delay $\overline{D}_0$

Figure 5.6: Corresponding optimal parameters for the example in Fig. 5.5.

5.3.2 Analyses of multi-hop transmission

On the basis of the results of one-hop transmission, we can extend the corresponding results to multi-hop transmissions in a scenario of one source and one destination in a fixed distance $d >> \overline{d}_{tx}$.

According to $\overline{d}_{tx}$, the average number of hops is:

$$\overline{N}_{hop} = \frac{d}{\overline{d}_{0tx}}, \tag{5.20}$$

where d_{0tx} is the optimal expected ETD for one-hop transmission. Then the average end-to-end energy consumption $\overline{E}_{e2e}$ and delay $\overline{D}_{e2e}$ are computed respectively by:

$$\overline{E}_{e2e} = \overline{N}_{hop} \cdot \overline{E}_{1hop}(Pt_0, \rho_0). \tag{5.21}$$

$$\overline{D}_{e2e} = \overline{N}_{hop} \cdot \overline{D}_0. \tag{5.22}$$

5.4 Simulations

In the simulations, $\overline{d_{tx}}$ is evaluated in a square area A with the surface area $S_A = 500 \times 500m^2$ in AWGN and Rayleigh block fading channels. The nodes are uniquely deployed according to a Poisson distribution with the density $0.0003\pi/\psi$ for each ψ to keep the P_{iso} constant. BPSK is adopted in the simulations and the bit rate is 1Mbps. In each simulation, the source node $\mathcal{S}$ sends a packet of 2560 bits with a transmission power of $10mW$. The nodes in the communication sector of $\mathcal{S}$ try to receive the packet. In each simulation, the recorded ETD corresponds to the node receiving successfully the packet and being the closest to the destination. The simulations are run 10000 times for each ψ.

The differences between simulation results and theoretical results obtained by (5.13) are smaller than 0.5% as shown in Fig. 5.4, which proofs the correctness of (5.13).

5.5 Summary

Firstly, we propose an analytical framework of opportunistic communication, which provides a method for optimizing the different opportunistic schemes. Meanwhile, the energy efficiency of opportunistic communications with respect to different forwarding areas is studied in regard to the optional transmission power and the optional node density in AWGN and Rayleigh block fading channels. The analyses show that opportunistic communications are more efficient in Rayleigh block fading channel than that in AWGN channel from an energy point of view. Further, the mechanism of selecting the forwarding candidates which locate around the linear path between the source and the destination is more energy efficient than that of selecting all neighbor nodes.

6

Energy-Delay Trade-off of Opportunistic Communications

6.1 Introduction

The energy efficiency performance of opportunistic communications is analyzed in Chapter 5, in which all neighbors in its communication area of a source act as forwarding candidates. The results of Chapter 5 show the importance of selection of relay candidates to the energy efficiency. Therefore, considering the optimal number of forwarding relays, we evaluate the maximal efficiency that can be achieved with such opportunistic routing in this chapter.

Concerning this question, we propose in this chapter to calculate the lower bound of the energy-delay trade-off for opportunistic communications under a hard end-to-end reliability constraint. To compute this bound, we consider the size of candidate cluster and the transmission power as variables of the optimization problem. As stated previously, we focus on the two following questions: what is the best set of relay candidates and what is the performance of the optimized set of candidates?

With regard to the routing policy, we assume that for a given cluster, only the candidate closest to the destination is selected to forward the packet. Such a strategy obviously relies on the assumption that each node has the full knowledge of the position of itself and the destination. Once a node has a packet to send, it appends the locations of itself and the intended relay cluster to the packet, then broadcasts it. The relay

candidates which successfully receive the packet (solid nodes in Fig. 4.1) assess their own priorities of acting as relay, based on how close they are to the destination. The *best relay* which is the closest to the destination relays the packet, as shown in Fig. 4.1. In contrast with the the aforementioned schemes, this scheme utilizes an optimized candidate cluster, instead of all the active neighbors, to receive the packet for the purpose of saving energy and taking advantage of the spatial diversity.

The main contributions of this chapter are:

- A general framework for evaluating the maximal efficiency of the opportunistic routing principle is provided. Energy and delay are compromised under an end-to-end reliability constraint.
- The Pareto front of energy-latency trade-off is derived for different scenarios. A close-form expression of energy-delay tradeoff when the number of relay candidates is fixed, and an algorithm to find the optimal number of relay candidates is proposed. The simulations results verify the correctness of this lower bound in a 2-dimension Poisson distributed network. The numerical analyses show that opportunistic routing is inefficient in AWGN channel, while efficient in Rayleigh block fading channel on the condition of a small cluster size.
- The lower bound of energy efficiency is derived and its corresponding maximal delay is obtained.
- An opportunistic relay selection mechanism is proposed to minimize energy consumption under a delay constraint.

The rest of this chapter is organized as follows: Section 6.2 describes the utilized models and metrics in this chapter. In Section 6.3, the lower bounds of energy-delay tradeoff and energy efficiency are obtained for one-hop transmissions. Then, this result is extended to the scenario of multi-hop transmissions in section 6.4, and the gain of opportunistic communication on energy efficiency is analyzed in this section. The optimization of the physical and protocol layer parameters on the lower bound is presented in Section 6.5. In Section 6.6, the theoretical results about lower bound of energy-delay tradeoff are verified and a new opportunistic protocol is introduced. Section 6.7 discusses the effects of these results and gives some conclusions.

6.2 Models and metric

In this section, we introduce the energy and delay models, the realistic link model and the metric $\overline{EDRb}$ and $\overline{DDR}$ used in this work. The cluster size of relay candidates is given by N_R.

6.2.1 System model

In this thesis, the nodes in a network are assumed to be independently and randomly distributed according to a random Poisson process of density ρ, which is defined in (3.1).

We consider the case of a source node $\mathcal{S}$ forwarding a packet to a sink/destination node $\mathcal{D}$. n_i is one of $\mathcal{S}$'s neighbors which is closer to $\mathcal{D}$ than $\mathcal{S}$.

In addition, each n_i is associated with a pair, (pl_i, d_i), where pl_i is the link probability between n_i and $\mathcal{S}$ which is defined in (2.10) and d_i is the effective transmission distance which is calculated by:

$$d_i = Dist(S, D) - Dist(n_i, D) \tag{6.1}$$

where $Dist(i, D)$ and $Dist(n_i, D)$ are the Euclidian distance between $\mathcal{S}$ and $\mathcal{D}$ and between n_i and $\mathcal{S}$ respectively.

$\mathcal{S}$ has the knowledge of the location of itself, all neighbors and $\mathcal{D}$, and the link probability pl_i. $\mathcal{S}$ selects the forwarding candidate set among all neighbors according to some priority on the basis of these information about neighbors. Let $\mathcal{F}$ denote the forwarding candidate set, which includes all the nodes involved in the local collaborative forwarding and the number of nodes in $\mathcal{F}$ is N_R.

6.2.2 Energy consumption model

According to the models of energy consumption in Chapter 5, the energy consumption per bit is:

$$E_b = \frac{E_p}{N_b} = E_c + K_1 \cdot P_t \tag{6.2}$$

where E_p is defined in (5.14), P_t is the transmission power. Here, $K_1 \cdot P_t$ stands for the radio emission energy and E_c denotes the circuit energy per node, which are obtained by:

$$E_c = (1 + \tau_{ack}) \cdot \left((N_R + 1) \cdot \frac{T_{start} \cdot P_{start}}{N_b} + (1 + \tau_{head}) \left(N_R \frac{P_{rxElec}}{R_b R_{code}} + \frac{P_{txElec}}{R_b R_{code}} \right) \right), \tag{6.3}$$

$$K_1 = (1 + \tau_{ack})(1 + \tau_{head}) \cdot \frac{\beta_{amp}}{R_b R_{code}}, \tag{6.4}$$

where τ_{ack} and τ_{head} are defined in (2.5) and (2.9) respectively, and the related parameters are described in Table 2.1.

6.2.3 Realistic unreliable link models

According to the opportunistic relaying principle, the successful transmission means that at least one node receives the packet correctly. Therefore, for N_R forwarding nodes whose sequence is based on the protocol priority, the probability of a successful transmission is:

$$p_s = \sum_{i=1}^{NR} pl_i \prod_{j=1}^{i-1}(1 - pl_j), \tag{6.5}$$

where pl is the link probability between two nodes and is defined in (2.10).

In this part, retransmissions and acknowledgement mechanism also are adopted in this thesis to ensure a reliable transmission. The mean of transmission $\overline{N}_{tx}$ is:

$$\begin{aligned} \overline{N}_{tx} &= \sum_{n=1}^{\infty} n \cdot p_{sdata} \cdot p_{sack} \cdot (1 - p_{sdata} \cdot p_{sack})^{(n-1)} \\ &= \frac{1}{p_{sdata} \cdot p_{sack}}, \end{aligned} \tag{6.6}$$

where n is the number of transmissions, p_{sdata} and p_{sack} are the successful transmission probability of DATA packet and ACK packet respectively calculated by (6.5).

In the acknowledgment process, as described in Chapter 2 we can assume that $p_{sack} = 1$, in another words, only one ACK packet is sent with high probability of success to the source of the message. Therefore, $\overline{N}_{tx}$ can be approximated by:

$$\overline{N}_{tx} \approx \frac{1}{p_s}, \tag{6.7}$$

where p_s replaces for p_{sdata} for simplification.

6.2.4 mean Energy Distance Ratio per bit ($\overline{EDRb}$)

According to the definition of $\overline{EDRb}$, we have:

$$\overline{EDRb} = \frac{E_b(P_t) \cdot \overline{N}_{tx}}{\overline{d}_{tx}}, \tag{6.8}$$

where $\overline{d}_{tx}$ is the expected transmission distance for opportunistic communication . It should be noticed that this metric integrates all factors of physical and link layers.

Then, we focus on $\overline{d}_{tx}$ [85]:

$$\overline{d}_{tx} = \frac{1}{p_s} \cdot \sum_{i=0}^{N_R} d_i \cdot pl(d_i, P_t) \prod_{j=1}^{i-1}(1 - pl(d_j, P_t)). \tag{6.9}$$

Substituting (6.7), (6.2) and (6.9) into (6.8), we obtain:

$$\overline{EDRb} = \frac{Ec + K_1 P_t}{\sum_{i=0}^{NR} d_i \cdot pl(d_i, P_t) \prod_{j=1}^{i-1}(1 - pl(d_j, P_t))}. \tag{6.10}$$

6.2.5 Delay Distance Ratio ($\overline{DDR}$)

The delay of a packet to be transmitted over one hop, D_{hop}, is defined in (2.23) as the sum of three delay components. The first component is the queuing delay during which a packet waits for being transmitted, T_{queue}. The second component is the transmission delay that is equal to $\frac{N_b}{R_b R_{code}}$. The third component is T_{ACK}. Note that we neglect the propagation delay because the transmission distance between two nodes is usually short in multi-hop networks.

Furthermore, a reliable one-hop transmission will suffer from the delay caused by retransmissions. According to (6.7), the mean delay of a reliable one-hop transmission is:

$$\overline{D}_{hop} = D_{hop}\overline{N}_{tx}. \tag{6.11}$$

$\overline{DDR}$ is adopted as the metric of delay also. It is defined in opportunistic communications as:

$$\overline{DDR} = \frac{D_{hop}\overline{N}_{tx}}{\overline{d}_{tx}} = \frac{D_{hop}}{\sum_{i=0}^{NR} d_i \cdot pl(d_i, P_t) \prod_{j=1}^{i-1}(1 - pl(d_j, P_t))}. \tag{6.12}$$

6.3 Energy-delay trade-off for one-hop transmission

In this section, we analyze the energy-delay trade-off under the reliability constraint in the scenario of one-hop transmission. The optimal transmission power and the optimal number of receivers will be analyzed and the close-form expression of lower bound of energy-delay tradeoff is obtained.

The energy-delay trade-off of one-hop transmission can be abstracted as an optimization problem:

$$\begin{aligned} \text{minimize}: \quad & \overline{EDRb} \\ \text{subject to}: \quad & N_R \geq 1,\ N_R \in Integer, P_t > 0,\ \ \overline{DDR} = ddr, \\ & d_{iopt} > 0\ (i = 1, \ldots N_R)), \end{aligned} \tag{6.13}$$

where ddr is a delay constraint. Consequently, minimizing energy under a delay constraint can be achieved by finding the three parameters $(P_{opt}, N_{Ropt}, d_{iopt}(i = 1, \ldots N_R))$ for one-hop transmission, where P_{opt} is the optimal transmission power, N_{Topt} is the optimal number of opportunistic relay candidates, d_{iopt} is the optimal transmission distance for each relay candidate.

This is a mixed integer nonlinear programming (MILNP) problem. We can solve this optimization problem using the branch-and-bound algorithm [50] in order to find the lower bound of energy-delay tradeoff, but it is time-consumed and complex. In the following part, we will solve this problem to derive this lower bound.

6.3.1 Energy-delay trade-off for a given number of receivers

According to (2.11), we have $d_{hop} = \left(\frac{K_2 P_t}{\bar{\gamma}}\right)^{\alpha}$. In turn, the expressions of (6.10) and (6.12) are converted to the function of P_t and $\bar{\gamma}$ as follows:

$$\overline{DDR}(\langle\bar{\gamma}_i\rangle, P_t, N_R) = \frac{D_{hop}}{(K_2 P_t)^{\frac{1}{\alpha}}} \cdot g(\langle\bar{\gamma}_i\rangle, N_R) \tag{6.14}$$

$$\overline{EDRb}(\langle\bar{\gamma}_i\rangle, P_t, N_R) = \frac{E_c(N_R) + K_1 P_t}{(K_2 P_t)^{\frac{1}{\alpha}}} \cdot g(\langle\bar{\gamma}_i\rangle, N_R) \tag{6.15}$$

where $\langle\bar{\gamma}_i\rangle = \bar{\gamma}_1, \cdots, \bar{\gamma}_i, \cdots \bar{\gamma}_{N_R}$ and

$$g(\langle\bar{\gamma}_i\rangle, N_R) = \frac{1}{\sum_{i=0}^{N_R} \bar{\gamma}_i^{-\frac{1}{\alpha}} \cdot pl(\bar{\gamma}_i) \prod_{j=1}^{i-1}(1 - pl(\bar{\gamma}_j))}. \tag{6.16}$$

First, we consider the scenario that N_R is fixed.

Theorem 4. *When N_R is a constant, the lower bound of energy-delay trade-off is provided by the equations (6.14) and (6.15) if the minimum value of $g(\langle\bar{\gamma}_i\rangle)$ is obtained.*

Proof. Refer to the proof of Theorem 3. ■

According to (6.15) and (6.14), we get the relation between $\overline{EDRb}$ and $\overline{DDR}$:

$$\overline{EDRb}(\langle\bar{\gamma}_i\rangle, P_t) = \frac{\overline{DDR}(\langle\bar{\gamma}_i\rangle, P_t)}{D_{hop}} \cdot (E_c + K_1 P_t) \tag{6.17}$$

On the basis of Theorem 4, we obtain the lower bound of energy-delay trade-off when we minimize $g(\langle\bar{\gamma}_i\rangle)$. Finally, when the N_R is fixed, the lower bound of energy-delay trade-off is:

$$\overline{EDRb}(\langle\bar{\gamma}_{iopt}\rangle, P_t) = \frac{\overline{DDR}(\langle\bar{\gamma}_{iopt}\rangle, P_t)}{D_{hop}} \cdot (E_c + K_1 P_t) \tag{6.18}$$

where $\langle\bar{\gamma}_{iopt}\rangle$ are the whole value of $\langle\bar{\gamma}_i\rangle$ minimizing $g(\langle\bar{\gamma}_i\rangle)$.

Next, we analyze how to obtain the minimum value of $g(\langle\bar{\gamma}_i\rangle)$.

Theorem 5. *For a given N_R nodes whose corresponding $\bar{\gamma}$ is $\bar{\gamma}_1, \ldots, \bar{\gamma}_{N_R}$, the minimum value of $g(\langle\bar{\gamma}_i\rangle)$ can only be obtained by giving the higher relay priority to the node whose $\bar{\gamma}$ is smaller.*

Proof. Refer to Appendix B. ■

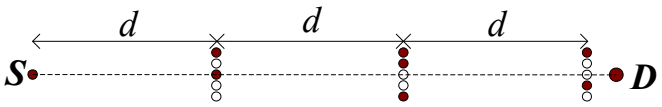

Figure 6.1: Approximation solution

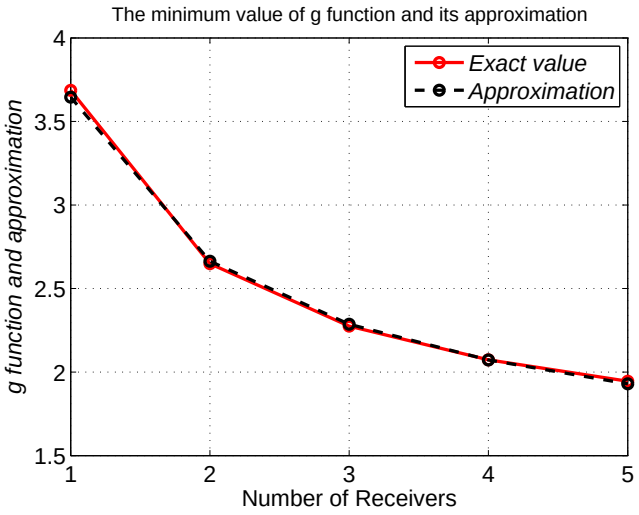

Figure 6.2: Approximation of the minimum value of $g(\langle\bar{\gamma}_{iopt}\rangle)$

According to Theorem 5, the minimum value of $g(\langle\bar{\gamma}_i\rangle)$ can be calculated by optimizing each $\bar{\gamma}_i$, but we can not find the close-form expression of $\overline{EDRb}$ if using the exact expression of $g(\langle\bar{\gamma}_{iopt}\rangle)$ directly. Therefore, in order to get the close-form expression of $\overline{EDRb}$, we introduce the approximation of $g(\langle\bar{\gamma}_{opti}\rangle)$ where we assume the N_R receivers has the same effective transmission distance d and are deployed around the line between a source node and a destination node as shown in Fig. 6.1. $g(\langle\bar{\gamma}_{opti}\rangle)$ is approximated by:

$$\widetilde{g}(\bar{\gamma}_{opt}) = \frac{\left(1+\frac{N_R}{90}\right)\cdot\bar{\gamma}_{opt}^{\frac{1}{\alpha}}}{1-(1-pl(\bar{\gamma}_{opt}))^{N_R}} \tag{6.19}$$

Fig. 6.2 shows the exact value of minimum $g(\langle\bar{\gamma}_{opti}\rangle)$ and its approximation, $\widetilde{g}$, in the same condition. Note that the difference between the exact value and the approximation is very small. Therefore, we use $g(\langle\bar{\gamma}_{opti}\rangle)$ to analyze $\overline{EDRb}$ and $\overline{DDR}$ in the following part.

The minimum value of $\widetilde{g}(\bar{\gamma})$ is available by solving $\frac{\partial\widetilde{g}(\bar{\gamma})}{\partial\bar{\gamma}} = 0$. Thus, we get:

$$\bar{\gamma}_{opt} = \frac{1-(1-pl(\bar{\gamma}_{opt}))^{N_R}}{\alpha\cdot N_R\cdot(1-pl(\bar{\gamma}_{opt}))^{N_R-1}\cdot pl'(\bar{\gamma}_{opt})} \tag{6.20}$$

where $pl'(\cdot)$ is the derivation of $pl(\cdot)$. (6.20) implies the close-form expression of $\bar{\gamma}_{opt}$ tightly depends on $pl(\cdot)$, thus we should consider different channels.

First, we focus on AWGN, Rayleigh flat fading and Rayleigh block fading channels, then, a general solution of obtaining $\widetilde{g}$ is given for all other scenarios.

The unreliable link models are provided by (2.15), (2.19) and (2.18) for AWGN, Rayleigh flat fading channel and Rayleigh block fading channel respectively.

Substituting (2.15), (2.18) and (2.19) into (6.20) respectively yields $\bar{\gamma}_{opt}$ in different channels:

AWGN

$$\gamma_{optg} = \frac{1}{0.5418\beta_m} \ln \left(\frac{0.1826\alpha_m}{1 - \left(1 - \left(-\alpha \mathrm{W}_{-1}\left(\frac{(0.1826 N_b \alpha_m)^{-NR}}{-\alpha}\right)\right)^{-\frac{1}{N_R}}\right)^{\frac{1}{N_b}}} \right) \tag{6.21}$$

where $\mathrm{W}_{-1}[\cdot]$ is the branch of the Lambert W function satisfying $\mathrm{W}(x) < -1$ [16].

Rayleigh block fading channel

$$\bar{\gamma}_{optb} = \frac{-4.25 \log_{10}(N_b) + 2.2}{\beta_m \ln\left(1 - \left(\frac{1}{\alpha N_R}\right)^{\frac{1}{NR}}\right)} \tag{6.22}$$

Rayleigh flat fading channel

$$\bar{\gamma}_{optf} = \frac{\alpha_m}{2\beta_m \left(1 - \left(1 - \left(\frac{1}{1+\alpha N_R}\right)^{\frac{1}{N_R}}\right)^{\frac{1}{N_b}}\right)} \tag{6.23}$$

Substituting $\bar{\gamma}_{optg}$, $\bar{\gamma}_{optb}$ and $\bar{\gamma}_{optf}$ into (6.19) respectively yields $\widetilde{g}(\bar{\gamma}_{opt})$ in the three kinks of channel. Except the above channels mentioned, there are a lot of scenarios in which we can not find the close-form expression of $\bar{\gamma}_{opt}$ and $\widetilde{g}(\bar{\gamma}_{opt})$, which will be presented in the following part.

Other scenarios

Besides the scenarios that the close-form expression of $\bar{\gamma}_{opt}$ can be obtained, there are other cases where $\bar{\gamma}_{opt}$ and $\widetilde{g}(\bar{\gamma}_{opt})$ have to be calculated by other methods.

The first case is the expression of link probability could be obtained but it is different to deduce the close-form expression of $\bar{\gamma}_{opt}$. For example, the type of channel is Nakagami block fading channel and a coding scheme is employed. In this kind of situation, the sequential quadratic programming (SQP) method algorithm in [67] can

be adopted to solve the optimization problem of minimizing $\widetilde{g}(\bar{\gamma})$. Then the exact value of $\bar{\gamma}_{opt}$ and $\widetilde{g}(\bar{\gamma}_{opt})$ are obtained.

Another case is that we are not able to get the expression of link probability. As for this situation, we have to measure the value of $\widetilde{g}(\bar{\gamma}_{opt})$. The searching method is:

- Set a transmission power, for example, 0dB.
- Measure the value of $pl(\bar{\gamma})$ and the corresponding $\bar{\gamma}$ in different distance and try to find its maximum value, i.e., $max((1-(1-pl)^{N_R})\cdot d_{hop})$ and recode the corresponding $\bar{\gamma}$.
- Calculate the value of $g(\bar{\gamma})$ according to (6.19) and find the minimum value of $\widetilde{g}(\bar{\gamma})$ and the corresponding $\bar{\gamma}_{opt}$.

So far, the value $\widetilde{g}(\bar{\gamma}_{opt})$ can be obtained in any condition.

Then, substituting $\widetilde{g}(\bar{\gamma}_{opt})$ in (6.14) yields the optimal transmission power for a delay constraints ddr:

$$P_{opt}(N_R) = \frac{1}{K_2}\cdot\left(\frac{D_{hop}}{ddr}\cdot\widetilde{g}(\bar{\gamma}_{opt},N_R)\right)^{\alpha}. \tag{6.24}$$

According to (2.11) and (6.24), we have the equivalent optimal transmission distance:

$$d_{opt}(N_R) = \left(\frac{K_2 P_{opt}}{\bar{\gamma}_{opt}}\right)^{\frac{1}{\alpha}} = \frac{\widetilde{g}(\bar{\gamma}_{opt},N_R)\cdot D_{hop}}{\bar{\gamma}_{opt}^{1/\alpha}\cdot ddr}. \tag{6.25}$$

Then, substituting $\widetilde{g}(\bar{\gamma}_{opt})$ in (6.18), we obtain the lower bound of energy-delay tradeoff in the scenario of fixed N_R.

$$\overline{EDRb}_{opt}(N_R) = E_c(N_R)\cdot\frac{ddr}{D_{hop}} + \widetilde{g}(\bar{\gamma}_{opt},N_R)^{\alpha}\cdot\frac{K_1}{K_2}\cdot\left(\frac{ddr}{D_{hop}}\right)^{1-\alpha}. \tag{6.26}$$

6.3.2 Optimal number of receivers

In previous subsection, the lower bound of energy delay tradeoff is obtained in the scenario that the number of receivers is fixed. In this subsection, we will analyze how to select the optimal number of receivers for a given ddr.

Theorem 6. *$\overline{EDRb}$ is a convex function with respect to N_R.*

Proof. Refer to Appendix C. ■

Theorem 6 implies the minimum value of $\overline{EDRb}$ exists and this value is global minimum value. In addition, P_{opt} is calculated by (6.24) under a delay constraint ddr. Therefore, we can find the minimum value of $\overline{EDRb}$ for a given delay constraint ddr

by searching the optimal number of receivers and . The searching algorithm is given in Algorithm 1.

Algorithm 1 Search the optimal number of receivers N_{Ropt}

$N_R \leftarrow 1$, $\overline{EDRb}1 \leftarrow Inf$, $flag \leftarrow 0$, ddr
while $flag == 0$ **do**
  Calculate $\widetilde{g}(\bar{\gamma}_{opt}, N_R)$
  $\overline{EDRb} \leftarrow E_c(N_R) \cdot \frac{ddr}{D_{hop}} + \widetilde{g}(\bar{\gamma}_{opt}, N_R)^{\alpha} \cdot \frac{K_1}{K_2} \cdot \left(\frac{ddr}{D_{hop}}\right)^{1-\alpha}$
  if $\overline{EDRb} > \overline{EDRb}1$ **then**
    $flag \leftarrow 1$, $N_{Ropt} \leftarrow N_R - 1$
    return N_{Ropt}
  else
    $\overline{EDRb}1 \leftarrow \overline{EDRb}$, $N_R \leftarrow N_R + 1$
  end if
end while

6.3.3 Lower bound of energy-delay tradeoff

we obtain N_{Ropt}, P_{opt} and d_{opt} under a delay constraint ddr in the above subsections, then we have the lower bound of energy-delay tradeoff for one-hop transmission with opportunistic communication:

$$\overline{EDRb}_{opt} = E_c(N_{Ropt}) \cdot \frac{ddr}{D_{hop}} + \widetilde{g}(\bar{\gamma}_{opt}, N_{Ropt})^{\alpha} \cdot \frac{K_1}{K_2} \cdot \left(\frac{ddr}{D_{hop}}\right)^{1-\alpha}. \tag{6.27}$$

Substituting N_{Ropt} into (6.24) and (6.25), we obtain the corresponding optimal transmission power and distance.

Similar to Chapter 2, in order to obtain Pareto front of energy-delay tradeoff, the lowest point will be derived in following subsection.

6.3.4 Minimum energy consumption

In this section, as to the lowest point, we derive the lower bound of energy efficiency and corresponding energy-optimal transmission power and distance without the delay constraints.

Optimal transmission power

Assuming N_R is constant, in order to get the minimum value of $\overline{EDRb}$, it is obvious that we should minimize $\widetilde{g}(\bar{\gamma})$ and $f(P_t) = \frac{E_c(N_R)+K_1P_t}{(K_2P_t)^{\frac{1}{\alpha}}}$ at the same time in (6.15). Letting $\bar{\gamma} = \gamma_{opt}$, we have $g(\gamma_{opt})$.

Employing Lagrange algorithm, we have:

$$\frac{d}{dP_t}\left(\frac{E_c + K_1 P_t}{(K_2 P_t)^{\frac{1}{\alpha}}}\right) = 0. \tag{6.28}$$

Solving the above equation yields:

$$P_0(N_R) = \frac{E_c(N_R)}{(\alpha - 1)\cdot K_1}. \tag{6.29}$$

which is the transmission power minimizing $f(P_t)$. Substituting (6.3) and (6.4) into (6.29) yields:

$$P_0(N_R) = \frac{(N_R + 1)\cdot T_{start}\cdot P_{start}}{\beta_{amp}\cdot(\alpha-1)\cdot\frac{N_b}{R_b R_{code}}} + \frac{N_R P_{rxElec} + P_{txElec}}{\beta_{amp}\cdot(\alpha-1)}, \tag{6.30}$$

where $\frac{N_b+N_{head}}{R_b R_{code}}$ is the transmission duration of a packet. Since $\frac{N_b+N_{head}}{R_b R_{code}} \gg T_{start}$ generally, the first part of (6.30) can be neglected. Thus, we get:

$$P_0(N_R) \approx \frac{N_R P_{rxElec} + P_{txElec}}{\beta_{amp}\cdot(\alpha-1)}. \tag{6.31}$$

It should be noted that P_0 is tightly related with N_R, so that we should apply Algorithm 1 to find the optimal number of receivers N_{R0} which is tightly related to the modulation, the type of channel of a network. Then, substituting N_{R0} into yields:

$$P_0 \approx \frac{N_{R0} P_{rxElec} + P_{txElec}}{\beta_{amp}\cdot(\alpha-1)}. \tag{6.32}$$

Meanwhile, (6.32) also shows that the characteristics of the amplifier have a strong impact on P_0. When the efficiency of the amplifier is high, i.e., $\beta_{amp} \to 1$, P_0 reaches its maximum value. As well, it is clear that when the environment of transmission deteriorates, namely, α increases, P_0 decreases correspondingly. However, P_0 is independent of τ_{ack}.

Lower bound of $\overline{EDRb}$ and its corresponding delay

The lower bound of $\overline{EDRb}$ is obtained by substituting (6.19) and (6.32) into (6.15):

$$\overline{EDRb}_0 = \frac{E_c(N_{R0}) + K_1 P_0}{(K_2 P_0)^{\frac{1}{\alpha}}}\cdot\widetilde{g}(\bar{\gamma}_{opt}, N_{R0}) \tag{6.33}$$

Based on this result, we can set the transmission power of node according to (6.32) to minimize the total energy consumption for the applications without delay request. Moreover, the transmission power of a node should not be smaller than this value, otherwise the node will be running in an inefficient state as shown on the right side

curve of the lowest point in Fig. 6.3, Fig. 6.4 and Fig. 6.5.

Moreover, on the basis of (6.14) and P_0, the maximal mean delay is obtained:

$$\overline{D}_{max} = d_{SD} \cdot \frac{D_{hop}}{(K_2 P_0)^{\frac{1}{\alpha}}} \cdot \widetilde{g}(\bar{\gamma}_{opt}, N_{R0}), \tag{6.34}$$

where d_{SD} is the distance between a source node and a destination node.

Minimum mean transmission distance

By P_0, $\bar{\gamma}_{opt}$ and (2.11), we obtain the minimal mean transmission distance:

$$d_0 = \left(\frac{K_2 P_0}{\bar{\gamma}_{opt}} \right)^{\frac{1}{\alpha}} \tag{6.35}$$

This distance shows the minimal distance between a source node and a destination node, otherwise, too small hop distance results in more energy consumption or too many hops, namely, too much delay.

6.3.5 Energy-delay tradeoff in different channels

According to the analyses in previous subsections, we obtain P_{opt} and N_{Ropt} under a delay constraint ddr, then we have the lower bound of energy-delay tradeoff for one-hop transmission with opportunistic communication, (6.27). Because (N_{Ropt}, P_{opt}, d_{opt}) tightly depends on the function of link probability, $pl(\cdot)$, we analyze the lower bound of energy-delay tradeoff in three different channels mentioned in this section.

Fig.6.3, Fig. 6.4 and Fig. 6.5 show the lower bound of energy-delay tradeoff and the corresponding optimal transmission power and the optimal number of receivers in three kinds of channels on the basis of (6.27). It should be noticed that the lowest point exists in each curve, this is to say, there is the most energy saving point without the delay constraints for each channel and the corresponding mean delay is the maximum mean delay of a pair of nodes. In Section 6.3.4, we will analyze the most energy saving point in detail. The left side of the lowest point shows the energy consumption increases with the decrease of the delay constraint which coincides with our intuition. However, in the right of the lowest point, the energy consumption increases with the increase of the delay because both the transmission power and the number of receives are too small which results in very small hop distance, i.e., the increase of the hop number. Certainly, this is a work state should be avoided in practice.

It should be noted that the the optimal number of receivers corresponding to the lowest point in each curve is 2 in Rayleigh block fading channel and flat fading channel and is 1 in AWGN channel. The result implies that too many nodes will lead to the

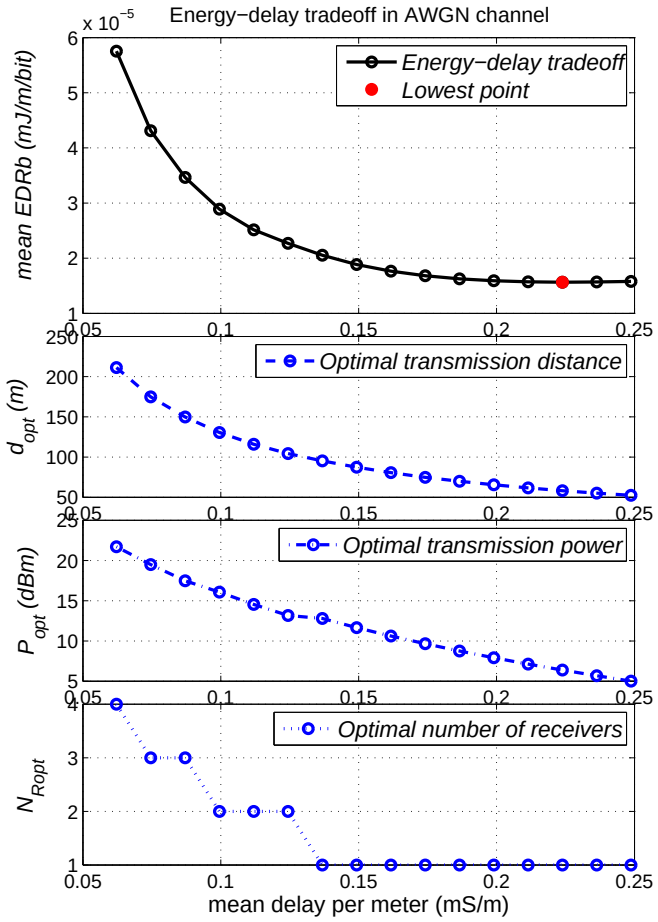

Figure 6.3: Lower bound of energy-delay tradeoff in AWGN channel

waste of energy, this is to say, we should avoid acting all neighbor nodes as the relay candidates. In addition, the optimal number of receivers raises with the decrease of delay limit. AS for the corresponding optimal transmission power, it is not monotonically decrease as we saw in traditional P2P communications. Conclusively, it is clear that the transmission power and the number of relay candidates should be adjusted correctly according to a delay constraint in order to avoid too much energy consumption. Algorithm 1 and (6.24) provide the approach to calculate the optimal transmission power and a distributed algorithm to select the optimal relay candidates will be introduced in Section 6.6.

Though the lower bound on the energy-delay trade-off is derived in linear networks, it will be shown by simulations in the following section 6.6 that this bound is proper for 2-dimensional Poisson distributed networks.

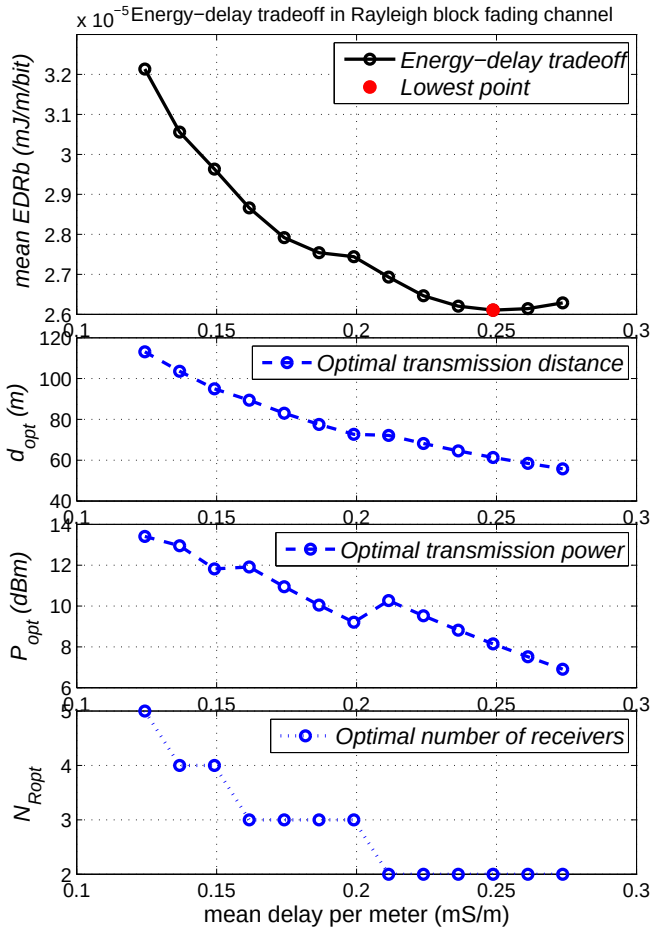

Figure 6.4: Lower bound of energy-delay tradeoff in Rayleigh block fading channel

6.4 Energy-delay trade-off of multi-hop transmission

In this section, we extend the result of one-hop transmission in Section 6.3 to the scenarios of multi-hop transmission. Meanwhile, the energy efficiency gain of opportunistic communication are analyzed.

6.4.1 Lower bound of energy-delay tradeoff

The lower bound of energy-delay trade-off can be abstracted as an optimization problem:

$$\text{minimize}: \ \overline{E}_{tot} \quad \text{subject to}: \ \overline{D}_{tot} = \text{delay constraint}, \tag{6.36}$$

where $\overline{E}_{tot}$ and $\overline{D}_{tot}$ are the end to end energy consumption and delay between a source node and a destination node.

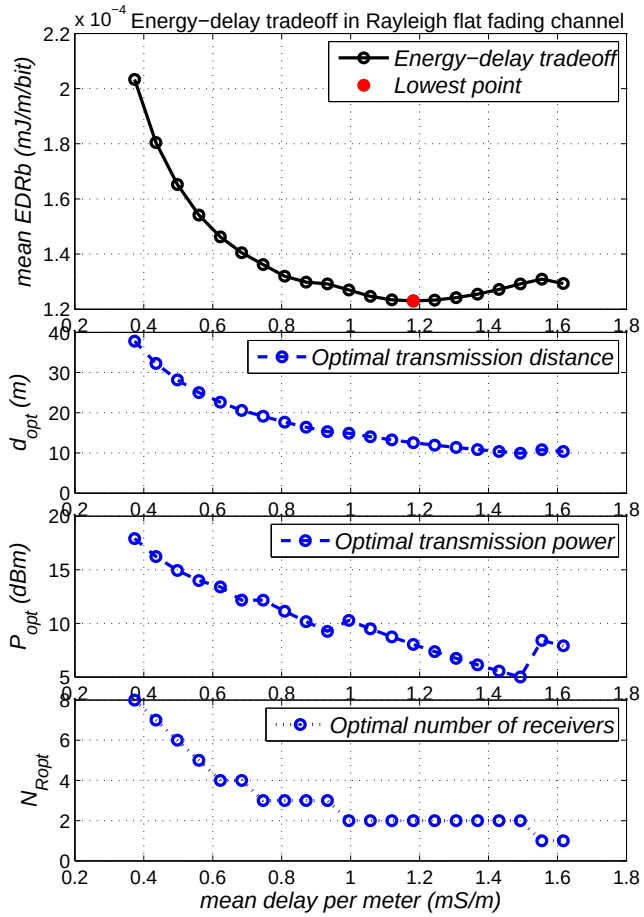

Figure 6.5: Lower bound of energy-delay tradeoff in Rayleigh fading channel

In order to obtain the low bound of energy-latency trade-off of multi-hop transmission, the theorems about *equivalent distance transmission* are introduced as follows:

Theorem 7. *In an homogeneous network, a source node x sends a packet of N_b bits to a destination node x' using n hops in opportunistic communication mode. The n relaying clusters are located around (x, x') line, as shown in Fig. 6.1, and each cluster has the same number of relay candidates N_R. The distance between x and x' is d. The length of each hop is d_1, d_2, ..., d_n respectively, and the average EDRb is denoted as $\overline{EDRb}(d)$. The minimum mean total energy consumption $\overline{Etot}_{min}$ is obtained if and only if $d_1 = d_2 = \ldots = d_n$:*

$$\overline{Etot}_{min} = N_b \cdot \overline{EDRb}(d/n) \cdot d. \tag{6.37}$$

Proof. The mean energy consumption for each hop of index m is set to $\overline{E}_m = N_b \cdot \overline{EDRb}(d_m) \cdot d_m$, $m = 1, 2, \ldots, n$. Since each hop is independent from the other hops,

the mean total energy consumption is $\overline{Etot} = \overline{E}_1 + \overline{E}_2 + \ldots + \overline{E}_n$. Hence, the problem of finding the minimum mean total energy consumption can be rewritten as:

$$\begin{array}{ll} \text{minimize} & \overline{Etot} \\ \text{subject to} & d_1 + d_2 + \ldots + d_n = d. \end{array}$$

Set

$$F = \overline{E}_1 + \overline{E}_2 + \ldots + \overline{E}_n + \lambda(d_1 + d_2 + \ldots + d_n - d),$$

where $\lambda \neq 0$ is the Lagrange multiplier.

According to the method of the Lagrange multipliers, we obtain:

$$\begin{cases} \dfrac{\partial \overline{E_1}}{\partial d_1} + \lambda = 0 \\ \ldots \\ \dfrac{\partial \overline{E_n}}{\partial d_n} + \lambda = 0 \\ d_1 + d_2 + \ldots + d_n = d \end{cases} \tag{6.38}$$

(6.38) shows that the minimum value of F is obtained in the case: $\frac{\partial \overline{E_1}}{\partial d_1} = \ldots = \frac{\partial \overline{E_n}}{\partial d_n} = -\lambda$. Moreover, in a homogeneous linear network, the properties of each node are identical. Therefore,

$$\overline{E_m} = \overline{EDRb}(d_m) \cdot d_m = (E_c + \frac{K_1 \bar{\gamma}_{opt}}{K_2} d_m^{\alpha}) \cdot \frac{g(\bar{\gamma}_{opt})}{\bar{\gamma}_{opt}^{\frac{1}{\alpha}}} \tag{6.39}$$

Because

$$\frac{\partial^2 \overline{E_m}}{\partial^2 d_m} = \alpha \cdot (\alpha - 1) d^{\alpha - 2} \frac{K_1 \bar{\gamma}_{opt}}{K_2} \cdot \frac{g(\bar{\gamma}_{opt})}{\bar{\gamma}_{opt}^{\frac{1}{\alpha}}} > 0 \tag{6.40}$$

when $\alpha > 1$, we deduce $\frac{\partial \overline{E}}{\partial d}$ is a monotonic increasing function of d when the path-loss exponent follows $\alpha > 1$. Therefore, the unique solution of Eq. (6.38) is $d_1 = d_2 = \ldots = d_n = \frac{d}{n}$. Finally, we obtain:

$$\overline{Etot}_{min} = N_b \cdot \overline{EDRb}(d/n) \cdot d.$$

■

Theorem 8. *On the same assumption as Theorem 7, the mean delay of one-hop transmission is referred to as $\overline{D}(d)$. The minimum mean end-to-end delay $\overline{Dtot}_{min}$ is given by:*

$$\overline{Dtot}_{min} = \overline{D}(d/n) \cdot n \tag{6.41}$$

if and only if $d_1 = d_2 = \ldots = d_n$.

Proof. The theorem can be proved in the same way as shown in Theorem7. this theorem is valid if and only if $\frac{\partial \overline{D}}{\partial d}$ is a monotonic increasing function of d which holds with the attenuation model in (2.11).

$$\overline{D}(d) = DDR \cdot d = \frac{D_{hop}}{p_s(d)}$$

$$\frac{\partial^2 \overline{D}(d)}{\partial^2 d} = D_{hop}\left(\frac{2(p_s'(d))^2}{p_s(d)^3} - \frac{p_s''(d)}{p_s(d)}\right) > 0 \tag{6.42}$$

where $p_s'(d))$ and $p_s''(d)$ are the first and second derivative of (6.5) with respect to d. Because $p_s'(d)) < 0$ and $p_s''(d) < 0$ in case of $\alpha \geq 2$ in many practical scenarios, (6.42) is great than 0. Thus, $\frac{\partial \overline{D}}{\partial d}$ is a monotonic increasing function with respect to d. ■

Based on Theorem 7 and 8, we conclude that, regarding a pair of source and destination nodes with a given number of hops, the single scenario, which minimizes both mean energy consumption and mean transmission delay, is that each hop with uniform distance along a linear path. As a result, the optimization about energy and delay for a single hop will bring the optimization of the same performance for the multi-hop transmission. Hence, the results about the lower bound of energy-delay tradeoff in Section 6.3 can be used directly in multi-hop transmission.

6.4.2 Gain of opportunistic communication

We analyze the gain of opportunistic communication in energy efficiency compared with traditional multi-hop communications in this subsection. The benefit of opportunistic communication in terms of energy efficiency, as shown in Fig. 6.6, is measured with the energy gain defined as:

$$Gain = \frac{\overline{EDRb}_{p2p} - \overline{EDRb}_{opp}}{\overline{EDRb}_{p2p}}. \tag{6.43}$$

Here, $\overline{EDRb}_{p2p}$ is the optimal $\overline{EDRb}$ under a delay constraint ddr in traditional multi-hop communications, which is obtained according to the approach proposed in Chapter 2, and $\overline{EDRb}_{opp}$ is referred to as the optimal $\overline{EDRb}$ under the same delay constraint using opportunistic communications obtained by (6.27).

Fig. 6.6 provides an example in three kinds of channel and the physical parameters are shown in Table 2.1. In this example, the gain of opportunistic communications decrease from 25% to 0 with the increase of the delay constraint. The gain becomes 0 when the delay constraint is greater than $0.11mS/m$ which implies that the opportunistic communication has changed to the traditional multi-hop communication which is coincide with the result in Fig. 6.3, where the optimal number of receivers becomes

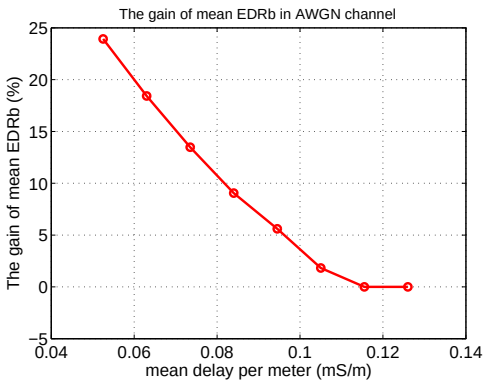

(a) AWGN channels

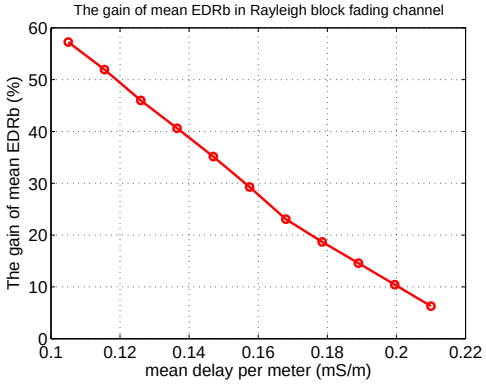

(b) Rayleigh block fading channel

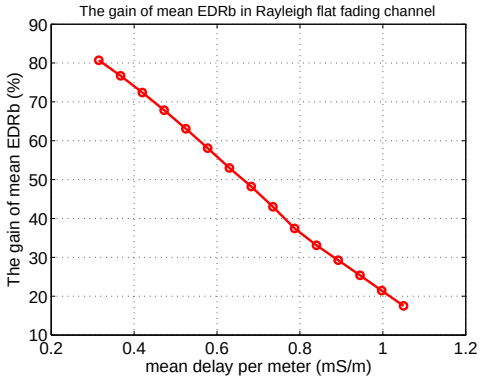

(c) Rayleigh flat fading channel

Figure 6.6: Comparison between P2P and opportunistic communications

1 for the corresponding delay constraint. In other words, when the delay constraint is greater than a threshold, traditional multi-hop communications are more energy efficiency than opportunistic communications in AWGN channel.

In Rayleigh block fading channel and Rayleigh flat fading channel the gain of opportunistic communication is always greater than 0 which reveals the opportunistic communication outperforms traditional multi-hop communications in these two kinds of channel. Obviously, opportunistic routing benefits from the effect of diversity and improves the energy efficiency. While, the gain decrease with the increase of the delay constraint.

According to these results, it can be concluded that opportunistic communications are more energy efficient for fading channels than for AWGN channels.

6.5 Effect of parameters

On the basis of (6.27), the effects of physical layer and protocol layer parameters on the lower bound of energy-delay trade-off are studied in this section. All related parameters are provided in Table 2.1 except the parameters mentioned especially for analyzing.

6.5.1 The effect of physical layer parameters

Circuitry power

According to the definition of $\overline{EDRb}$ (6.10) and (6.3) (6.4), it is deduced easily that the increase of circuitry power leads to the increment of total energy consumption which coincides with our intuition. Meanwhile, E_c is independent of P_{opt} and d_{opt} under a delay constraint. Therefore, we should reduce the circuitry power in the design of sensor node and should select a node which has minimum circuitry power.

Channel coding

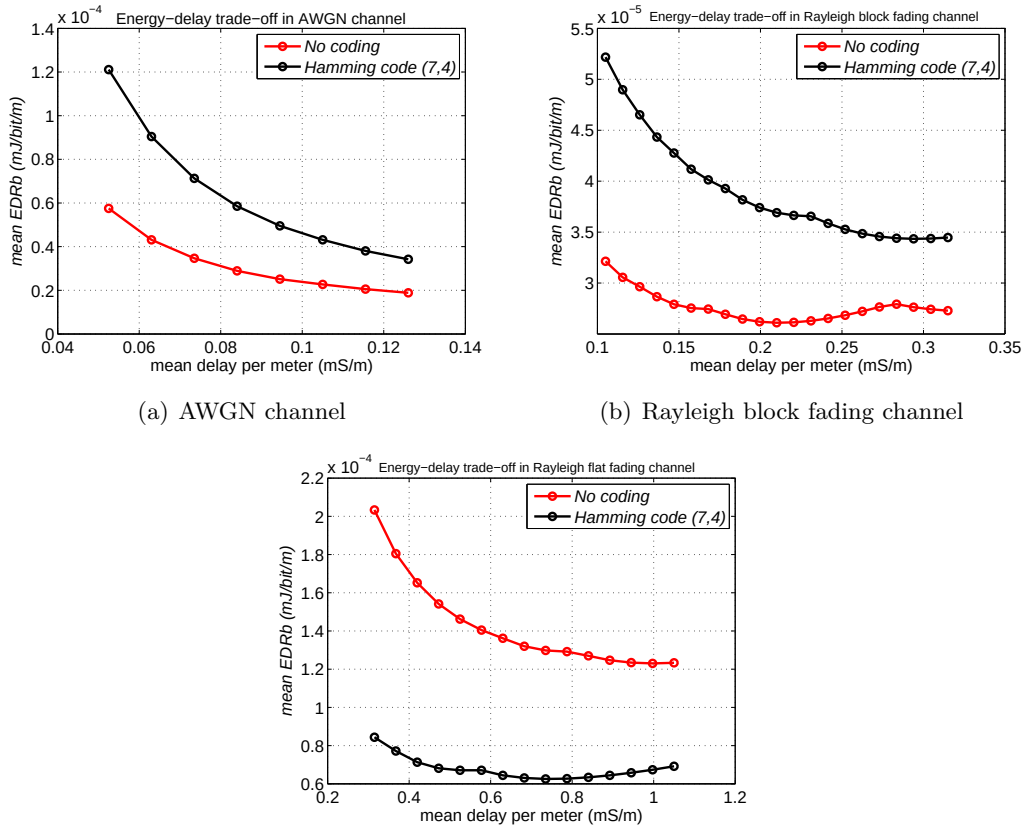

(a) AWGN channel

(b) Rayleigh block fading channel

(c) Rayleigh flat fading channel

Figure 6.7: Effect of coding on energy-delay trade-off in different channels

Coding can reduce the probability of bit or block error but introduce more bits resulting to more energy consumption. What is the benefit of coding in the viewpoint of energy-delay trade-off will be revealed in the following part in three kinds of channels. Here, Hamming code $(7, 4)$ is used as an example. The results in Fig. 6.7 indicate that this kind of coding brings some benefit in both energy and delay in Rayleigh flat fading channel, however, introduces more energy and delay in AWGN channel and Rayleigh block fading channel. Therefore, it is dependent on the type of channel to decide if a coding scheme should be used.

Modulation

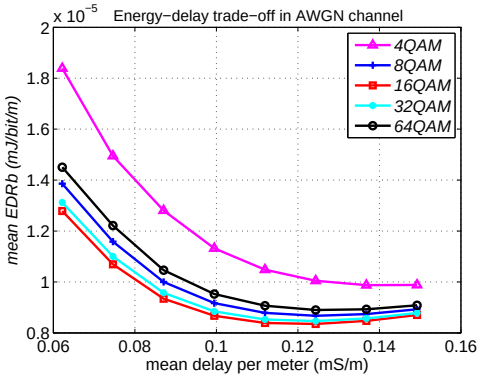

(a) AWGN channel

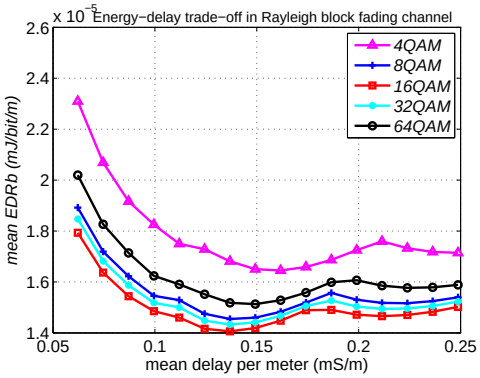

(b) Rayleigh block fading channel

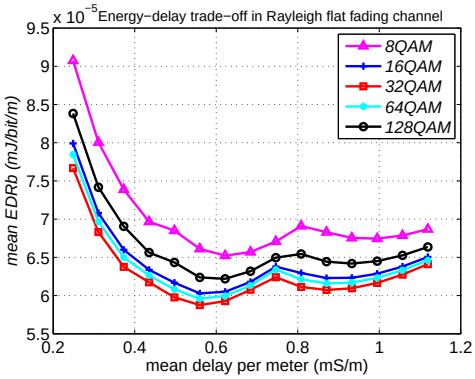

(c) Rayleigh flat fading channel

Figure 6.8: Effect of modulation on energy-delay trade-off in different channels

High order modulation brings high BER but reduces the transmission time and energy when in the same symbol rate due to the increase of bit rate. The effect of modulation on the lower bound of energy-delay trade-off in three kinds of channel is shown in Fig. 6.8.

Transmission Rate

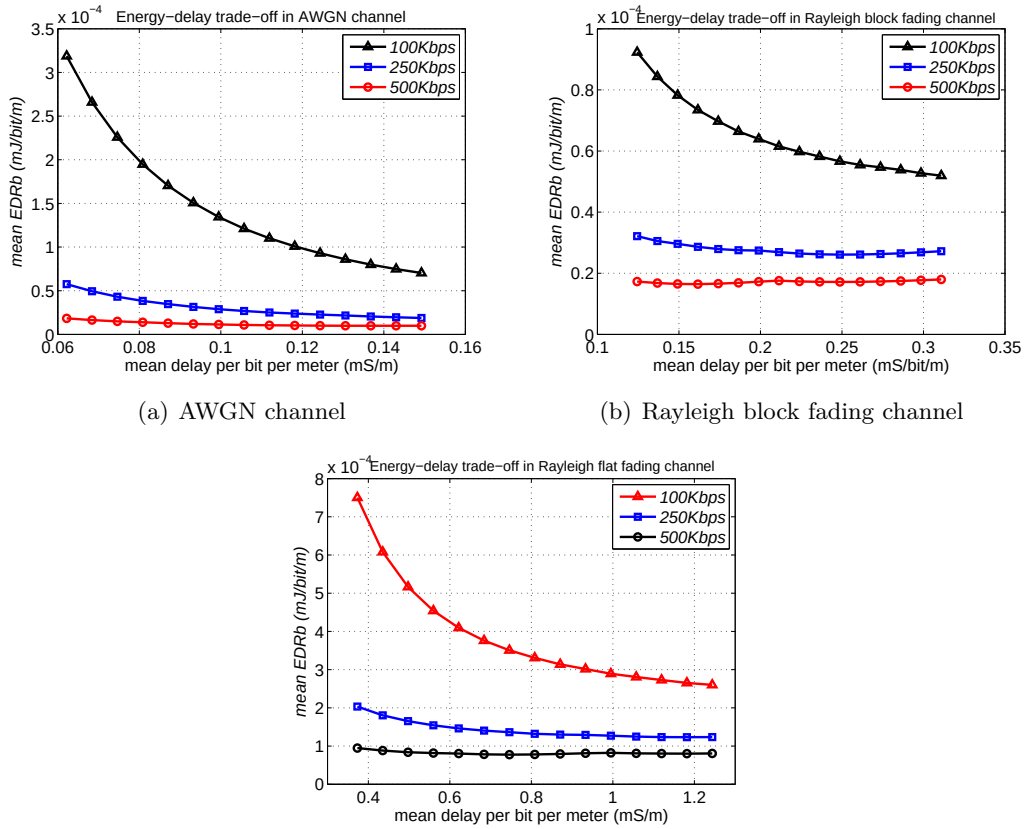

(a) AWGN channel

(b) Rayleigh block fading channel

(c) Rayleigh flat fading channel

Figure 6.9: Effect of R_s on energy-delay trade-off in different channels

On the basis of (6.10) and (6.12), we know that the higher transmit rate is, the smaller E_c and $\overline{DDR}$ is in any type of channel. Meanwhile, the increase of transmission rate leads to the decrease of SNR according to (2.11) which brings the rise of BER. In other words, the increase of transmit rate will bring two oppositive effect on the optimal $\overline{EDRb}$ and thus an optimal transmit rate should be existed. While, the results in Fig. 6.9 show that $\overline{EDRb}$ and $\overline{DDR}$ decrease simultaneously with respect to the increase of transmit rate in the three kinds of channel. Hence, the energy saving from the decrease E_c can compensate for the increase of energy consumption because of the augment of BER. Finally, according to this conclusion, the maximum transmit rate that a node can reach should be used in order to minimize both $\overline{EDRb}$ and $\overline{DDR}$.

6.5.2 The effect of protocol layer parameters

Number of bits in a ACK packet N_{ack}

According to (6.3) (6.4) and the definition of $\overline{EDRb}$ (6.10), it is deduced easily that the increase of N_{ack} leads to the increment of total energy consumption because of increase of τ_{ack}. Therefore, similarly to P2P communications, $N_b ack$ should be removed or reduced as less as possible.

Number of bits in a packet N_b

As analyzed above, diminishing τ_{ack} can improve the energy efficiency. Another method of diminishing τ_{ack} is to increase N_b according to (2.5). Meanwhile, this will lead to the decrease of link probability based on (6.5), which results in more energy consumption. Finally, these two contrary effects bring on an optimal number of bits. Fig. 6.10, Fig. 6.11 and Fig. 6.12 show how the optimal $\overline{EDRb}$ varies with N_b in three kinds of channel. Because τ_{ack} is related with both N_{ack} and N_b, the optimal N_b is tightly dependent on N_{ack}. This kind of impact is also shown in Fig. 6.10, Fig. 6.11 and Fig. 6.12. The conclusion obtained from these figures is the increase of N_{ack} will lead to the great increase of optimal N_b.

It should be noticed that the difference of $\overline{EDRb}$ from the different number of bits is small when N_{ack} is very small especially in AWGN channel and Rayleigh block fading channel. Considering the conclusion about N_{ack}, we should do our best to reduce N_{ack} so that the optimization about N_b can be neglected.

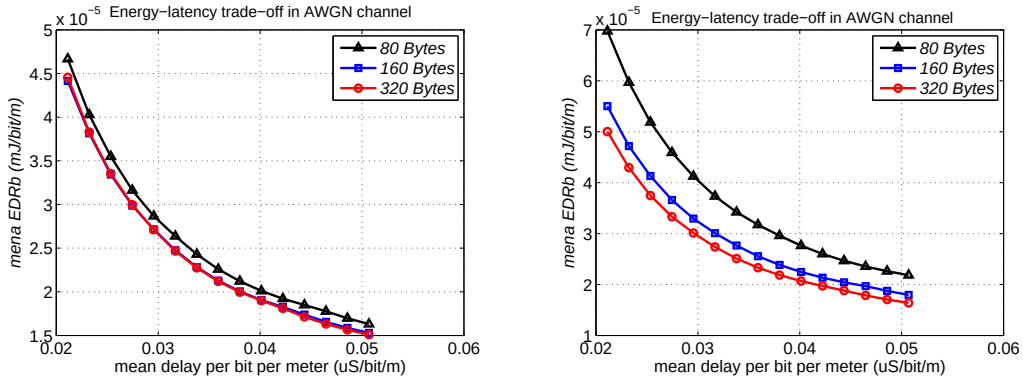

(a) ACK = 11 bytes (b) ACK = 26 bytes

Figure 6.10: Effect of N_b on energy-delay trade-off in AWGN channels

Delay from MAC protocol

According to (6.12) , the increase of T_{queue} will lead to the increment of $D_h op$ and it can be deduced that the transmission power should be increased to satisfy the same delay constraint on the basis of (6.18). In turn, the $\overline{EDRb}$ will increase. The results

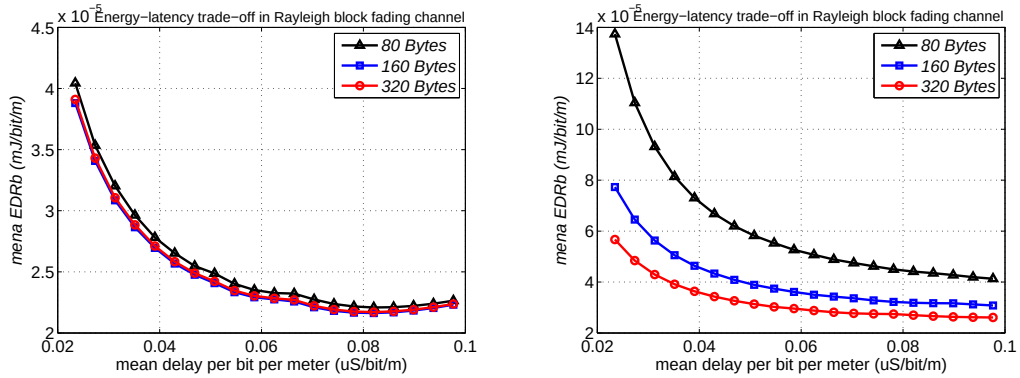

(a) ACK = 11 bytes (b) ACK = 78 bytes

Figure 6.11: Effect of N_b on energy-delay trade-off in Rayleigh block fading channels

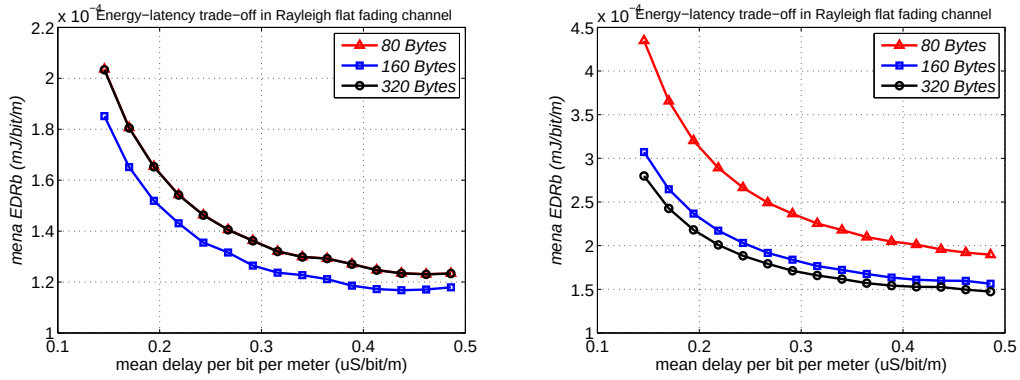

(a) ACK = 78 bytes (b) ACK = 150 bytes

Figure 6.12: Effect of N_b on energy-delay trade-off in Rayleigh flat fading channels

in Fig. 6.13 verify the above analyses. This conclusion shows that during the design of protocol the process leading to the increase of T_{queue} should be reduced or removed such as RTS and CTS process to improve the energy efficiency of a network.

Besides the above parameters, the integration of several parameters can be analyzed also according to the different applications because this framework includes every parameters in physical and protocol layer. On the basis of these analysis result, we can adjust the parameter to obtain the best performance of a network.

6.6 Simulations

The purpose of this section is to verify the lower bound on the energy-delay trade-off and on the energy efficiency in a 2-dimensional Poisson distributed network using simulations. The goal is to show that the theoretical results obtained in a linear network using approximation approach still hold for such a more realistic scenario. First, we

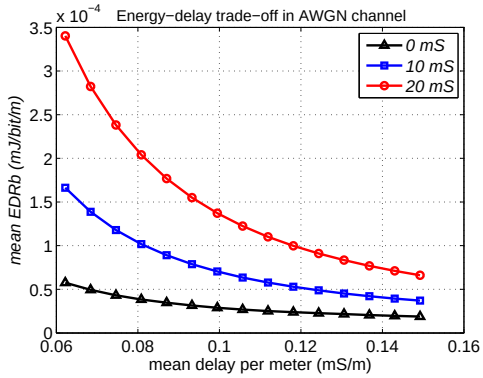

(a) AWGN channel

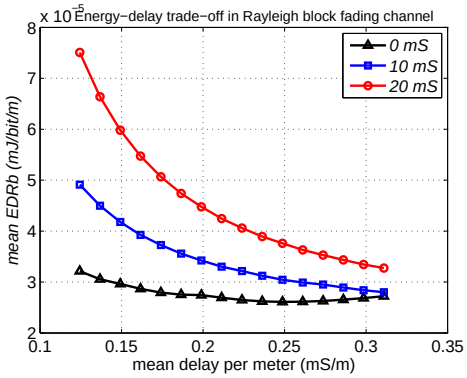

(b) Rayleigh block fading channel

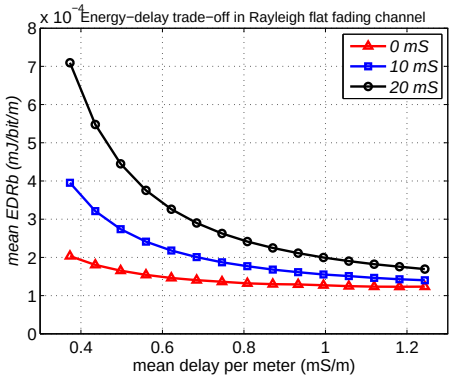

(c) Rayleigh flat fading channel

Figure 6.13: Effect of T_{queue} on energy-delay trade-off in different channels

introduce a new opportunistic protocol on the basis of the theoretical analyzes.

6.6.1 Opportunistic Protocol

The analyses in Section 6.3 reveal that an optimal transmission power and an optimal number of receivers should be configured in order to approach the lower bound of energy-delay tradeoff. Meanwhile, a algorithm of searching the optimal number of receivers to evaluate the energy-delay performance of a network is proposed. However, this algorithm needs the global parameters of a network, so that it can not be applied directly to the distributed networks. Here, a new distributed algorithm is introduced based on the algorithm propose in [85] and the analyses in Section 6.3 and Section 6.4.

The containing property in Lemma 3.4 proposed in [85] shows that a straightforward way to find an optimal node set containing r nodes is to add a new node into the optimal node set containing $r-1$ nodes. Furthermore, when a local minimum $\overline{EDRb}$ is found, it is the global minimum according to Theorem 6. Based on this idea, a distributed algorithm for finding the optimal receiver set of each hop in order to minimize the

energy consumption and satisfy the delay constraint ddr is proposed in Algorithm 2.

Algorithm 2 Search the optimal set of receivers

$B \leftarrow C$, $F^* \leftarrow F_c^* \leftarrow F \leftarrow \emptyset$, ddr
while $C \neq \phi$ **do**
  for each node i $\in B$ **do**
    $F^* \leftarrow F \cup \{i\}$;
    Sorting the nodes in F^* according to their effective transmission distance;
    $ddr^* \leftarrow \overline{DDR}(F^*)$
    if $ddr^* > ddr_c^*$ **then**
      $ddr_c^* \leftarrow ddr^*$; $F_c^* = F^*$
    end if
  end for
  if $ddr_c^* < ddr$ **then**
    $F \leftarrow F_c^*$; $B \leftarrow C - F$
  else
    return F_c^*
  end if
end while

where C is the set of neighbor nodes of a source node, F is the set of nodes selected to receive the packet from the source node.

Next, we introduce the protocol process:

1. Search the forward candidates according to Algorithm 2.

2. Assign a priority to each node according to its effective transmission distance.

3. Transmit the Data packet including the information of forward candidates ID and its corresponding priority.

4. Nodes in the set of forward candidates try to receiver packet.

5. A node which receives the packet correctly calculates the back-off time according to the priority and waits for the ack packet from the nodes with the priority higher than that of itself.

6. If a node does not receive any ack packet, it broadcasts its ACK packet and then is ready to transmit the received packet to next hop or destination. If a node receives an ack packet, it draws the received data packet and do nothing.

7. The source waits for the ack packet from one of forwarding candidates. If an ack packet is received, the source node removes the packet from the buffer, otherwise, it is ready to transmit the data packet again.

6.6.2 Simulation setup

In the simulations, the lower bounds on energy-delay trade-off and on $\overline{EDRb}$ are evaluated in an area $\mathcal{A}$ of surface $S_{\mathcal{A}} = 100 \times 1200m^2$ using the simulator Wsnet [2]. The nodes are uniquely deployed according to Poisson distribution.

All the other simulation parameters concerning a node are listed in Table 2.1. The distance between the source node and the destination node is $1000m$. The source node transmits only one DATA packet of 320 bytes to the destination with BPSK modulation. the size of ACK packet is 26 bytes. For every hop, the transmitter will retransmit the DATA packet until the DATA packet is received by the next relay node, this is to say, there is no limit to the number of retransmissions in order to ensure the reliability of each hop. The opportunistic protocol proposed in Subsection 6.6.1 is used in all simulations. A simulation will be repeated for 1000 times in each same configuration.

The network model used in the simulations assumes the following statements:

- After the initial phase, the network is geographical-aware, i.e., each node knows the position of itself, the sink node and all the neighbor nodes in the simulation network.

- Each node in the simulation network has the same fixed transmission.

6.6.3 Results and analyses

Effect of node density

The first simulation is run in order to analyze the variety of energy-delay tradeoff with the increase of node density. The simulations is done in three case: 200 nodes, 400 nodes and 800 nodes are deployed in the simulation area. The transmission power of each node is configured as the optimal transmission power according to (6.24).

Fig. 6.14 provides the simulation results which are compared with the theoretical lower bound of energy-delay trade-off in Rayleigh block fading channel which reveal that, with the increase of the node density, the simulation result is approaching the theoretical lower bound because relays node selected by the routing scheme are more and more near the optimal transmission distance of each hop when the node density increases. The corresponding mean number of receivers in each hop shown in Fig. 6.15 also can verify this phenomenon because the mean number of receivers reduces with the increase of node density. And we can deduce that the lower bound can be reached when the node density is big enough. Hence, it is concluded that the theoretical lower bound on $\overline{EDRb}$ is adequate for a 2-D Poisson network although its derivation is based on a linear network using approximation method.

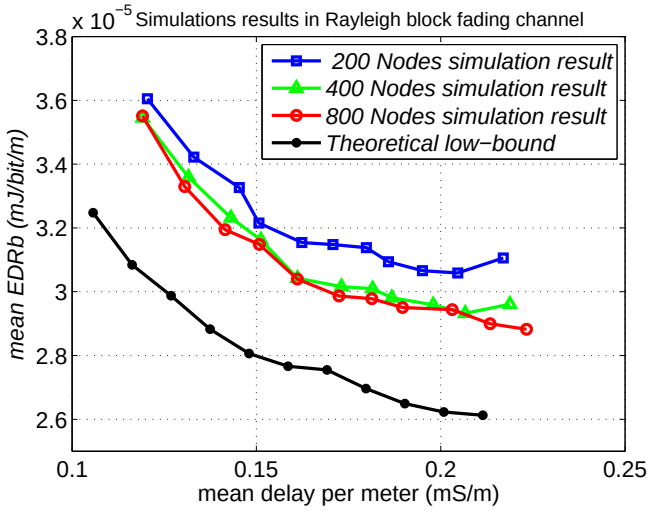

Figure 6.14: Simulation results about EDRb-DDR tradeoff

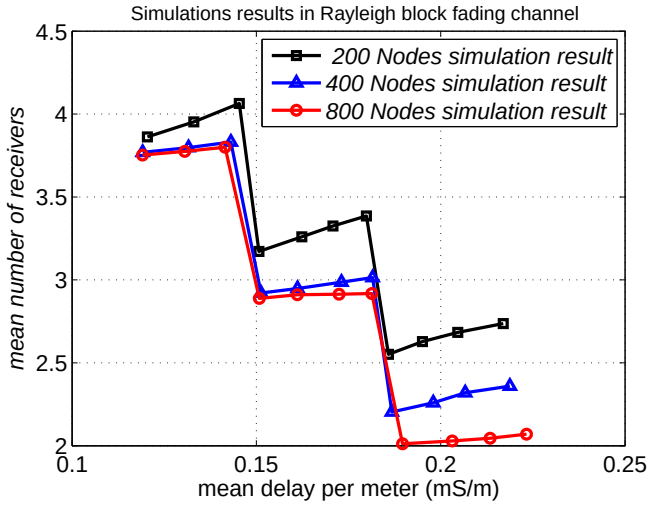

Figure 6.15: Simulation results about mean number of receivers

Furthermore, these results imply that unreliable links play an important role in energy savings because the mechanism of opportunistic protocol used in these simulations decide the link between a source node and each forward candidate is unreliable.

Effect of transmission power

The aim of the second simulations is to show the importance of optimal transmission power to the reduction of energy consumption.

Fig. 6.16 shows the simulation result of energy-delay tradeoff with the optimal transmission power Pt_{opt} and $Pt_{opt} \pm 2dB$ where 800 nodes are placed in the simulation area and Fig.6.17 shows the corresponding mean number of receivers for each hop.

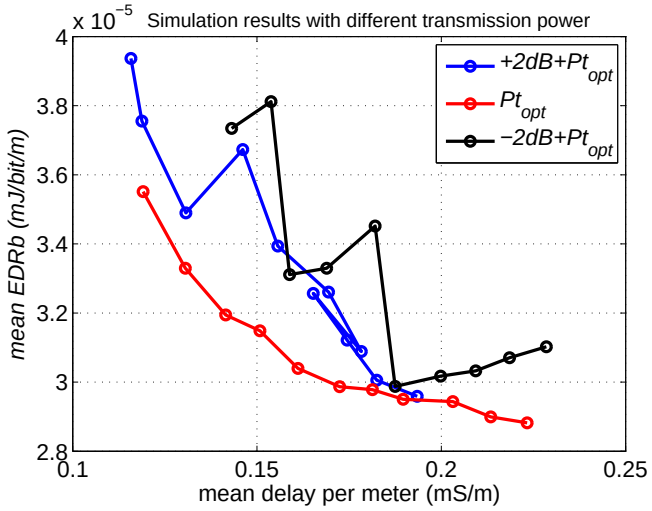

Figure 6.16: Simulation results about EDRb-DDR tradeoff with different P_t

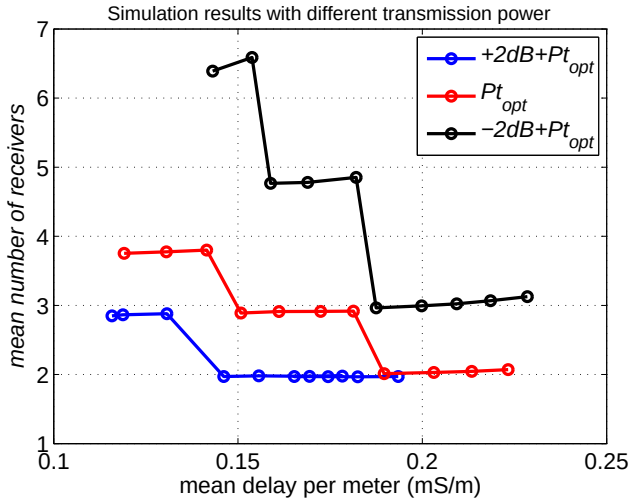

Figure 6.17: Mean number of receivers with different P_t

When the transmission power is greater than the optimal transmission power, the transmission delay is reduced and is smaller than the delay constraint *ddr*. However, the energy consumption increases. At the same time, the increase of transmission power leads to the decrease of the number of forward candidates. While, a transmission power smaller than the optimal transmission power results in the increase of both delay and energy consumption. Finally, the optimal physical configuration is importance to achieve the best of network performance.

6.7 Summary

In this chapter, we first integrate an unreliable link model into our energy model using a specific metric for energy efficiency: $\overline{EDRb}$. By optimizing $\overline{EDRb}$ for AWGN, Rayleigh block fading and Rayleigh block fading channels with and without delay constraint, we show that the channel state impacts the optimal number of receivers in a cluster. Meanwhile, the corresponding optimal transmission power and the optimal transmission range are derived. The energy-delay trade-off for one-hop and multi-hop transmissions are analyzed and compared with the trade-off given by traditional multi-hop communications. The simulations using the proposed opportunistic scheme verify the theoretical lower bound of energy-delay tradeoff. The main conclusion is that opportunistic communications exploiting spatial diversity are beneficial for Rayleigh block fading and Rayleigh block fading channels when a delay constraint is considered.

7

Energy-Delay Trade-off of Cooperative MIMO Scheme

7.1 Introduction

In the previous chapter, we introduce the concept of cooperation by opportunistic relaying but only at the receiver side. In this chapter, the cooperation is extended to both the transmitter side and the receiver side by cooperative multi-input multi-output (MIMO) systems.

Concerning this question, the lower bound of energy-delay tradeoff of CMIMO is exploited under unreliable links in this chapter, by optimizing the number of cooperative nodes in both transmitter side and reception side, as well as the transmission power. Here, we assume perfect synchronization among the cooperative nodes and the performance reduction from the time jitter is out of the scope this chapter. [44] investigated the effect of time synchronization errors on the performance of cooperative MIMO systems, and concluded that CMIMO schemes has a good tolerance of up to 10 clock jitter.

The contributions of this chapter:

- The lower bound of energy-delay tradeoff of CMIMO schemes is obtained when the number of cooperative transmitters and receivers is fixed, and an algorithm for searching the optimal number of cooperative nodes in both two sides is proposed.

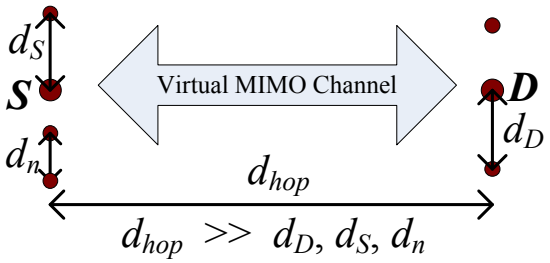

Figure 7.1: Single hop cooperative MIMO communication

- A cross-layer framework to optimize the parameters at the physical and MAC layers in CMIMO scheme is introduced.
- The lower bound of energy efficiency of CMIMO scheme is achieved, and the corresponding optimal parameters are deduced.
- The lower bounds of the three communication schemes mentioned in this thesis are compared in different channels respectively. The results show that in order to achieve better energy-delay performance, the corresponding communication scheme should be adopted for different channel type: traditional multi-hop communications for AWGN channel, opportunistic communications for Rayleigh block fading channel and CMIMO for Rayleigh flat fading channel.

The rest of this chapter is organized as follows: Section 7.2 describes the utilized models and metrics in this chapter. In Section 7.3, the lower bound of energy-delay tradeoff of CMIMO is deduced and the lower bound of energy efficiency is obtained. Using the lower bound, the effectiveness of CMIMO in AWGN, block fading and flat fading channels is analyzed in Section 7.4. In Section 7.5, the lower bound of energy-delay tradeoff in Nakagami-m flat fading channel and the gain of CMIMO on energy efficiency are analyzed. The optimization of the physical layer and protocol layer parameters on the lower bound is presented in Section 7.6. Section 7.7 gives some conclusions.

7.2 Models and metric

In this section, we introduce the energy and delay models, the realistic link model, the metric $\overline{EDRb}$ and $\overline{DDR}$ of CMIMO communications used in this work.

7.2.1 System model

As described in Chapter 4, a CMIMO system is composed of N_T cooperative transmitters including a source node and N_R cooperative receivers including a destination node. Here, the distance between cooperative transmitters and cooperative receivers, d_{hop}, is

greatly greater than the distance among cooperating nodes, d_n, the distance between $\mathcal{S}$ and its cooperative neighbors d_S and the distance between the destination node $\mathcal{D}$ and its cooperative nodes, d_D, i.e., $d \gg d_S, d_D, d_n$ as shown in Fig. 7.1. Meanwhile, we assume the distance between each pair of cooperative transmitter and receiver is the same as d_{hop}. STBC technique and Alamouti space-time code are utilized in this chapter where $R_c = 1$ when $N_T \leq 2$ and $R_c = 1/2$ when $N_T > 2$. A multi-hop transmission repeats the one-hop transmission in each hop. In addition, each cooperative transmitter has the same transmit power.

7.2.2 Energy consumption model

According to the previous assumptions and transmission processes described in Chapter 4, the energy consumption for transmitting one packet E_p is composed of four parts:

$$E_p = E_{broad} + E_{agg} + E_{mimo} + E_{ack}, \tag{7.1}$$

where E_{broad} is the energy consumed in the broadcast process, E_{mimo} is in CMIMO transmission phase, E_{agg} is in the aggregation phase at the receiver side and E_{ack} is for transmitting an ACK packet. The model of each part is presented as follows.

$$E_{broad} = S_{mimo} \cdot \frac{N_b + N_{head}}{R_b R_{code}} \cdot (P_{txElec} + P_{broagg} + (N_T - 1) \cdot P_{rxElec}) \tag{7.2}$$

where S_{mimo} presents the switch of MIMO communication where $S_{mimo} = 1$ when $N_T > 1$, otherwise $S_{mimo} = 0$; P_{broagg} is the transmission power during the broadcast phase and the aggregation phase. The other parameters are listed in Table 2.1.

$$E_{mimo} = \frac{N_b}{R_b R_{code} R_c}(N_T \cdot P_{txElec} + N_R \cdot P_{rxElec} + \beta_{amp} \cdot N_T \cdot P_t) \tag{7.3}$$

where P_t is the transmission power at each antenna, R_c is the code rate of STBC code, the other parameters are described in Table 2.1.

According to the transmission scheme of CMIMO, during the aggregation phase, the cooperative nodes transmit received packet to the destination node in different time slot. Therefore, the energy consumption in this phase is:

$$E_{agg} = \frac{N_r + N_{head}}{R_b R_{code}} \cdot (N_R - 1)(P_{txElec} + P_{broagg} + P_{rxElec}) \tag{7.4}$$

where N_r is the number of bits of received data by a cooperative node and we set $N_r = N_b$.

Concerning the acknowledgement process, we assume it has a transmission scheme

similar to the one of a data packet. The minimal energy expenditure for acknowledgement is thus given by:

$$E_{ACK} = \tau_{ack} \cdot (E_{broad} + E_{agg} + E_{mimo}), \tag{7.5}$$

where τ_{ack} represents the ratio of size between ACK packet and data packet defined in (2.5). We assume that ACK packet is much smaller than data packet, i.e., $0 \leq \tau_{ack} \ll 1$.

Therefore, the energy consumption per bit is:

$$E_b = \frac{E_p}{N_b} = E_c + K_1 \cdot P_t \tag{7.6}$$

Here, $K_1 \cdot P_t$ stands for the radio emission energy and E_c denotes the circuit energy per node, which are obtained by:

$$\begin{aligned} E_c = \frac{1+\tau_{ack}}{R_b R_{code}} \Big\{ & N_T P_{txElec} + N_R P_{rxElec} \\ & + \frac{S_{mimo}}{R_c}(P_{tx} + (N_T - 1)P_{rxElec}) + \eta(N_R - 1)(P_{tx} + P_{rx}) \Big\}, \end{aligned} \tag{7.7}$$

where $\eta = (N_r + N_{head})/(N_b + N_{head})$ and is set to 1 in this chapter.

$$K_1 = (1 + \tau_{ack}) \frac{N_T \beta_{amp}}{R_b \cdot R_{code} \cdot R_c} \tag{7.8}$$

The related parameters are described in Table 2.1.

7.2.3 Realistic unreliable link models

As claimed in Chapter 1, it is very crucial to take transmission errors into account to ensure a reliable transmission. Hence, we consider herein a radio link probability which is derived from the packet error rate (PER) according to (2.10) as follows:

$$pl = 1 - PER.$$

In [72], an equivalent SISO system of a MIMO system is provided. The relationship between $\bar{\gamma}_s$ and γ_{STBC} is presented, where $\bar{\gamma}_s$ is the average SNR at each receiver antenna and γ_{STBC} is the SNR after Alamouti decoding at the receiver of the equivalent SISO system. They are related as follows:

$$\gamma_{STBC} = \frac{\sum_{i=1}^{N_R} \sum_{j=1}^{N_T} |h_{i,j}|^2}{N_T R_c} \bar{\gamma}_s, \tag{7.9}$$

where $h_{i,j}$ is the transfer function between transmitter antenna i and receiver antenna

j and $\bar{\gamma}_s$ is obtained by:

$$\bar{\gamma}_s = \frac{K_2 \cdot N_T \cdot P_t}{d_{hop}^{\alpha}}, \tag{7.10}$$

where K_2 is presented in (2.12).

Because PER depends on the type of channel and modulation, the expression of pl in AWGN, Nakagami-m block fading and Nakagami-m flat fading channel are provided respectively in the following part.

AWGN channel

In AWGN channel the value of $|h_{i,j}|^2$ in (7.9) is 1. Therefore, γ_{STBC} in AWGN channel is:

$$\gamma_{STBC} = \frac{N_R}{R_c}\bar{\gamma}_s = \frac{N_R \cdot N_T \cdot K_2 \cdot P_t}{R_c \cdot d_{hop}^{\alpha}}. \tag{7.11}$$

Then, we have the link probability in AWGN channel:

$$pl = \left(1 - BER\left(\frac{N_R \cdot N_T \cdot K_2 \cdot P_t}{b \cdot R_c \cdot d_{hop}^{\alpha}}\right)\right)^{N_b}, \tag{7.12}$$

where $BER(\gamma)$ is provided in (2.14), γ_s is the SNR at the antenna of each cooperative node, $b = \log_2(M)$ is the order of modulation.

Nakagami-m block fading channel

In [72], the pdf of γ_{STBC} under the condition of $\bar{\gamma}_s$ is derived as a gamma distribution:

$$p_{\gamma_{STBC}}(\gamma|\bar{\gamma}_s) = \frac{(mN_TR_c)^{mN_TN_R}\gamma^{mN_TN_R-1}}{\Gamma(mN_TN_R)\bar{\gamma}_s^{mN_TN_R}} \exp\left(-\frac{mN_TR_c\gamma}{\bar{\gamma}_s}\right). \tag{7.13}$$

According to (2.19), we have the link probability of MIMO in block fading channel:

$$pl(\bar{\gamma}_s) = \int_{\gamma=0}^{\infty}(1 - BER(\frac{\gamma}{b}))^{N_b} \cdot p_{\gamma_{STBC}}(\gamma|\bar{\gamma}_s)d\gamma, \tag{7.14}$$

where $BER(\cdot)$ provided in (2.14) and γ_s is obtained by (7.10).

Nakagami-m flat fading cannel

In [72, 60], the symbol error rate (SER) of MIMO communication is provided in a Nakagami-m flat fading channel for MPSK modulation and MQAM modulation as follows:

MPSK modulation:

$$P_{spsk}(\bar{\gamma}_s) = M_{\gamma STBC}^{i.i.d.Naka}(-g_{psk})\Big\{\frac{\Gamma(q+1)}{2\sqrt{\pi}\Gamma(q+1)}\ {}_2F_1\left(q,\frac{1}{2};q+1;x\right) + \frac{\sqrt{z}}{\pi}F_1\left(\frac{1}{2},q,\frac{1}{2}-q;\frac{3}{2};y,z\right)\Big\} \tag{7.15}$$

where $M_{\gamma STBC}^{i.i.d.Naka}(s) = (1+s\bar{\gamma}_s/(mN_TR_c))^{-q}$, $x = 1/(1+(g_{psk}\bar{\gamma}_s)/(mN_TR_c))$, $y = (1-g_{psk})/(1+(g_{psk}\bar{\gamma}_s)/(mN_TR_c))$, $g_{psk} = \sin^2(\pi/M)$, $q = mN_TN_R$, $z = 1-g_{psk}$, $F_1(\cdot)$ and ${}_2F_1(\cdot)$ are the hypergeometric functions, and $\Gamma(\cdot)$ is Gamma function.

MQAM modulation:

$$\begin{aligned} P_{sqam}(\bar{\gamma}_s) =& \frac{2gM_{\gamma STBC}^{i.i.d.Naka}(-g_{qam})}{\sqrt{\pi}}\frac{\Gamma(q+1/2)}{\Gamma(q+1)}\ {}_2F_1\left(q,\frac{1}{2};q+1;x_1\right) \\ &- M_{\gamma STBC}^{i.i.d.Naka}(-2g_{qam})\frac{g^2\Gamma(q+1/2)}{\pi\Gamma(q+3/2)}F_1\left(1,q,1;q+\frac{3}{2};y,\frac{1}{2}\right) \end{aligned} \tag{7.16}$$

where $g = 1-1/\sqrt{M}$, $g_{qam} = 1.5/(M-1)$, $x_1 = 1/(1+(g_{qam}\bar{\gamma}_s)/(mN_TR_c))$, $y = (1+(g_{qam}\bar{\gamma}_s)/(mN_TR_c))/(1+(2g_{qam}\bar{\gamma}_s)/(mN_TR_c))$.

Hence, the link probability is formulated as:

$$pl(\bar{\gamma}_s) = (1-P_s(\bar{\gamma}_s))^{\frac{N_b}{\log_2(M)}} \tag{7.17}$$

where $P_s(\bar{\gamma}_s)$ is obtained by (7.16) or (7.15) for QAM or PSK modulation respectively.

7.2.4 Reliable transmission

Furthermore, a reliable one-hop transmission will suffer from the delay caused by retransmissions. The average number of transmissions, $\overline{N}_{tx}$, is calculated by:

$$\overline{N}_{tx} = \sum_{n=1}^{\infty} n\cdot pl_s\cdot(1-pl_s)^{(n-1)} = \frac{1}{pl_s}, \tag{7.18}$$

where n is the number of packet transmissions including retransmissions, pl_s is the probability of one-time successful transmission which is obtained by:

$$pl_s = pl_{broad}^{N_T-1}\cdot pl_{mimo}\cdot pl_{agg}^{N_R-1}\cdot pl_{ack}, \tag{7.19}$$

where pl_{broad} is the link probability between a source node and a its cooperative node, and pl_{agg} is the link probability between a destination and a its cooperative node, pl_{mimo} and pl_{ack} are link probabilities in the CMIMO transmission phase and the acknowledgement phase respectively.

According to the assumption in Chapter 4 about CMIMO, as shown in Fig. 4.2,

$d \gg d_D, d_S$, this it to say, the distance between a source and a destination is greater than that between the source or the destination and its cooperative nodes, so that the channels between the source or the destination and its cooperative nodes can be considered as AWGN channel. Then, according to the result in Chapter 2, the reliable links should be used in AWGN channel to obtain high energy efficiency. Therefore, we assume that pl_{broad} and pl_{agg} approximate to 1. In the acknowledgment process, it is assumed that $pl_{ack} \approx 1$ on the basis of analysis in Chapter 2.

Hence, $\overline{N}_{tx}$ can be approximated by:

$$\overline{N}_{tx} \approx \frac{1}{pl}, \tag{7.20}$$

where pl stands for pl_{mimo} for the sake of simplification and is given in (7.12), (7.14) and (7.17) in the different channels respectively.

7.2.5 mean Energy Distance Ratio per bit ($\overline{EDRb}$)

To evaluate the energy efficiency, we adopt the metric: mean Energy Distance Ratio per bit ($\overline{EDRb}$) also in CMIMO communications.

According to the definition of $\overline{EDRb}$, we have:

$$\overline{EDRb} = \frac{E_b(P_t)}{d_{hop} \cdot pl} = \frac{E_c + K_1 \cdot P_t}{d_{hop} \cdot pl}. \tag{7.21}$$

Here, d_{hop} is the transmission distance

7.2.6 Delay Distance Ratio ($\overline{DDR}$)

The delay of a packet to be transmitted over one hop in CMIMO, D_{hop}, is defined as the sum of four delay components. The first component is from the broadcast phase, T_{broad}. The second component is the CMIMO transmission delay T_{mimo}. The third component is T_{agg} due to the aggregation phase and the last component is T_{ack} because of the acknowledge process. Note that we neglect the propagation delay because the transmission distance between two nodes is usually short in multi-hop networks.

$$D_{hop} = S_{mimo} \cdot T_{broad} + T_{mimo} + T_{agg} + T_{ack} \tag{7.22}$$

where $T_{broad} = (N_b + N_{head})/(R_b \cdot R_{code})$, $T_{mimo} = N_b + N_{head}/(R_b \cdot R_{code} \cdot R_c)$, $T_{agg} = (N_R - 1) \cdot (N_b + N_{head})/(R_b \cdot R_{code})$ and $T_{ack} = \tau_{ack} \cdot (S_{mimo} \cdot T_{broad} + T_{mimo} + T_{agg})$.

Furthermore, a reliable one-hop transmission will suffer from the delay caused by retransmissions. According to (7.20), the mean delay of a reliable one-hop transmission is:

$$\overline{D}_{hop} = D_{hop}\overline{N}_{tx}. \tag{7.23}$$

Then, $\overline{DDR}$ is defined as:

$$\overline{DDR} = \frac{D_{hop}\overline{N}_{tx}}{d_{hop}} = \frac{D_{hop}}{d_{hop} \cdot pl}. \tag{7.24}$$

7.3 Energy-delay trade-off of CMIMO

In this section, we analyze the energy-latency trade-off under the reliability constraint in the scenarios of one-hop transmission. The optimal transmission power and the optimal number of node in transmitter cluster and receiver cluster will be analyzed and the lower bound of energy-delay tradeoff is obtained.

The energy-delay trade-off of one-hop transmission can be abstracted as an optimization problem:

$$\begin{aligned} \text{minimize} &: \overline{EDRb} \\ \text{subject to} &: N_T, N_R \geq 1,\ N_T, N_R \in \text{Integer}, \\ &\quad P_t > 0,\ d_{hop} > 0,\ \overline{DDR} = ddr, \end{aligned} \tag{7.25}$$

where ddr is a delay constraint. Consequently, minimizing energy and delay in a multi-hop transmission can be achieved by finding the four parameters $(d_{opt},\ P_{opt}, N_{Topt}, N_{Ropt})$ for one-hop transmission, where d_{opt} is the optimal hop distance, P_{opt} is the optimal transmission power, N_{Topt} and N_{Ropt} are the optimal number of cooperative transmitters and receivers respectively.

This is a mixed integer nonlinear programming (MILNP) problem which can be solved by the branch-and-bound algorithm [50] in order to find the lower bound of energy-delay tradeoff. But this method is time-consumed and complex. In the following part, we will solve this problem to derive this lower bound. First, we consider the scenario with N_T and N_R fixed.

7.3.1 Lower bound of energy-delay trade-off with fixed N_T and N_R

According to (7.10), we have $d_{hop} = \left(\frac{K_2 N_T P_t}{\bar{\gamma}}\right)^{\alpha}$. In turn, the expressions of (7.21) and (7.24) are converted to the function of P_t and $\bar{\gamma}$ as follows:

$$\overline{EDRb}(\bar{\gamma}, P_t, N_T, N_R) = \frac{E_c(N_T, N_R) + K_1 P_t}{(K_2 N_T P_t)^{\frac{1}{\alpha}}} \cdot g(\bar{\gamma}, N_T, N_R) \tag{7.26}$$

$$\overline{DDR}(\bar{\gamma}, P_t, N_T, N_R) = \frac{D_{hop}}{(K_2 N_T P_t)^{\frac{1}{\alpha}}} \cdot g(\bar{\gamma}, N_T, N_R) \tag{7.27}$$

where

$$g(\bar{\gamma}, N_T, N_R) = \frac{\bar{\gamma}^{\frac{1}{\alpha}}}{pl(\bar{\gamma}, N_T, N_R)}. \tag{7.28}$$

Theorem 9. *When N_T and N_R are constant, the optimal $\overline{EDRb}$ under a given delay constraint $\overline{DDR}(\bar{\gamma}, P_t, N_T, N_R) = ddr$ is obtained when*

$$\bar{\gamma}_{opt} = \arg\min_{\gamma} g(\bar{\gamma}, N_T, N_R).$$

Proof. Refer to the proof of Theorem 3. ■

According to Theorem 9, the lower bound of energy-delay trade-off is obtained by $g(\bar{\gamma}_{opt}, N_T, N_R)$ when N_T and N_R are fixed. By the traditional optimization method, such as Gauss-Newton algorithm [50], $\bar{\gamma}_{opt}$ and $g(\bar{\gamma}_{opt}, N_T, N_R)$ can be obtained.

Meanwhile, when the ddr is given, according to (7.27) the optimal transmission power to minimize the total energy consumption is obtained by:

$$P_{opt}(N_T, N_R) = \frac{1}{K_2 \cdot N_T} \cdot \left(\frac{D_{hop}}{ddr} \cdot g(\bar{\gamma}_{opt}, N_T, N_R) \right)^{\alpha}. \tag{7.29}$$

According to (7.10) and (7.29), we have the optimal transmission distance:

$$d_{opt}(N_T, N_R) = \left(\frac{K_2 P_{opt}}{\bar{\gamma}_{opt}} \right)^{\frac{1}{\alpha}} = \frac{g(\bar{\gamma}_{opt}, N_T, N_R) \cdot D_{hop}}{\bar{\gamma}_{opt}^{1/\alpha} \cdot ddr}. \tag{7.30}$$

The corresponding optimal $\overline{EDRb}$ is:

$$\overline{EDRb}_{opt}(N_T, N_R) = E_c(N_T, N_R) \cdot \frac{ddr}{D_{hop}} + g(\bar{\gamma}_{opt}, N_T, N_R)^{\alpha} \cdot \frac{K_1}{K_2 \cdot N_T} \cdot \left(\frac{ddr}{D_{hop}} \right)^{1-\alpha}. \tag{7.31}$$

In following subsection, the optimal N_T and N_R under a ddr constraint will be analyzed.

7.3.2 Optimization of N_T and N_R

According to (7.31), the optimal number of transmitters and receivers, N_{Topt} and N_{Ropt}, are found by Algorithm 3.

Then, substituting N_{Topt} and N_{Ropt} into (7.30), (7.29) and (7.31), we have the optimal transmission power, the optimal transmission distance, and the lower bound of energy-delay tradeoff respectively as follows:

$$P_{opt} = \frac{1}{K_2 \cdot N_{Topt}} \cdot \left(\frac{D_{hop}}{ddr} \cdot g(\bar{\gamma}_{opt}, N_{Topt}, N_{Ropt}) \right)^{\alpha} \tag{7.32}$$

$$d_{opt} = \frac{g(\bar{\gamma}_{opt}, N_{Topt}, N_{Ropt}) \cdot D_{hop}}{\bar{\gamma}_{opt}^{1/\alpha} \cdot ddr}. \tag{7.33}$$

Algorithm 3 Searching optimal N_T and N_R

$N_T \leftarrow 1$, $N_R \leftarrow 1$, $N_{Topt} \leftarrow 1$, $N_{Ropt} \leftarrow 1$
$\overline{EDRb}2 \leftarrow Inf$, $flag \leftarrow 0$, ddr
while $flag == 0$ **do**
  $\overline{EDRb}1 \leftarrow Inf$, $flag1 \leftarrow 0$, $N_R \leftarrow 1$
  while $falg1 == 0$ **do**
    Calculate $\bar{\gamma}_{opt}$ and $g(\bar{\gamma}_{opt}, N_T, N_R)$
    $\overline{EDRb} \leftarrow E_c(N_T, N_R) \cdot \frac{ddr}{D_{hop}(N_T,N_R)} + g(\bar{\gamma}_{opt}, N_T, N_R)^{\alpha} \cdot \frac{K_1}{K_2 \cdot N_T} \cdot \left(\frac{ddr}{D_{hop}(N_T,N_R)}\right)^{1-\alpha}$
    if $\overline{EDRb} > \overline{EDRb}1$ **then**
      $flag1 \leftarrow 1$, $N_{Ropt} \leftarrow N_R - 1$
    else
      $\overline{EDRb}1 \leftarrow \overline{EDRb}$, $N_R \leftarrow N_R + 1$
    end if
  end while
  if $\overline{EDRb}1 > \overline{EDRb}2$ **then**
    $flag \leftarrow 1$, $N_{Topt} \leftarrow N_T - 1$
    return N_{Ropt}, N_{Topt}
  else
    $\overline{EDRb}2 \leftarrow \overline{EDRb}1$, $N_T \leftarrow N_T + 1$
  end if
end while

$$\overline{EDRb}_{opt} = E_c(N_{Topt}, N_{Ropt}) \cdot \frac{ddr}{D_{hop}} + g(\bar{\gamma}_{opt}, N_{Topt}, N_{Ropt})^{\alpha} \cdot \frac{K_1}{K_2 \cdot N_{Topt}} \cdot \left(\frac{ddr}{D_{hop}}\right)^{1-\alpha}. \tag{7.34}$$

Though the lower bound of energy-delay tradeoff, (7.34), is derived from one-hop CMIMO transmission, it can be extended directly to multi-hop scenario on the basis of Theorem 1 and 2 in Chapter 2. To reach the lower bound, the physical parameters of each hop in a multi-hop transmission should have the same optimal configuration (N_{Topt}, N_{Ropt}, P_{opt}, d_{opt}), obtained by Algorithm 3, (7.32) and (7.33).

Obviously, the lower bound of energy-delay tradeoff (7.34) is composed of two components with respect to ddr. Therefore, it can be deduced easily that $\overline{EDRb}_{opt}$ is a convex function with respect to ddr when $g(\gamma_{opt})$ is given, and a lowest point is existed. Similar to Chapter 2, in order to obtain Pareto front of energy-delay tradeoff, the lowest point will be derived in following subsection.

7.3.3 Minimum energy consumption

In this subsection, as to the lowest point, we derive the lower bound of energy efficiency and corresponding energy-optimal transmission power and distance without the delay constraints.

Optimal transmission power

First, we analyze the scenario that N_T and N_R are constant. In order to get the minimum value of $\overline{EDRb}$ defined in (7.26), it is obvious that we should minimize $g(\bar{\gamma})$ and $f(P_t) = \frac{E_c(N_R,N_T)+K_1P_t}{(K_2N_TP_t)^{\frac{1}{\alpha}}}$ at the same time. Letting $\bar{\gamma} = \bar{\gamma}_{opt}$, we have the minimum $g(\bar{\gamma}_{opt})$. Then, employing Lagrange algorithm, we have:

$$\frac{d}{dP_t}\left(\frac{E_c + K_1P_t}{(K_2N_TP_t)^{\frac{1}{\alpha}}}\right) = 0. \tag{7.35}$$

Solving the above equation yields:

$$P_0(N_T, N_R) = \frac{E_c(N_T, N_R)}{(\alpha - 1)\cdot K_1}. \tag{7.36}$$

which is the transmission power minimizing $f(P_t)$. Substituting (7.7) and (7.8) into (7.36) yields:

$$\begin{aligned} P_0(N_T, N_R) =& \frac{R_c}{\beta_{amp}N_T}\left(N_T \cdot R_c \cdot P_{elecTx} + (P_{txElec} + P_{broagg})(S_{mimo} + \eta(N_R - 1)\right) \\ &+ \frac{R_c}{\beta_{amp}N_T}\left(P_{rxElec}(N_R + S_{mimo}(N_T - 1) + \eta(N_R - 1))\right). \end{aligned} \tag{7.37}$$

N_{T0} and N_{R0}

Notice that P_0 is tightly related with N_T, N_R, so that we should apply Algorithm 3 to find the optimal number of cooperative transmitters and receivers N_{T0} and N_{R0} which are tightly related to the modulation, the type of channel of a network. Then, substituting N_{T0} and N_{R0} into (7.37), the optimal transmission power P_0 is obtained.

Minimum mean transmission distance d_0

By P_0, $\bar{\gamma}_{opt}$ and (7.10), we obtain the minimal mean transmission distance:

$$d_0 = \left(\frac{K_2 \cdot N_{T0} \cdot P_0}{\bar{\gamma}_{opt}}\right)^{\frac{1}{\alpha}} \tag{7.38}$$

This distance shows the minimal distance between a source node and a destination node, otherwise, too small hop distance results in more energy consumption which is similar with the result in [20].

Lower bound of $\overline{EDRb}$ and its corresponding delay

The lower bound of $\overline{EDRb}$ is obtained by substituting (7.28) and (7.36) into (7.26):

$$\overline{EDRb}_0 = \frac{E_c(N_{T0}, N_{R0}) + K_1 P_0}{(K_2 N_{T0} P_0)^{\frac{1}{\alpha}}} \cdot g(\gamma_{opt}, N_{T0}, N_{R0}) \tag{7.39}$$

Based on this result, we can set the transmission power of node according to (7.37) to minimize the total energy consumption for the applications without delay request. Moreover, the transmission power of a node should not be smaller than this value, otherwise the node will be running in an inefficient state as shown on the right side curve of the lowest point in Fig. 7.4.

Moreover, on the basis of (7.27) and P_0, the maximal mean delay is obtained:

$$\overline{Delay}_{max} = d_{SD} \cdot \frac{D_{hop}}{(K_2 N_{T0} P_0)^{\frac{1}{\alpha}}} \cdot g(\gamma_{opt}, N_{T0}, N_{R0}), \tag{7.40}$$

where d_{SD} is the distance between a source node and a destination node.

Because (N_{Topt}, N_{Ropt}, P_{opt}, d_{opt}) tightly depends on the function of link probability, $pl(\cdot)$, we analyze the lower bound of energy-delay tradeoff in three different channels mentioned in the following section.

7.4 Effectiveness of CMIMO in different channels

As describe in Chapter 4, a CMIMO transmission includes three phases: broadcast, MIMO transmission and aggregation. Obviously, the phases broadcast and aggregation introduce additional energy consumption and delay. In order to reveal the effectiveness of CMIMO more clearly, we consider two scenarios: the first one we call it 'pure MIMO', the second one is CMIMO. In 'pure MIMO', the energy consumption and delay from broadcast and aggregation is set to 0 to show the benefit of CMIMO directly. Then, in CMIMO, all energy consumption and delay are considered in three phases.

7.4.1 Pure MIMO

In this subsection, the energy consumption and delay from broadcast and aggregation are set to 0 and only the energy and delay from MIMO transmission phase are consider. Here, the energy-delay tradeoffs of SISO (1×1), SIMO (1×2), MISO (2×1) and MIMO (2×2) are provided in three kind of channels. Meanwhile, the lower bound of energy-delay tradeoff obtained by (7.34) is shown. Related parameters are provided in Table 2.1. $BPSK$ is adopted in all channels.

Fig. 7.2 shows that CMIMO brings some benefit on the energy efficiency in three kinds of channels, especially in flat fading channel.

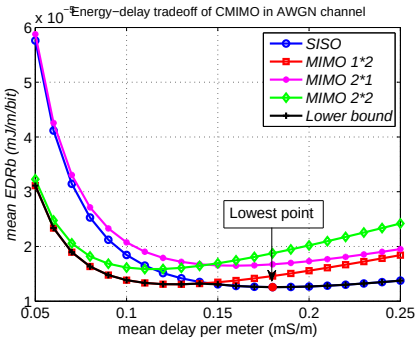

(a) AWGN

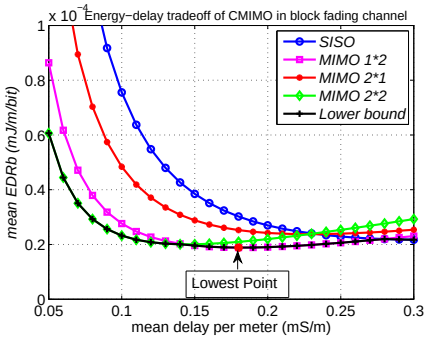

(b) Nakagami-m block fading (m=1)

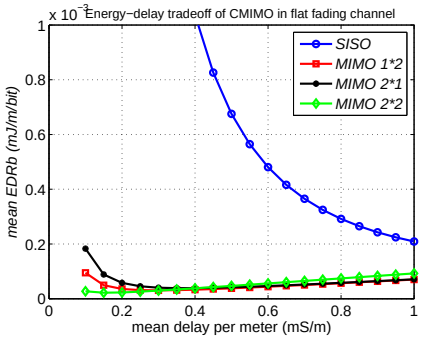

(c) Nakagami-m flat fading (m=1)

Figure 7.2: Energy-delay tradeoff of pure CMIMO in different channels

7.4.2 CMIMO

In this subsection, all energy consumption and delay from three phases are considered. The energy-delay tradeoffs of SISO (1×1), SIMO (1×2), MISO (2×1) and MIMO (2×2) in three kind of channels are shown in Fig. 7.3 where all parameters are presented in Table 2.1 and $BPSK$ is adopted in all channels.

Fig. 7.3 shows that SISO becomes the optimal scheme in AWGN and block fading channels and CMIMO has better energy efficiency than SISO in flat fading channel still. Comparing Fig. 7.3 with Fig. 7.2, we can deduce that the advantage of CMIMO in energy efficiency and delay can not compensate for the additional energy consumption and delay from the broadcast and aggregation phases. This result reveal that we should reduce the energy consumption and delay caused by broadcast and aggregation by some technologies, for example, increasing transmit rate.

In flat fading channel, CMIMO can bring a lot of advantage. In following section, we will analyze CMIMO in Nakagami-m flat fading channel in detail.

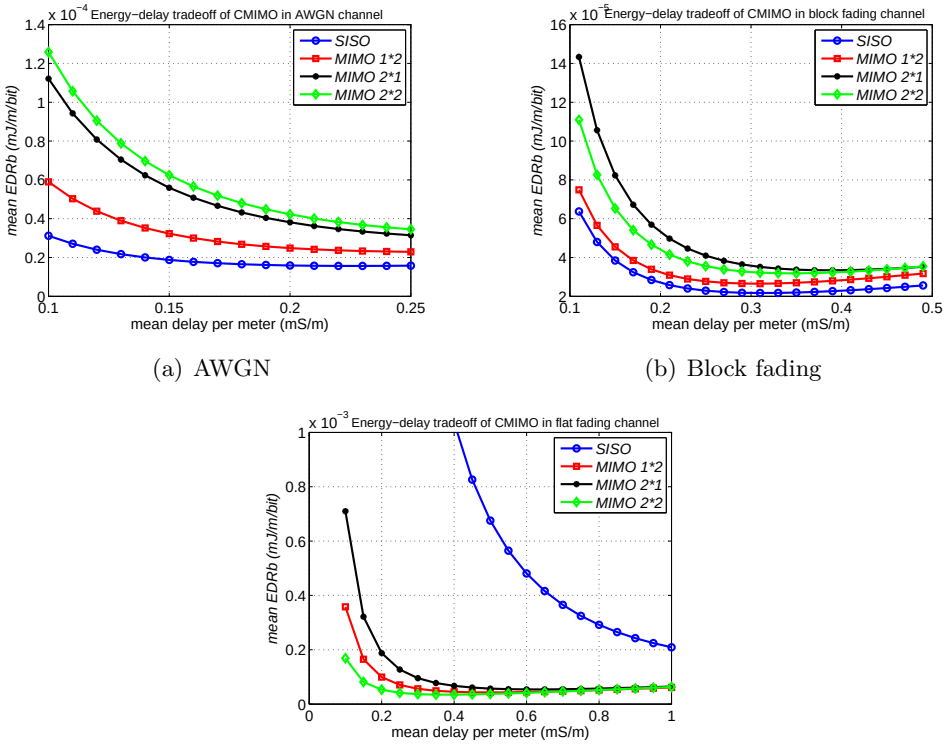

(a) AWGN

(b) Block fading

(c) Flat fading

Figure 7.3: Energy-delay tradeoff of CMIMO in different channels

7.5 Analysis in Nakagami-m flat fading channel

In this section, we focus on the lower bound of energy-delay tradeoff of CMIMO in Nakagami-m flat fading channel and the gain on energy efficiency compared with tradition multi-hop transmission and opportunistic communications.

7.5.1 Lower bound of CMIMO

The energy-delay tradeoff in Nakagami (m=1) flat fading channel is provided in Fig. 7.4 and the corresponding physical parameters N_{Topt}, N_{Ropt}, P_{topt}, d_{opt} are shown also. First we notice the lowest point ($ddr = 0.5mS/m$, $\overline{EDRb} = 0.5mJ/m/bit$) in the curve about the energy-delay tradeoff in Fig. 7.4. It is the most energy efficient point. The corresponding optimal transmission power $P_0 = 8.805mW$, $N_{T0} = 2$, $N_{R0} = 2$, the corresponding minimum hop distance $d_0 = 40.44m$. At the right side of the lowest point, $\overline{EDRb}$ rises with the increase of ddr which should be avoided in practice. Furthermore, as shown in Fig. 7.4, the corresponding transmission power at the right side of the lower point is smaller than P_0, the number of transmitters and receivers are not greater than N_{T0}, N_{T0}, and the optimal transmission distance is smaller than d_0. Therefore,

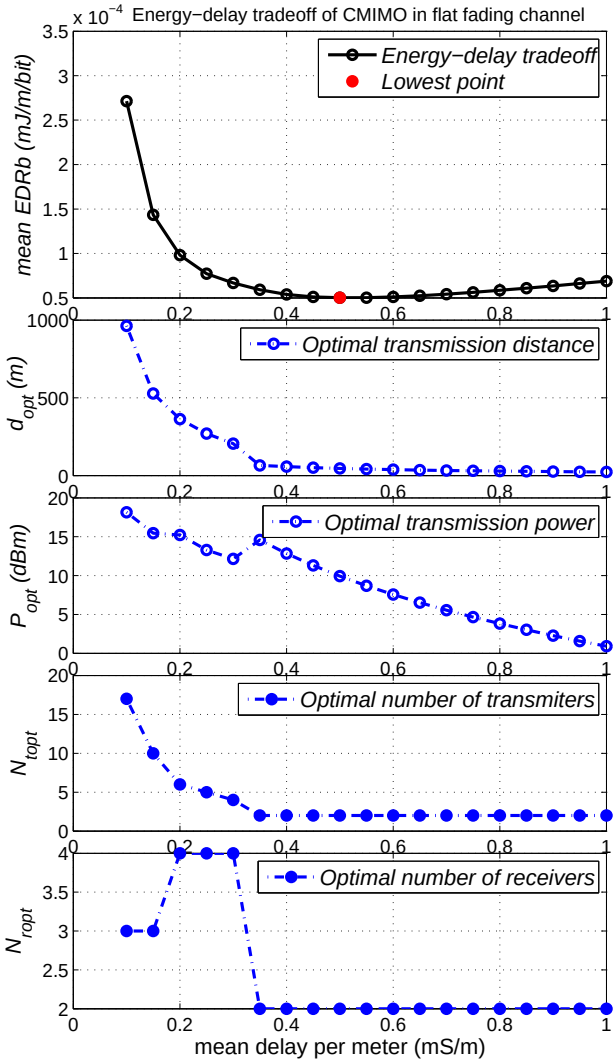

Figure 7.4: Energy-delay tradeoff of CMIMO in Rayleigh flat fading channel

each value provides a threshold for the corresponding physical parameter under which a network will operate in an inefficient state, which is very useful in the design phase of a network. Another point should be pointed out that the link probability of the lowest point is 91.06% and $P_b = 3.658 \times 10^{-5}$, which reveals that unreliable links can improve energy efficiency of a network in a CMIMO scheme also.

Then, we focus on the left side of the lowest point. At the left side, the energy consumption increases with the decrease of ddr, which coincides with our intuition. Meanwhile, N_{Topt} increases with the reduction of ddr. N_{Ropt} and P_{opt} are adjusted simultaneously with a tendency of increasing. The optimal transmission distance rises monotonically and the optimal link probability raises as shown in Fig. 7.4. Notice that the optimal link probability shown in Fig. 7.5 varies with ddr. Therefore, we can

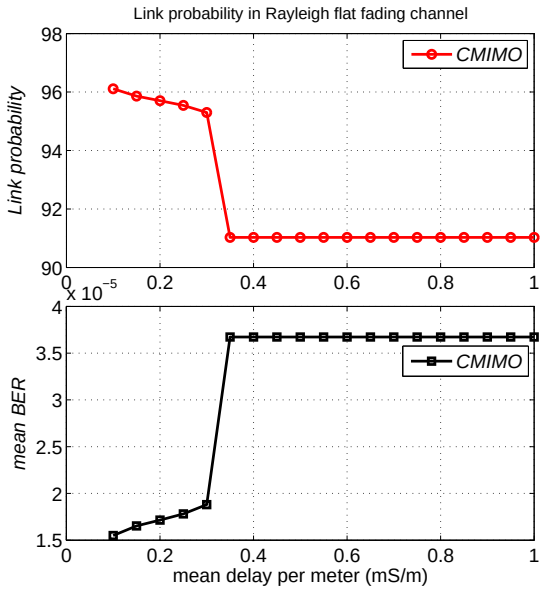

Figure 7.5: Optimal link probability

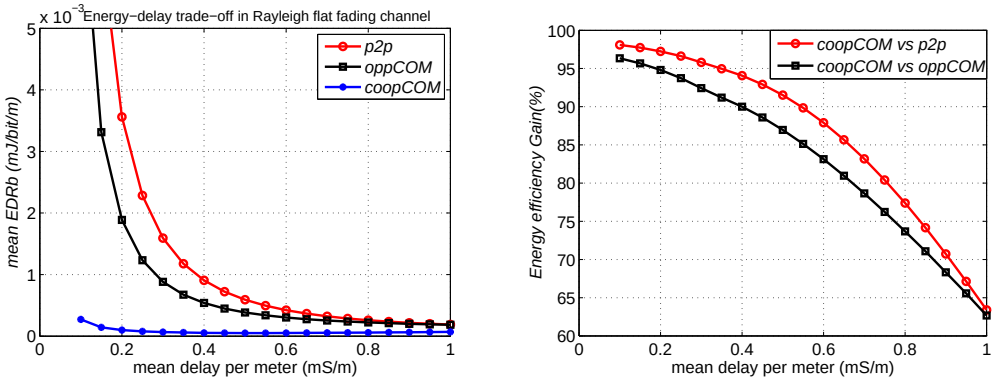

(a) Comparison (b) Gain

Figure 7.6: Energy gain of CMIMO in Rayleigh fading channel

deduce that a fixed mean BER (i.e. link probability) will result in the inefficiency of the system as realized in previous works.

7.5.2 Energy efficiency gain of CMIMO

We analyze the gain of cooperative communications in energy efficiency compared with traditional P2P communications and opportunistic communications in this section. The benefit of cooperative communications in terms of energy efficiency is shown in Fig. 7.6 under a delay constraint *ddr* in Rayleigh flat fading channel.

In Rayleigh flat fading channel, the energy gain of CMIMO compared with traditional point-to-point communications and opportunistic communications is analyzed

with the following formula:

$$Gain = \frac{\overline{EDRb}_{p2p,\ opp} - \overline{EDRb}_{Cmimo}}{\overline{EDRb}_{p2p,\ opp}}, \tag{7.41}$$

where $\overline{EDRb}_{p2p}$ and $\overline{EDRb}_{opp}$is obtained according to (2.42) proposed in Chapter 2 and (6.27) in Chapter 6. In this example, the minimum gain is greater than 60% which shows CMIMO outperform than the other two schemes.

7.6 Optimization of parameters

On the basis of the analyses in Section 7.3, the effects of physical layer and protocol layer parameters on the lower bound of energy-delay trade-off are studied in this section. All related parameters are provided in Table 2.1 except the parameters mentioned especially for analyzing.

7.6.1 The effect of physical layer parameters

Circuitry power

According to the definition of $\overline{EDRb}$ (7.21) and (7.7) (7.8), it is deduced easily that the increase of circuitry power will lead to the increment of total energy consumption similarly to the other schemes described in Chapter 2 and 6. Therefore, we should reduce the circuitry power in the design of sensor node and should select a node which has minimum circuitry power.

Fading

The increasing strength of fading worsens the link between two nodes which results to the augmentation of total energy consumption. The results in Fig. 7.7 proofs the correction of our deduction.

Modulation

Higher order modulation brings bigger BER under the condition of the same SNR but reduces transmission time and energy expenditure when in the same symbol rate due to the increase of bit rate. Hence, according to (7.21) and (7.24), an optimal modulation scheme should exist, which can balance these two kinds of effect and minimize both energy consumption and transmission delay. In Fig. 7.7, the lower bound of energy-delay tradeoff using different order QAM are shown, where the symbol rate is kept the same for all examples. Here, $8QAM$ is the best choice.

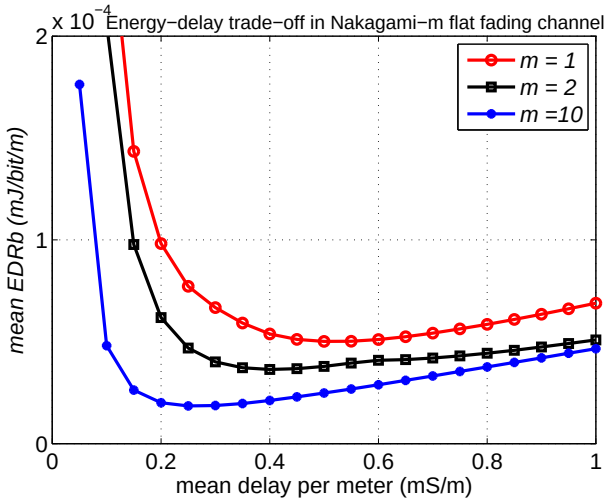

Figure 7.7: Effect of fading strength on energy-delay tradeoff

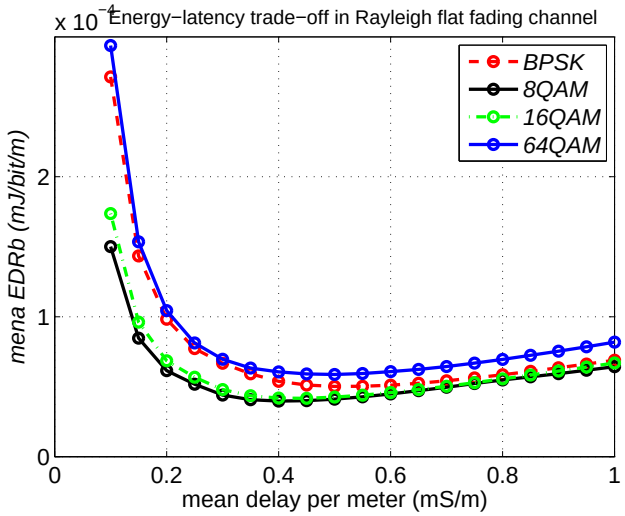

Figure 7.8: Effect of modulation on energy-delay tradeoff

Transmit Rate

On the basis of (7.21) and (7.24), we know that the higher transmit rate brings the smaller E_c and $\overline{DDR}$ in all type of channel. However, the increase of transmission rate leads to the decrease of SNR according to (2.11) which cases the rise of BER. In other words, the increase of transmit rate will bring two oppositive effects on the optimal $\overline{EDRb}$ and thus an optimal transmit rate should be existed. While, the results in Fig. 7.9 show that $\overline{EDRb}$ and $\overline{DDR}$ decrease simultaneously with respect to the increase of transmit rate. This result is same at the other communication schemes in Chapter 2 and 6. Hence, we should adopt the maximum transmit rate that a node can reach to minimize both $\overline{EDRb}$ and $\overline{DDR}$ in CMIMO.

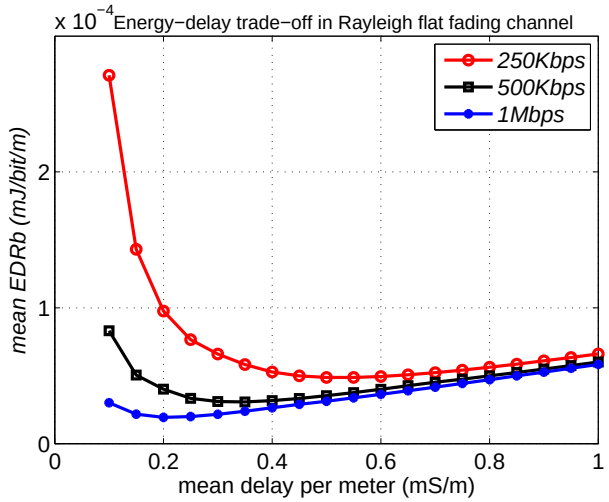

Figure 7.9: Effect of transmit rate on energy-delay tradeoff

7.6.2 The effect of protocol layer parameters

Number of bits in a ACK packet N_{ack}

According to (7.7) (7.8) and the definition of $\overline{EDRb}$ (2.22), it is deduced easily that the increase of N_{ack} leads to the increment of total energy consumption because of the rise of τ_{ack}. Therefore, removing the ACK packet is a best solution from the viewpoint of energy saving. At least, N_{ack} should be reduced as less as possible.

Number of bits in a packet N_b

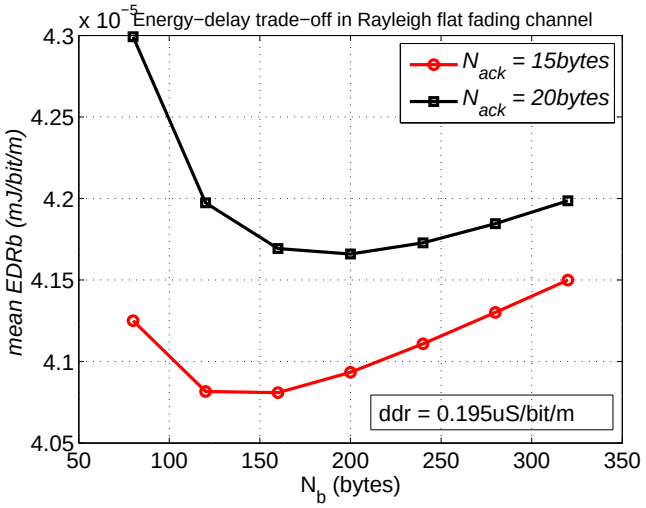

Figure 7.10: Effect of N_b on energy-delay trade-off in Rayleigh flat fading channels

Another method of diminishing τ_{ack} is to increase N_b according to (2.5). While,

this will lead to the decrease of link probability based on (7.17) which results in more energy consumption. Finally, these two contrary effects bring on an optimal number of bits. Fig. 7.10 shows how the optimal $\overline{EDRb}$ varies with N_b. Because τ_{ack} is tightly related with both N_{ack} and N_b, the optimal N_b is tightly dependent on N_{ack}, which is the same with the other schemes. This kind of impact is also shown in Fig. 7.10. When $N_{ack} = 15bytes$, the optimal N_b is $160bytes$. When $N_{ack} = 20bytes$, the optimal N_b is greater than $200bytes$. The conclusion obtained from these curves is the increase of N_{ack} will lead to the increase of the optimal N_b.

It should be noticed that the difference of $\overline{EDRb}$ from the different number of bits is small when N_{ack} is very small. Moreover, considering the conclusion about N_{ack}, we should do our best to reduce N_{ack} so that the optimization about N_b can be neglected.

7.7 Summary

In this chapter, we first introduce an energy model $\overline{EDRb}$ including protocol energy consumption and a delay model $\overline{DDR}$ based on an unreliable link model. On the basis of these models, the lower bound of energy-delay tradeoff of cooperative communications is deduced on the condition that the number of cooperative transmitters and receivers is fixed. Then, an algorithm for searching the optimal number of cooperative transmitters and receivers is proposed. Meanwhile, the effects of physical layer and protocol parameters on this lower bound are analyzed. In other side, the lower bound of energy efficiency is studied. Finally, we show the gain of energy efficiency of cooperative communications compared with P2P communications and opportunistic communications. There comparison shows that the choice of communication scheme is dependent on the type of channel. In AWGN channel and block fading channel, P2P communications better than cooperative communications. While, in Rayleigh flat fading channel, cooperative communications are best choice from the viewpoint of energy efficiency.

Part III

Conclusions et perspectives

8

Conclusions and Perspectives

8.1 Conclusions

In WSNs, many applications require only low data rates. The capacity is therefore not a critical issue. Instead, the objective is to ensure the transmission of a packet with a high probability, ensuring a low delay at the price of low energy consumption.

We considered in this work the success of a data transmission as a hard constraint, and we therefore investigate different acknowledged multi-hop strategies with respect to the two other constraints: energy consumption and transmission delay. To derive the performance of different strategies, we computed the set of Pareto-optimal solutions in different wireless channels.

In Chapter 2, using realistic unreliable link models, we explored the lower bound of energy-delay trade-off and energy efficiency in AWGN, Rayleigh flat fading and Nakagami block fading channel. For this purpose, we derived two metrics, the energy-distance ratio per bit $\overline{EDRb}$ for energy efficiency, and the delay/distance ratio per packet $\overline{DDR}$, respectively. We considered a multivariate problems (emitter/receiver distance and transmission power) with a multiobjective optimization target ($\overline{EDRb}$ and $\overline{DDR}$).

This study shows the existence of an optimal SNR, related to the PHY parameters (modulation, packet size, $\cdots$) at which the optimization with respect to $\overline{EDRb}$ and $\overline{DDR}$ is achieved for any possible trade-off. This optimal SNR is large enough in AWGN channel to ensure reliable radio links ($pl > 95\%$), but leads to unreliable links in fading

channels. Once the optimal SNR is computed, we found that a minimal energy can be achieved when no delay constraint is required, by adapting accordingly the transmission power and the inter-nodes distance. Theoretical analyses and simulations show that unreliable links in fading channels contributes to improve the energy efficiency of a system constrained by a maximum global delay. The close-form expression on energy-delay tradeoff provides a framework to evaluate the energy-delay performance of a network according to its PHY parameters.

In Chapter 3, some applications of the energy-delay lower bound are presented. A parameter optimization process is proposed to adjust the parameters including PHY and other protocol layers with or without delay constraint. Meanwhile, the simulations in a 2-dimension Poisson network exhibited the adequacy of the theoretical lower bound of energy-delay tradeoff. Two geographic routing schemes were used. Note that our framework can be used for non-geography routing schemes as well because the transmission distance is an inherent property of all routing schemes.

The second section of this thesis is then devoted to the study of cooperative approaches, as introduced in chapter 4. In Chapter 5, we proposed an analytical framework for opportunistic relaying schemes. Meanwhile, the energy efficiency of opportunistic communication with respect to different forwarding areas is studied as a function of the optional transmission power and the optional node density in AWGN and Rayleigh block fading channels. The analyses show that opportunistic communications are very efficient in Rayleigh block fading channels but not in AWGN from an energetic point of view. Further, the mechanism of selecting the forwarding candidates located around the linear path between the source and the destination is more energy efficient than that of selecting all neighbor nodes.

In Chapter 6, we extended the framework about energy-delay performance derived in Chapter 3 to the case of opportunistic communications. By optimizing $\overline{EDRb}$ for AWGN, Rayleigh block fading and Rayleigh block fading channels with and without delay constraint, we show that the channel state impacts the optimal number of receivers in a cluster. Meanwhile, the corresponding optimal transmission power and the optimal transmission range were derived. The energy-latency trade-off for one-hop and multi-hop transmissions are analyzed and compared with the trade-off given by traditional multi-hop communications. The main conclusion is that opportunistic communications exploiting spatial diversity are beneficial for Rayleigh block fading channels when a delay constraint is considered.

In Chapter 7, we extended the same framework to the case of MIMO and cooperative MIMO transmissions. We found that cooperative MIMO approaches appeared efficient in fading channels, but the energy cost for the broadcast and aggregation phases reduce this benefit.

As a summary, we can conclude that reducing energy consumption in WSNs in AWGN channels rely mostly on choosing appropriately the node density and power transmissions (these parameters are also related to the circuit energy consumption). The knowledge of the exact values will be helpful for designing sleeping mechanisms in order to keep alive enough nodes to comply with the node density constraint. We also found that there exist an optimal SNR which relies on the channel properties and the link probability function only. We then observed that opportunistic relaying and cooperative MIMO mechanisms increase energy consumption because of the circuit energy, with only a poor capacity increase in the case of AWGN channels.

While, in the context of fading channels, the results are opposite. Opportunistic relaying allows exploiting spatial diversity in reception and improves significantly the energy-delay trade-off. Cooperative MIMO is also efficient but suffers from the need of nodes synchronization and energy consumption for the broadcasting and aggregation phases.

In the block fading case, opportunistic relaying appears to be the most efficient approach and some existing routing algorithms already exploit this diversity. It should be noticed that in this thesis, we considered an ideal block fading, having a total independency of fading states between successive frames. In practice we can conjecture that the retransmission process used in our scheme to increase the reliability would be less efficient due to the time-correlation of block-fading states, and therefore opportunistic relaying mechanisms would be even more efficient.

Finally, in the case of flat fading, the packet error rate is computed assuming that fading states are different for each bit in a frame. This model is less realistic in WSNs, because we don't expect high mobility scenario. However, such channel could be achieved when using interleaving, or when using OFDMA, with independent fading states in each sub-carrier. We observed in this case, very bad performance as usually in this kind of channel. However, CMIMO and opportunistic schemes were proved to be very efficient to reduce this inefficiency.

8.2 Future works

In our framework, we obtained analytical expressions in the case of classical multi-hop transmission schemes and opportunistic relaying schemes. However, in several cases, we derived our results on a numerical analysis framework. We found in the literature a lack of realistic analytic expressions for the PER in block fading, albeit block fading is probably the most adequate model for WSNs. We proposed an approximation in the Rayleigh case, but we didn't extend this approximation to the case of other Nakagami-m conditions.

Further, the framework derived in this thesis considered neither shadowing variability nor irregular node distribution. In the case of a real deployment, we will have to face this variability. Finally, we also didn't consider the case of interference and multi-source transmissions.

We then suggest that the following research axes would be exciting.

Realistic channels In this work, we studied how unreliable links can be exploited. Some steps forward are still needed to cope with realistic channels. First, in realistic channels, each radio link could be subject to shadowing variations around the path-loss [34]. In this thesis, we derived an optimal set of parameters (P_{opt}, d_{opt}) for optimizing the energy-delay trade-off. In the case of shadowing variations, this optimal couple of parameters should be adapted to account for possible shadowing states. Note that if the shadowing is not stationary, the analysis about shadowing effect could be assessed by replacing the block fading pdf in (2.19) by the shadowing pdf.

The second question concerns the case of block fading channels. We guess that successive fading states are probably correlated during the transmission of successive packets in many applicative frameworks. In this case, our retransmission procedures would fail since successive retransmissions in a fading hole would experience identical conditions. The consequence would be an even better performance of opportunistic relaying since time diversity would be lower than spatial diversity. However, modeling the time-correlation in the packet error probability formulations would be a hard task.

Interfering networks In this thesis, we assume an interference-free scenario in all communication schemes because of low traffic applications. In the case of multiple simultaneous transmissions, our framework could not be used directly. However, an interesting extension of the model derived in chapter 2 could be easily extended to interfering networks from a statistical point of view. From (2.32) and (2.33), we proved that an optimal SNR can be derived. To take interference into account, it would be possible to replace the SNR by a SINR measure, exploiting an estimate of the interference distribution. Since this SINR would be related to the transmission power, we would be able to formulate the optimal power that achieving a trade-off between data rates and interference. This approach could open a new perspective to derive the theoretical capacity of WSNs.

Distributed coding In our models, we never consider the opportunity to encode the data. We think at this point that combining opportunistic communications with network coding [51] is a promising research direction. Further, in the case of having continuous data flows, mixing source coding, distributed coding and channel

coding could lead to a high improvement of the energy-delay performance.

Distributed mechanisms The results about cooperative communications in Chapter 4 are based on the assumption that the network is static and the optimal design can be performed off-line in a centralized fashion. However, for a dynamic network, a real-time adaptation is needed, and a distributed approach to select the best relay nodes is mandatory. In this thesis, we studied the optimal transmission policies, but we didn't provide the mechanisms for selecting the relays at a low energy cost. This problem is partially studied in the literature, but not with unreliable links.

Part IV

Appendices

A

Optimal γ in different channels

A.1 Derivation of γ_{opt} in AWGN channel

In Chapter 2, the close-form expression of link model in AWGN channel is given by (2.15). However, the closed form expression of γ_{optg} can not be obtained using the exact BER(γ). A simplified tight approximation of BER(γ) is obtained when $\beta_m \cdot \gamma_b \geq 2$ by using the fitting method:

$$\mathrm{BER}_g(\gamma_b) \approx 0.1826\alpha_m \cdot \exp(-0.5415\beta_m\gamma_b) \quad \text{if } \beta_m \cdot \gamma_b \geq 2, \tag{A.1}$$

where exp($\cdot$) represents the exponential function. Fig. A.1 shows the relation between the approximation and the exact values of the BER.

Substituting (A.1) and (2.13) into (2.50) and solving the equation of γ yield:

$$\gamma_{optg} = \frac{-1 - \alpha N_b \mathrm{W}_{-1}\left[\frac{-\exp(-\frac{1}{\alpha N_b})}{0.1826\alpha_m N_b \alpha}\right]}{0.5415\beta_m \cdot \alpha \cdot N_b} \tag{A.2}$$

where $\mathrm{W}_{-1}[\cdot]$ is the branch satisfying $\mathrm{W}(x) < -1$ of the Lambert W function [16].

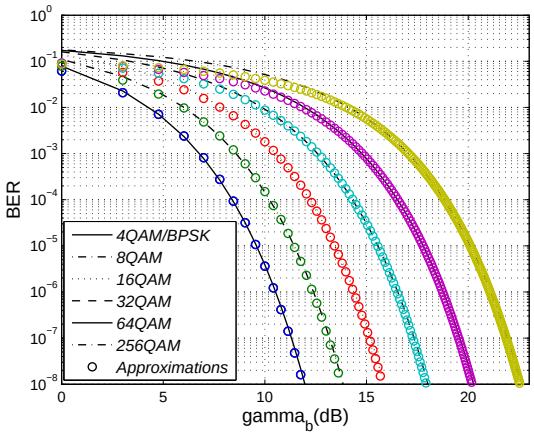

Figure A.1: BER approximations for MQAM

A.2 Derivation of γ_{opt} in Rayleigh flat fading channel

The substituting (2.18) into (2.50) and solving this equation, we have:

$$\gamma_{optf} = \frac{\alpha_m}{2\beta_m}(1 + \alpha N_b). \tag{A.3}$$

A.3 Derivation of γ_{opt} in Rayleigh block fading channel

The exact link model in Nakagami block fading channel is introduced by (2.19) in Chapter 2. However, the closed form expression of γ_{optb} can not be obtained directly using (2.19).

When $m = 1$ (Rayleigh block fading) and $\alpha_m = 1$, the approximation of (2.19) is found:

$$pl(\overline{\gamma}) = \exp\left(\frac{-4.25\log_{10}(Nb) + 2.2}{\beta_m \overline{\gamma}}\right). \tag{A.4}$$

Fig. A.2 shows the approximations for different values of N_b compared with the exact results.

Substituting (A.4) into (2.50) and solving the equation, we obtain:

$$\gamma_{optb} = \frac{\alpha(4.25\log 10(N_b) - 2.2)}{\beta_m}. \tag{A.5}$$

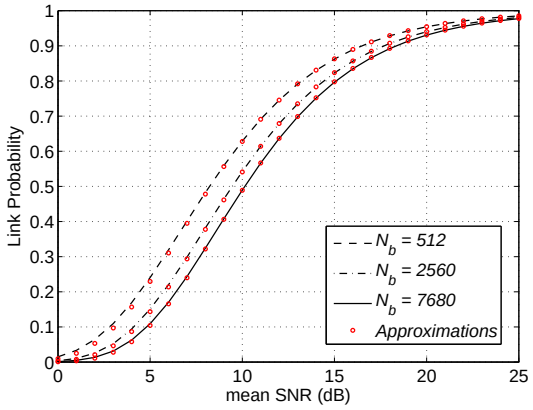

Figure A.2: Approximations of link probability for Rayleigh block fading

B

Minimum G Function

Refer to the Theorem 5. For a given N_R nodes whose corresponding $\bar{\gamma}$ is $\bar{\gamma}_1, \ldots, \bar{\gamma}_{N_R}$, the minimum value of $g(\langle\bar{\gamma}_i\rangle)$ can only be obtained by giving the higher relay priority to the node whose $\bar{\gamma}$ is smaller.

Proof. Let us introduce a new function $g' = \frac{1}{g(\langle\bar{\gamma}_i\rangle)}$. It can easily be seen that maximizing the value of g' leads to minimizing g. Next, we prove this theorem by maximizing g'.

When $N_R = 1$, the maximum value of g' can be gotten directly. Then, we assume it holds for $N_R = m - 1$ $(m \geq 2)$ where the relationship between is $\bar{\gamma}_1 < \cdots < \bar{\gamma}_k < \bar{\gamma}_{k+1} < \cdots < \bar{\gamma}_{m-1}$ $(k < m - 1)$ and its corresponding priority is $pri_{\bar{\gamma}_1} > \cdots > pri_{\bar{\gamma}_k} > pri_{\bar{\gamma}_{k+1}} > \cdots > pri_{\bar{\gamma}_{m-1}}$. Therefore, the theorem will be proved if we can show that it holds for $N_R = m$.

Without loss of generality, we may assume $\bar{\gamma}_m$ is the SNR of the m_{th} node and $\bar{\gamma}_k < \bar{\gamma}_m < \bar{\gamma}_{k+1}$. Here, there are three scenarios for assigning the priority of the m_{th} node,$pri_{\bar{\gamma}_m}$: $pri_{\bar{\gamma}_k} > pri_{\bar{\gamma}_m} > pri_{\bar{\gamma}_{k+1}}$, $pri_{\bar{\gamma}_m} > pri_{\bar{\gamma}_{k+1}}$ and $pri_{\bar{\gamma}_m} < pri_{\bar{\gamma}_{k+1}}$.

When $pri_{\bar{\gamma}_k} > pri_{\bar{\gamma}_m} > pri_{\bar{\gamma}_{k+1}}$,

$$\begin{aligned} g_1' = & \sum_{i=0}^{k} \bar{\gamma}_i^{-\frac{1}{\alpha}} \cdot pl(\bar{\gamma}_i) \prod_{j=1}^{i-1}(1 - pl(\bar{\gamma}_j)) \\ & + \bar{\gamma}_m^{-\frac{1}{\alpha}} pl(\bar{\gamma}_m) \prod_{j=0}^{l-1}(1 - pl(\bar{\gamma}_j)) \\ & + (1 - pl(\bar{\gamma}_m)) \sum_{i=k+1}^{m-1} \bar{\gamma}_i^{-\frac{1}{\alpha}} \cdot pl(\bar{\gamma}_i) \prod_{j=1}^{i-1}(1 - pl(\bar{\gamma}_j)). \end{aligned} \tag{B.1}$$

$$\begin{aligned} g_2' = & \sum_{i=0}^{l-1} \bar{\gamma}_i^{-\frac{1}{\alpha}} \cdot pl(\bar{\gamma}_i) \prod_{j=1}^{i-1}(1 - pl(\bar{\gamma}_j)) \\ & + \bar{\gamma}_m^{-\frac{1}{\alpha}} pl(\bar{\gamma}_m) \prod_{j=0}^{l-1}(1 - pl(\bar{\gamma}_j)) \\ & + (1 - pl(\bar{\gamma}_m)) \sum_{i=l}^{k} \bar{\gamma}_i^{-\frac{1}{\alpha}} \cdot pl(\bar{\gamma}_i) \prod_{j=1}^{i-1}(1 - pl(\bar{\gamma}_j)) \\ & + (1 - pl(\bar{\gamma}_m)) \sum_{i=k+1}^{m-1} \bar{\gamma}_i^{-\frac{1}{\alpha}} \cdot pl(\bar{\gamma}_i) \prod_{j=1}^{i-1}(1 - pl(\bar{\gamma}_j)). \end{aligned} \tag{B.2}$$

The difference between g_1' and g_2' is:

$$g_1' - g_2' = pl(\bar{\gamma}_m) \sum_{i=l}^{k-1} (\bar{\gamma}_i^{-\frac{1}{\alpha}} - \bar{\gamma}_m^{-\frac{1}{\alpha}}) \cdot pl(\bar{\gamma}_i) \prod_{j=1}^{l-1}(1 - pl(\bar{\gamma}_j)) \tag{B.3}$$

Because $\bar{\gamma}_m > \bar{\gamma}_i$ when $l < i < k$, we can obtain that $g_1' > g_2'$.

When $pri_{\bar{\gamma}_m} < pri_{\bar{\gamma}_{k+1}}$, using the similar method, the same result is obtained.

Thus, we conclude that the theorem holds. ■

C

Proof of $\overline{EDRb}$ convexity

Refer to Theorem 6. $\overline{EDRb}$ is a convex function with respect to N_R.

Proof. According to the definition of convex, the theorem will be proved if we can show: $\overline{EDRb}(N_R-1)+\overline{EDRb}(N_R+1) > 2\cdot\overline{EDRb}(N_R)$ where $N_R \geq 2$. Then, we will proof this condition holds.

$$\begin{aligned}&\overline{EDRb}(N_R-1)+\overline{EDRb}(N_R+1)-2\cdot\overline{EDRb}(N_R)= \\ &=\frac{(1+\tau_{ack})\bar{\gamma}^{\frac{1}{\alpha}}}{K_2P_t}\cdot\frac{(\bar{p}-1)\cdot\bar{p}^{N_R}\cdot(x+y)}{(1-\bar{p}^{N_R-1})\cdot(1-\bar{p}^{N_R+1})\cdot(1-\bar{p}^{N_R})}\end{aligned} \tag{C.1}$$

with

$$\begin{aligned}x &= E_{Tx}(\bar{p}-1)(1+\bar{p}^{N_R}) \\ y &= E_{Rx}(1+\bar{p}^{N_R+1}(N_R-1)-N_R+\bar{p}(N_R+1)-\bar{p}^{N_R}(1+N_R))\end{aligned}$$

where $\bar{p}=1-pl(\bar{\gamma})$ and $0<\bar{p}<1$.

Obviously, (C.1) is great than 0 if $x<0$ and $y<0$. Regarding x, it is easily concluded that $x<0$. Next, we proof $y<0$.

When $N_R=2$, we have $y(2)=E_{Rx}\cdot(\bar{p}-1)^3<0$. Meanwhile,

$$y(N_R+1)-y(N_R)=E_{Rx}\cdot(p-1)^3\cdot\sum_{i=1}^{N_R}i\cdot\bar{p}^{i-1}<0,$$

so y is a monotonic decreasing function. Thus, $y < 0$ for all N_R.

Finally, it is evident to see that $\overline{EDRb}$ is a convex function. ■

Part V

References

Bibliography

[1] http://ubimon.doc.ic.ac.uk/bsn.

[2] http://wsnet.gforge.inria.fr/.

[3] http://www.xbow.com.

[4] Micaz datasheet, available at *www.xbow.com*.

[5] Irfan Ahmed, Mugen Peng, Wenbo Wang, and Syed Ismail Shah. Joint rate and cooperative mimo scheme optimization for uniform energy distribution in wireless sensor networks. *Computer Communications*, 32(6):1072–1078, 2009.

[6] I. F. Akyildiz, W. Su, Y. Sankarasubramaniam, and E. Cayirci. Wireless sensor networks: a survey. *Computer Networks*, 38(4):393–422, 2002.

[7] H. Baldus, K. Klabunde, and G. MÃ$\frac{1}{4}$sch. Reliable set-up of medical body-sensor networks. In *Wireless Sensor Networks*, pages 353–363. 2004.

[8] S. Banerjee and A. Misra. Energy efficient reliable communication for multi-hop wireless networks. *Journal of Wireless Networks (WINET)*, 2004.

[9] P. Bauer, M. Sichitiu, R. Istepanian, and K. Premaratne. The mobile patient: wireless distributed sensor networks for patient monitoring and care. In *Information Technology Applications in Biomedicine, 2000. Proceedings. 2000 IEEE EMBS International Conference on*, pages 17–21, 2000.

[10] Sanjit Biswas and Robert Morris. Exor: opportunistic multi-hop routing for wireless networks. In *Proceedings of the 2005 conference on Applications, technologies, architectures, and protocols for computer communications*, pages 133–144, Philadelphia, Pennsylvania, USA, 2005. ACM.

[11] George Bravos and Athanasios G. Kanatas. Energy efficiency comparison of mimo-based and multihop sensor networks. *EURASIP J. Wirel. Commun. Netw.*, 8(3):1–13, 2008.

[12] A. Cerpa, J.L. Wong, L. Kuang, M. Potkonjak, and D. Estrin. Statistical model of lossy links in wireless sensor networks. In *Information Processing in Sensor Networks, 2005. IPSN 2005. Fourth International Symposium on*, 2005.

[13] D. Chen and P. K. Varshney. Qos support in wireless sensor networks: A survey. In *Proc. of the 2004 International Conference on Wireless Networks (ICWN 2004), Las Vegas, Nevada, USA*, 2004.

[14] P. Chen, B. O'Dea, and E. Callaway. Energy efficient system design with optimum transmission range for wireless ad hoc networks. In *Communications, 2002. ICC 2002. IEEE International Conference on*, volume 2, pages 945–952, 2002.

[15] Wenqing Cheng, Kanru Xu, Wei Liu, Zongkai Yang, and Zheng Feng. An energy-efficient cooperative mimo transmission scheme for wireless sensor networks. In *Wireless Communications, Networking and Mobile Computing, 2006. WiCOM 2006.International Conference on*, pages 1–4, 2006.

[16] R. Corless, G. Gonnet, D. Hare, D. Jeffrey, and D. Knuth. On the lambertw function. *Advances in Computational Mathematics*, 5(1):329–359, 1996.

[17] P. Coronel, S. Furrer, and W. Schott. An opportunistic energy-efficient medium access scheme for wireless sensor networks. In *Communications, 2005. ICC 2005. 2005 IEEE International Conference on*, volume 2, pages 1082–1086, 2005.

[18] S. Cui and A. J. Goldsmith. Cross-layer optimization of sensor networks based on cooperative mimo techniques with rate adaptation. In *Signal Processing Advances in Wireless Communications, 2005 IEEE 6th Workshop on*, pages 960–964, 2005.

[19] S. Cui, R. Madan, A. Goldsmith, and S. Lall. Joint routing, mac, and link layer optimization in sensor networks with energy constraints. In *Communications, 2005. ICC 2005. 2005 IEEE International Conference on*, volume 2, 2005.

[20] Shuguang Cui, A. J. Goldsmith, and A. Bahai. Energy-efficiency of mimo and cooperative mimo techniques in sensor networks. *Selected Areas in Communications, IEEE Journal on*, 22(6):1089–1098, 2004.

[21] Shuguang Cui and Andrea J. Goldsmith. Cross-layer design of energy-constrained networks using cooperative mimo techniques. *Signal Process.*, 86(8):1804–1814, 2006.

[22] Shuguang Cui, R. Madan, A. J. Goldsmith, and S. Lall. Cross-layer energy and delay optimization in small-scale sensor networks. *Wireless Communications, IEEE Transactions on*, 6(10):3688–3699, 2007.

[23] Estrin Deborah, Govindan Ramesh, Heidemann John, and Kumar Satish. Next century challenges: scalable coordination in sensor networks. In *Proceedings of the 5th annual ACM/IEEE international conference on Mobile computing and networking*, pages 263–270, Seattle, Washington, United States, 1999. ACM.

[24] I. Demirkol, C. Ersoy, and F. Alagoz. Mac protocols for wireless sensor networks: a survey. *Communications Magazine, IEEE*, 44(4):115–121, 2006.

[25] J. Deng, Y. S. Han, P. N. Chen, and P. K. Varshney. Optimal transmission range for wireless ad hoc networks based on energy efficiency. *Communications, IEEE Transactions on*, 55(7):1439–1439, 2007.

[26] M. Dohler, J. Dominguez, and H. Aghvami. Link capacity analysis for virtual antenna arrays. In *Vehicular Technology Conference, 2002. Proceedings. VTC 2002-Fall. 2002 IEEE 56th*, volume 1, pages 440–443, 2002.

[27] M. Dohler, E. Lefranc, and H. Aghvami. Space-time block codes for virtual antenna arrays. In *Personal, Indoor and Mobile Radio Communications, 2002. The 13th IEEE International Symposium on*, volume 1, pages 414–417, 2002.

[28] Gregory G. Finn. Routing and addressing problems in large metropolitan-scale internetworks. isi research report. Technical report, University of Southern California, Marina del Rey. Information Sciences Inst., 1987.

[29] D. Ganesan, B. Krishnamachari, A. Woo, D. Culler, D. Estrin, and S. Wicker. Complex behavior at scale: An experimental study of low-power wireless sensor networks. Technical report, 2003.

[30] J. L. Gao. Analysis of energy consumption for ad hoc wireless sensor networks using a bit-meter-per-joule metric. Technical report, 2002.

[31] Q. Gao, J. Zhang, X. S. Shen, and B. Larish. A cross-layer optimization approach for energy efficient wireless sensor networks: Coalition-aided data aggregation, cooperative communication, and energy balancing. *EURASIP Journal on Wireless Communications and Networking*, 2007.

[32] A. J. Goldsmith and P. P. Varaiya. Capacity of fading channels with channel side information. *Information Theory, IEEE Transactions on*, 43(6):1986–1992, 1997.

[33] A. J. Goldsmith and S. B. Wicker. Design challenges for energy-constrained ad hoc wireless networks. *Wireless Communications, IEEE [see also IEEE Personal Communications]*, 9(4):8–27, 2002.

[34] Andrea Goldsmith. *Wireless Communications*. cambridge university press, 2005.

[35] Jean-Marie Gorce, Ruifeng Zhang, and H. Parvery. Impact of radio link unreliability on the connectivity of wireless sensor networks. *EURASIP Journal on Wireless Communications and Networking*, 2007, 2007.

[36] M. Haenggi. The impact of power amplifier characteristics on routing in random wireless networks. In *Global Telecommunications Conference, 2003. GLOBECOM '03. IEEE*, volume 1, pages 513–517, 2003.

[37] M. Haenggi. On distances in uniformly random networks. *Information Theory, IEEE Transactions on*, 51(10):3584–3586, 2005.

[38] M. Haenggi. On routing in random rayleigh fading networks. *Wireless Communications, IEEE Transactions on*, 4(4):1553–1562, 2005.

[39] M. Haenggi and D. Puccinelli. Routing in ad hoc networks: a case for long hops. *Communications Magazine, IEEE*, 43(10):93–101, 2005.

[40] W. B. Heinzelman, A. P. Chandrakasan, and H. Balakrishnan. An application-specific protocol architecture for wireless microsensor networks. *Wireless Communications, IEEE Transactions on*, 1(4):660–670, 2002.

[41] R. Holman, J. Stanley, and T. Ozkan-Haller. Applying video sensor networks to nearshore environment monitoring. *Pervasive Computing, IEEE*, 2(4):14–21, 2003.

[42] Chalermekv Intanagonwiwat, Deborah Estrin, Ramesh Govindan, and John Heidemann. Impact of network density on data aggregation in wireless sensor networks. In *Proceedings of the 22 nd International Conference on Distributed Computing Systems (ICDCS'02)*. IEEE Computer Society, 2002.

[43] K. Jaffres-Runser, J. M. Gorce, and S. Ubeda. Multiobjective qos-oriented planning for indoor wireless lans. In *Vehicular Technology Conference, 2006. VTC-2006 Fall. 2006 IEEE 64th*, pages 1–5, 2006.

[44] S. Jagannathan, H. Aghajan, and A. Goldsmith. The effect of time synchronization errors on the performance of cooperative miso systems. In *Global Telecommunications Conference Workshops, 2004. GlobeCom Workshops 2004. IEEE*, pages 102–107, 2004.

[45] S. K. Jayaweera. Virtual mimo-based cooperative communication for energy-constrained wireless sensor networks. *Wireless Communications, IEEE Transactions on*, 5(5):984–989, 2006.

[46] Seada Karim, Zuniga Marco, Helmy Ahmed, and Krishnamachari Bhaskar. Energy-efficient forwarding strategies for geographic routing in lossy wireless sensor networks, 2004.

[47] H. Karl and A. Willig. *Protocols and Architectures for Wireless Sensor Networks*. John Wiley and Sons, 2005.

[48] Brad Karp and H. T Kung. Gpsr: greedy perimeter stateless routing for wireless networks, 2000.

[49] Bhaskar Krishnamachari, Deborah Estrin, and Stephen B. Wicker. The impact of data aggregation in wireless sensor networks, 2002.

[50] Duan Li and Xiaoling Sun. *Nonlinear Integer Programming*. Springer New York, 2006.

[51] S. Y. R. Li, R. W. Yeung, and Ning Cai. Linear network coding. *Information Theory, IEEE Transactions on*, 49(2):371–381, 2003.

[52] X. Y. Li, H. Chen, Y. Shu, and X. Chu. Energy efficient routing with unreliable links in wireless networks. In *Mobile Adhoc and Sensor Sysetems (MASS), 2006 IEEE International Conference on*, pages 160–169, 2006.

[53] Xiaohua Li. Energy efficient wireless sensor networks with transmission diversity. *Electronics Letters*, 39(24):1753–1755, 2003.

[54] Xiaohua Li, Mo Chen, and Wenyu Liu. Application of stbc-encoded cooperative transmissions in wireless sensor networks. *Signal Processing Letters, IEEE*, 12(2):134–137, 2005.

[55] Yingshu Li, My T. Thai, and Weili Wu, editors. *Wireless Sensor Networks and Applications*. Springer, 2008.

[56] Chun-Pong Luk, Wing-Cheong Lau, and On-Ching Yue. An analysis of opportunistic routing in wireless mesh network. In *Communications, 2008. ICC '08. IEEE International Conference on*, pages 2877 – 2883, 2008.

[57] Jian Ma, Qianbin Chen, Dian Zhang, and Lionel M. Ni. An empirical study of radio signal strength in sensor netoworks using mica2 nodes. Technical report, Hong Kong University of Science and Technology, 2006.

[58] R. Madan, Cui Shuguang, S. Lall, and N. A. Goldsmith. Cross-layer design for lifetime maximization in interference-limited wireless sensor networks. *Wireless Communications, IEEE Transactions on*, 5(11):3142–3152, 2006.

[59] K. Martinez, J. K. Hart, and R. Ong. Environmental sensor networks. *Computer*, 37(8):50–56, 2004.

[60] Philippe Mary. *Etude analytique des performances des systèmes radio-mobiles en présence d'évanouissements et d'effet de masque*. PhD thesis, 2008.

[61] Leonard E. Miller. Distribution of link distances in a wireless network. *Journal of Research of the National Institute of Standards and Technology*, 106:401–412, 2001.

[62] M. Nakagami. The m-distribution, a general formula of intensity distribution of rapid fading. *Statistical Methods in Radio Wave Propagation*, pages 3–36, 1960.

[63] J. Nemeroff, L. Garcia, D. Hampel, and S. DiPierro. Networked sensor communications. In *MILCOM 2002. Proceedings*, volume 2, pages 1462–1465, 2002.

[64] T. D. Nguyen, O. Berder, and O. Sentieys. Cooperative mimo schemes optimal selection for wireless sensor networks. In *Vehicular Technology Conference, 2007. VTC2007-Spring. IEEE 65th*, pages 85–89, 2007.

[65] E. M. Petriu, T. E. Whalen, R. Abielmona, and A. Stewart. Robotic sensor agents: a new generation of intelligent agents for complex environment monitoring. *Instrumentation and Measurement Magazine, IEEE*, 7(3):46–51, 2004.

[66] L. S. Pillutla and V. Krishnamurthy. Joint rate and cluster optimization in cooperative mimo sensor networks. In *Signal Processing Advances in Wireless Communications, 2005 IEEE 6th Workshop on*, pages 265–269, 2005.

[67] A. Ravindran, K. M. Ragsdell, and G. V. Reklaitis. *Engineering Optimization*. Wiley, second edition, 2006.

[68] C. Rose. Mean internodal distance in regular and random multihop networks. *Communications, IEEE Transactions on*, 40(8):1310–1318, 1992.

[69] R. Schmitz, M. Torrent-Moreno, H. Hartenstein, and W. Effelsberg. The impact of wireless radio fluctuations on ad hoc network performance. In *Local Computer Networks, 2004. 29th Annual IEEE International Conference on*, pages 594–601, 2004.

[70] R. C. Shah, S. Wietholter, and A. Wolisz. Modeling and analysis of opportunistic routing in low traffic scenarios. In *Modeling and Optimization in Mobile, Ad Hoc, and Wireless Networks, 2005. WIOPT 2005. Third International Symposium on*, pages 294–304, 2005.

[71] R. C. Shah, S. Wietholter, A. Wolisz, and J. M. Rabaey. When does opportunistic routing make sense? In *Pervasive Computing and Communications Workshops, 2005. PerCom 2005 Workshops. Third IEEE International Conference on*, pages 350–356, 2005.

[72] Hyundong Shin and Jae Hong Lee. Performance analysis of space-time block codes over keyhole nakagami-m fading channels. *Vehicular Technology, IEEE Transactions on*, 53(2):351–362, 2004.

[73] C. E. Smith, C. A. Richards, S. A. Brandt, and N. P. Papanikolopoulos. Visual tracking for intelligent vehicle-highway systems. *Vehicular Technology, IEEE Transactions on*, 45(4):744–759, 1996.

[74] Hsieh Tim Tau. Using sensor networks for highway and traffic applications. *Potentials, IEEE*, 23(2):13–16, 2004.

[75] N. F. Timmons and W. G. Scanlon. Analysis of the performance of ieee 802.15.4 for medical sensor body area networking. In *Sensor and Ad Hoc Communications and Networks, 2004. IEEE SECON 2004. 2004 First Annual IEEE Communications Society Conference on*, pages 16–24, 2004.

[76] M. A. M. Vieira, C. N. Jr. Coelho, D. C. Jr. da Silva, and J. M. da Mata. Survey on wireless sensor network devices. In *Emerging Technologies and Factory Automation, 2003. Proceedings. ETFA '03. IEEE Conference*, volume 1, pages 537–544, 2003.

[77] Mehmet Can Vuran. *CORRELATION-BASED CROSS-LAYER COMMUNICATION IN WIRELESS SENSOR NETWORKS*. PhD thesis, Georgia Institute of Technology, 2007.

[78] A. Woo and D. E. Culler. Evaluation of efficient link reliability estimators for low-power wireless networks. Technical report, Computer Science Division, University of California, 2003.

[79] Guang-Zhong Yang, editor. *Body Sensor Networks*. Springer, 2006.

[80] Wei Ye, J. Heidemann, and D. Estrin. An energy-efficient mac protocol for wireless sensor networks. In *INFOCOM 2002. Twenty-First Annual Joint Conference of the IEEE Computer and Communications Societies. Proceedings. IEEE*, volume 3, pages 1567–1576, 2002.

[81] Gai Yi, Zhang Lin, and Shan Xiuming. Energy efficiency of cooperative mimo with data aggregation in wireless sensor networks. In *Wireless Communications and Networking Conference, 2007.WCNC 2007. IEEE*, pages 791–796, 2007.

[82] Yong Yuan, Zhihai He, and Min Chen. Virtual mimo-based cross-layer design for wireless sensor networks. *Vehicular Technology, IEEE Transactions on*, 55(3):856–864, 2006.

[83] Marco Zuniga Zamalloa and Krishnamachari Bhaskar. An analysis of unreliability and asymmetry in low-power wireless links. *ACM Transactions on Sensor Networks*, 3(2):7, 2007.

[84] Marco Zuniga Zamalloa, Karim Seada, Bhaskar Krishnamachari, and Ahmed Helmy. Efficient geographic routing over lossy links in wireless sensor networks. *ACM Trans. Sen. Netw.*, 4(3):1–33, 2008.

[85] Kai Zeng, Wenjing Lou, Jie Yang, and D. R. Brown. On geographic collaborative forwarding in wireless ad hoc and sensor networks. In *Wireless Algorithms, Systems and Applications, 2007. WASA 2007. International Conference on*, pages 11–18, 2007.

[86] Lili Zhang and Boon-Hee Soong. Energy efficiency analysis of channel aware geographic-informed forwarding (cagif) for wireless sensor networks. *Wireless Communications, IEEE Transactions on*, 7(6):2033–2038, 2008.

[87] Ruifeng Zhang, J. M. Gorce, and Katia Jaffrès-Runser. Energy-delay bounds analysis in wireless multi-hop networks with unreliable radio links. Technical Report 6598, ARES / INRIA, 2008.

[88] Jerry Zhao and Ramesh Govindan. Understanding packet delivery performance in dense wireless networks. In *Proceedings of the 1st international conference on Embedded networked sensor systems*, pages 1–13, Los Angeles, California, USA, 2003. ACM Press.

[89] L. C. Zhong, J. M. Rabaey, and A. Wolisz. An integrated data-link energy model for wireless sensor networks. In *Communications, 2004 IEEE International Conference on*, volume 7, pages 3777–3783, 2004.

[90] M. Zorzi and R. R. Rao. Geographic random forwarding (geraf) for ad hoc and sensor networks: energy and latency performance. *Mobile Computing, IEEE Transactions on*, 2(4):349–365, 2003.

[91] M. Zuniga and B. Krishnamachari. Analyzing the transitional region in low power wireless links. In *Sensor and Ad Hoc Communications and Networks, 2004. IEEE SECON 2004. 2004 First Annual IEEE Communications Society Conference on*, pages 517–526.

List of publications

Journal

[1] J.M. Gorce, R. Zhang, and H. Parvery *Impact of Radio Links Unreliability on the Connectivity of Wireless Sensor Networks* EURASIP, Journal on Wireless Communications and Networking, 2007.

International Conferences

[2] R. Zhang, J.M. Gorce, and K. Jaffres-Runser. *Lower Bound of Energy-Latency Trade-Off of Opportunistic Routing in Multi-Hop Networks.* in Communications, 2009. ICC '09. IEEE International Conference on. 2009

[3] R. Zhang, , J.M. Gorce, and K. Jaffrès-Runser . *Energy Efficiency of Opportunistic Routing with Unreliable Links.* in Wireless Communications and Networking Conference, 2009. WCNC 2009. IEEE. 2009

[4] R. Zhang, and J.M. Gorce. *Optimal Transmission Range for Minimum Energy Consumption in Wireless Sensor Networks.* in Wireless Communications and Networking Conference, 2008. WCNC 2008. IEEE. 2008. Las Vegas, NV

[5] J.M. Gorce, R. Zhang, and H. Parvery. *Tight Bound for the Mean Node Degree in Ad Hoc Networks with Opportunistic Communications.* in Wireless and Mobile Computing, Networking and Communications, 2007. WiMOB 2007. Third IEEE International Conference on. 2007. White Plains, NY.

[6] R. Zhang and J.M. Gorce. *Connectivity of Wireless Sensor Networks with Unreliable Links.* in Communications and Networking in China, 2007. CHINACOM '07. Second International Conference on. 2007.

[7] R. Zhang, J.-M. Gorce, and K. Jaffrès-Runser. *Analyses of Energy-Latency Trade-off of Opportunistic Routing in Multi-hop Networks.* in COST 2100, 6th MCM. 2008. Lille, France.

National Conference

[8] R. Zhang, J.M. Gorce, and H. Parvery. *Mean node degree in fading channels with opportunistic communications.* in First IRAMUS Workshop on radio interfaces for WSN and MANET networks. 2007. Val Thorens, France.

Rapport de recherche

[9] R. Zhang, J.M. Gorce, and K. Jaffrès-Runser, *Energy-delay bounds analysis in wireless multi-hop networks with unreliable radio links.* 2008, ARES / INRIA.